Copper Coated Iron Particles: Magnetically Retrievable and Low-Leaching Heterogeneous Catalysts for the Azide-Alkyne Huisgen Cycloaddition

A thesis submitted to McGill University
in partial fulfillment of the requirements of the
Degree of Master's in Chemistry

by

Mary Bateman

Department of Chemistry

McGill University

Montreal, Quebec, Canada

February 2015

Abstract

Magnetically retrievable nanocatalysts have represented an emerging class of heterogeneous catalysts which offer both ease of separation and low-leaching with the high catalytic activity. These features were attractive not only in typical organic reactions but also in reactions of biologically relevant molecules, where removal of catalyst and leaching were important considerations. Cu(I)-catalyzed azide-alkyne cycloadditions (CuAAC) also called “click” reactions, have been well studied since its discovery in 2002. The remarkable regioselectivity, high tolerance for a wide range of reaction conditions and bioorthogonality make CuAAC an excellent choice for use in biological systems. However, the toxicity of Cu(I) has been problematic in its widespread use. This thesis examined the use of various copper coated iron particles as magnetically retrievable, low leaching and nontoxic nanocatalysts for CuAAC as a first step to develop a bio-compatible aromatase nanosensor. These particles are simple to prepare, under very mild conditions and can be recycled several times. They were successfully tested for several click reactions, including the coupling of rhodamine azide (Rhod-N_3) and ethisterone (testo-alkyne), to produce the product rhod-*triazole*-testo, a fluorescently-labeled testosterone to be used in the future development of the nanosensor. The reactivity and leachability of these particles were probed by monitoring time of reactions by NMR and ICP measurements of the product to determine Cu content, while optimizing a number of important reaction parameters. Toxicity tests were also undergone to verify the inequity of the Cu-based catalysts. It was found that nanoparticles of iron were not reliable as catalysts supports, while their micron-sized counterparts performed very well, in terms of catalytic activity and low leachability. Further improvements to achieve ultra-low leaching were obtained by modifying the surface of the copper coated iron particles with carbon, although the reaction took longer to proceed to completion.

Résumé

Les nanocatalyseurs recyclables magnétiquement constituent une nouvelle classe de catalyseurs hétérogènes qui offrent à la fois une facilité de séparation, un faible « leaching » et une activité catalytique élevée. Ces caractéristiques en font des catalyseurs de choix non seulement pour les réactions organiques classiques mais aussi pour des réactions entre molécules biologiquement pertinentes, où la récupération du catalyseur et le « leaching » sont des paramètres importants à prendre en considération. La cycloaddition entre azoture et alcyne catalysée par le Cu(I) (CAACu), également appelée réaction "clic", a fait l'objet de nombreuses recherche depuis sa découverte en 2002. Sa régiosélectivité remarquable, sa grande tolérance pour un large éventail de conditions de réaction et sa bioorthogonalité fait de la CAACu un excellent choix pour une utilisation dans des systèmes biologiques. Cependant, la toxicité du Cu(I) empêche son utilisation généralisée. Cette thèse présente l'utilisation de diverses particules de fer recouvertes de cuivre, magnétiquement récupérables et à faible « leaching » limité et leur utilisation comme nanocatalyseurs non toxiques pour la CAACu dans le but de développer un nanocapteur d'aromatase bio-compatible. Ces particules sont simples à préparer, dans des conditions très douces et peuvent être recyclées à plusieurs reprises. Elles ont été testés avec succès sur plusieurs réactions clic, y compris le couplage de la rhodamine azoture (Rhod-N_3) et l'éthistérone, pour produire le rhod-*triazole*-testo, une testostérone marqué par fluorophore qui pourra permettre le développement futur du nanocapteur. La réactivité et le « leaching » de ces particules ont été évalués en fonction du temps de réaction, obtenu par RMN et la teneur en Cu dans le produit, mesuré par PIC et a permis l'optimisation d'un certain nombre de paramètres réactionnels. Des tests de toxicité ont également révélé l'innocuité des catalyseurs à base de cuivre. Il a été constaté que les nanoparticules de fer entrainaient des problèmes de reproductibilité, tandis que leurs homologues micrométriques étaient beaucoup plus fiables, en termes d'activité catalytique et de faible « leaching ». En modifiant la surface des particules de fer couvertes de cuivre avec

du carbone, un « leaching » ultra faible a été obtenu, en notant toutefois que la réaction s’est révélée plus lente dans ces conditions.

To my family and friends for their unwavering support

Buda geçer, buda geçer
alışmalısın
alışmalısın
alışmalısın

Hemen karar, verme sabret, buda geçer
dayanmalısın
dayanmalısın
dayanmalısın

Böyle kalmaz zamanla
düzelir elbet
Buda geçer arkadaş
buna üzülme

Yarin başka bir gündür yarını bekler
Buda geçer arkadaş sakın üzülme

-Hamza Dekeli

Acknowledgements

I would like to begin by thanking my research supervisor, Dr. Audrey Moores. I can't thank you enough for all of the wonderful opportunities you've given me to further develop as a scientist and person. From conferences and exchanges to other labs in the world, I was allowed to interact and learn from many people. For that, I will be forever grateful. Additionally, thank you for your guidance and many discussions, not just about science, but about the world and life. You've given me great advice along the way that I'll always remember. It has truly been a pleasure working in your lab and I feel I've grown into an independent researcher who is not afraid to ask questions and learn.

There are several funding agencies and programs that have been important to my research: NSERC, the Canadian Foundation for Innovation (CFI), the Fonds de Recherche sur le Nature et les Technologies (FQRNT), the Centre for Green Chemistry and Catalysis and McGill University. A very special thank you to the Green Chemistry NSERC Collaborative Research and Training Experience (CREATE) for the additional funding to allow me to travel to conferences and exchanges as well as the numerous workshops at McGill. Thank you to Jacky Farrell who has organized these events and has been wonderful to work with.

A special thanks to the Moores group collaborators I had the opportunity to work with: Dr. Yasuhiro Uozumi and Dr. Takao Osaka at the Institute for Molecular Science in Okazaki, Japan as well as Dr. Bruce Koel and Peng Zhang at Princeton University.

I am grateful to everyone who I have had the pleasure of meeting and working with over the past two years. You have all played a role in making this experience truly unique and unforgettable. To the past and present Moores group members: Alain, Annie, Diogo, Hava, Huizhi, Karl, Luis, Madhu, Michael, Mitra, Monika, Monique, Olivia, Reuben, Sali, Shingo, Thomas and Yuting; where do I begin? I can't tell you how lucky I am to have met each and every one of you. We became such a tight knit (crazy) family and it has made my time at McGill that much more special. With our silly pranks (peanut

Mary, sexy dancing snake, 3% duck, rainbow dash), our Bollywood nights and music videos (I wanna love you every day!!), it truly made coming to the lab that much more exciting. I've also benefited tremendously from speaking to each of you about chemistry and knew I'd always leave with an idea (or at least a hug!). To Annie, I can't thank you enough for allowing me to work with you on your project. There were definitely ups and downs but you were always so positive and I learned so much from being around you. Your pink fumehood was definitely the best! To Yuting, thank you for being such a great person to work and being the azide queen! To Olivia, for being my first summer student and being a great researcher. To Huizhi, for the dumplings, and the funny jokes (Shi, Shi Shi poem). To Mitra, for being a great source of knowledge and discussion, amazing SEM pictures, and friend to have a good laugh with. To Alain, the sassiest Frenchman around (hon hon hon!). I know the group loves giving you a hard time but thanks for always giving it right back and for the endless chocolate and coffee. To Madhu for our lovely conversation about anything and everything, delicious Indian food, the endless Bollywood dance videos (Tattad Tattad!) and just dancing in general. Finally to Monika, my crazy, wonderful friend. My experience at McGill has been that much better after having met you. From the numerous animal facts, elaborate pranks, drive-by hugs (stranger-danger), brunch dates, and non-stop fun, you're truly a special person and have changed my life for the better. Thanks for being you!

A special shout-out to the friends I've made throughout grad school. The nail night girls, Monika, Laure, Julia, Isabelle and Michelle, for the laughs and beautiful nails. Just think, if the chemistry thing doesn't work out our nail business will be a hit! The cooking team, Graeme and Thomas, for the soup and mushrooms. My first friends at McGill, Yue-Chen and Davin, for always being supportive and finally Janane for being who you are and having an unfailing love for french fries and shawarma. Also a special thank you to my friend and roommate Michelle. We've known each other since our Dalhousie days and I'm so happy we reunited again here at McGill. I can always count on you for a funny story, to listen to me complain or just a beer after a long day.

Finally, I'd like to thank my family, who, without their constant support and

encouragement, I would not be here. To my parents, despite not completely understanding what I was doing in the lab every day, you were always there to listen when I needed it. To my sister for our trips together and for keeping it real with me no matter what, even if I didn't want to hear it. To my aunts, uncles and cousins, I'm so grateful to have family here in Montreal that have supported me these two years, whether it be for advice, moral support or cooking my favorite meals.

Without all these important people in my life, I would not be who I am today and for that I am extremely grateful.

Contribution of Authors

All chapters presented in this thesis were entirely written by Mary Bateman, with the exception of a short contribution on biology application from Dr. Annie Castonguay (post-doctoral fellow, Moores and Maysinger group) in the Chapter 1. All chapters were edited by Dr. Audrey Moores. Most of the experiments, data collection and analysis were undergone by Mary Bateman under Dr. Audrey Moores' supervision. Other contributors to the presented research are Dr. Annie Castonguay, Dr. Mitra Masnadi (post-doctoral fellow, Moores and Braidy group), Yuting Feng (undergraduate student, Moores group) and Prof. Dusica Maysinger (McGill Pharmacology) and their role is outlined below.

Chapter 2: Dr. Annie Castonguay helped with research conduct. The characterization of the nanoparticles presented in the chapter was performed by Dr. Mitra Masnadi.

Chapter 3: Dr. Annie Castonguay and Yuting Feng helped with research conduct. Prof. Dusica Maysinger of McGill Pharmacology supervised the toxicity tests. The characterization of the microparticles presented in the chapter was performed by Dr. Mitra Masnadi.

Chapter 4: Dr. Mitra Masnadi and Yuting Feng helped with research conduct. The characterization of the microparticles presented in the chapter was performed by Dr. Mitra Masnadi.

Table of Contents

List of Figures

List of Schemes

List of Tables

List of Graphs

Chapter 1- Introduction

In the world of green chemistry, catalysis is a central concept that touches on several principles. The ability to decrease the amount of waste and energy required through increased efficiency has been invaluable in the field of synthetic chemistry. Some reactions that were previously found to be not feasible due to high temperatures and pressure required are now possible with the use of a catalyst. One relatively new example is the Cu(I)-catalyzed azide-alkyne click reaction (CuAAC), which is a 1,3-dipolar addition.

1.1 Cu(I)-catalyzed azide-alkyne cycloadditions (CuAAC)

Before the discovery, Rolf Huisgen found the reaction between an azide and alkyne would occur at elevated temperatures and pressures and would yield a mixture of regioisomers[1]. Both Meldal and Sharpless independently found that in the presence of Cu(I), not only could the reaction conditions be dramatically decreased to room temperature and ambient pressures, with shortened reaction times but exclusively the 1,4-disubstituted product forms.[2] Furthermore, it was found that the reaction is robust in terms of steric and electronic properties of the functional groups attached to both the azide and alkyne. It should be noted that only terminal alkynes are able to react due to the nature of the mechanism involving copper acetylides[3].

A wide variety of solvents, both organic and aqueous, can be used by simply varying the method in which Cu(I) is introduced to the system. In the case of using organic solvents, Cu(I) salts should be used in conjunction with a base (such as DIPEA). This is to prevent the formation of unreactive polynuclear copper(I) acetylides, facilitate the coordination of the azide to copper center at the ligand exchange step, and increase the solubility of the copper complex to deliver higher concentrations of the necessary Cu(I)-species as well as help with the formation of the acetylide anion[3]. Reactions conducted in aqueous media utilize Cu(II) salts in the presence of a reductant which generates the Cu(I) ion in situ. Through the work of Folkin and coworkers[4], it was

found that either copper sulfate pentahydrate or copper acetate accompanied with sodium ascorbate was the best alternative to oxygen free conditions. Moreover, using this method in with water as a solvent is the most accepted and straightforward manner of preparing 1,2,3-triazoles. Water has been found to stabilize the reactive states of copper(I) acetylides especially when formed in situ.[3] This reaction has had so much success not only due to its robustness, efficiency and large scope but also the incredible stability of the resulting 1,2,3-triazole product. It is inert to oxidation, reduction and hydrolysis.The discovery of CuAAC has been widely applied in many fields of chemistry, such as synthesis and medicinal chemistry, molecular biology, and materials science. For instance, in medicinal chemistry, CuAAC is used in the modification of natural products and pharmaceuticals for enhancement of specific parameters such as solubility or bioavailability, attaching labels such as fluorophores or biotins and diversifying drug structures.[1] Other applications include synthesis of dendrimers and polymers, macrocyclic compounds, conjugation of carbohydrates and peptides, DNA and nucleotides, virus tracking, and modification of surfaces such as nanoparticles.

1.1.1 CuAAC stabilizing ligands

The use of stabilizing ligands for Cu(I) has been studied for various classes of ligands. The issue with Cu(I) is its thermodynamic instability which leads to potential oxidation or disproportionation. To maintain the concentration of the catalytically active Cu, nitrogen-containing ligands, such as amines, pyridines and polytriazoles are used, which are very efficient at stabilizing Cu(I). Well known stabilizing ligands, such as tris(benzyltriazolylmethyl)amine (TBTA) which contain three triazole groups, are frequently used after discovery by Fokin et al[5]. This is interesting because, the result of CuAAC reactions yields products containing triazoles, which implies that Cu chelation to the end product is inevitable. The review by Schibli et al[2] explains that Cu(I) chelates mostly to the *N3* position, but has also been found to chelate to *N2* and *C5*.

1.1.2 CuAAC mechanisms

In 2013, Fokin et al[6] were able to further elaborate on the homogeneous mechanism of the CuAAC reaction. Previously, Sharpless and coworekrs reported[4] that solely a copper acetylide intermediate was formed after deprotonation of the alkyne's acidic terminal hydrogen. This step was second order with respect to Cu. The Cu has a partially negative charge which coordinates to the positively charged nitrogen in the azide dipole, shown in Figure 1.1a. The Cu affects this cycloaddition step through weak π-interactions with the alkyne. What was unknown was the identity and nuclearity of the Cu and whether another Cu species coordinates. In Fokin's newly proposed mechanism, one of the key steps, the formation of Cu-acetylide, was formed then isolated and put in the presence of benzyl azide and additional Cu to yield the triazole product. Without the addition of the additional Cu, no reaction was seen. Therefore, it can be hypothesized that two copper atoms are required, where the second copper atom π-bonds to the triple bond. Through isotope labeling experiments, the two Cu centers were found to form a bridging dicopper μ-acetylide. However the roles of both Cu atoms in the formation of the triazole are interchangeable. Overall, the required steps are the following: 1) in situ formation of σ-bound Cu-acetylide; 2) π-bonding of a second copper atom, being the catalytically active species; 3) coordination of the organic azide to the π-bonded Cu; 4) loss of both Cu atoms forming the triazole product.

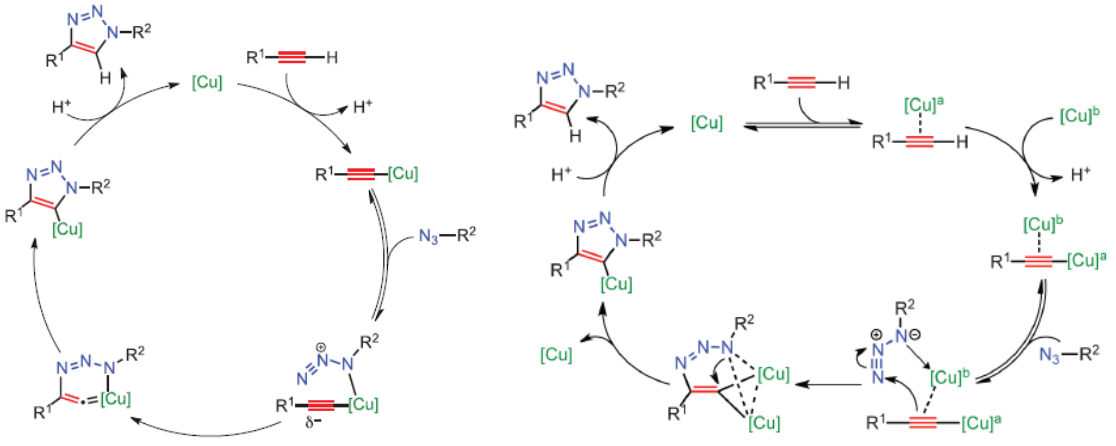

Figure 1.1a,b. a) Previously reported mechanism containing only one Cu center (left); **b)** Most recent mechanism containing two Cu centers (right).

Recently, Scaiano and coworkers[7] proved that CuAAC using CuNPs could also proceed in a purely heterogeneous fashion, with no catalytic contribution from potential leached Cu species, through single-molecule fluorescent studies. By using an alkyne conjugated to a donor dye and an azide conjugated to an acceptor dye, they could employ FRET energy transfer and monitor the acceptor emission by single-molecule spectroscopy. Based on the analysis of the bursting spots from fluorescence versus time, it was concluded that these bursting events were localized next to the catalyst. This implied a heterogeneous mechanism as opposed to bursting events located away from the catalyst which would imply leaching of Cu ions leading to a homogenous mechanism.

1.2 Toxicity of Cu(I) in biological systems

While Cu contamination in the product can be removed by several methods such as extractions, washing with EDTA solutions or ammonium salts and metal scavenger columns, there are instances where Cu removal is not practical or possible. Biological systems constitute an example where, depending on the system and whether it would be conducive to in vivo studies, Cu(I) removal is not practical. Cu(I) has been found to be toxic to biological systems. While exact concentrations for toxicity vary based on the system, the recommended health standard level for Cu in biologically relevant material should be below 15ppm[8]. Although copper-binding to specialized proteins and free amino acids is as an important mechanism for prevention of oxidative damage, under oxidant stress, Cu is released and can catalyze the formation of highly reactive oxygen species (ROS), such as hydroxyl radicals[9]. This leads to initiate oxidative damage of many biological targets and interference with important cellular events[10]. A study performed by Song and coworkers[11], probed the toxicity of CuNPs, CuMPs and leached Cu^{2+} ions in mammalian and piscine cells (e.g. fish cells). What was found was the morphologies, ion release and size of the particles all affected toxicity in these cells. In general, the larger MPs were found to be less toxic than their NP counterpart. Also, a morphology change from spherical nanoparticle to nanorod resulted in less toxicity to both mammalian and

piscine cells for nanorod CuNPs. This was attributed to the net surface area of the spherical NPs being larger, thus having a higher dissolution ability compared with the rod-shaped NP of the same size. Finally, leached Cu^{2+} was found to be toxic only to the mammalian cells, where the smallest sized NPs leached the most and were the most toxic, compared to a $Cu(NO_3)_2$ standard. This toxicity was found for all NP sizes except the nanorods. The nanorods were also found to have the least amount of leaching after 24h.

1.3 Strain-promoted azide-alkyne cycloadditions (SPAAC)

The utility and versatility of click reactions has been well established, yet in the context of biological systems, where the bioorthogonality of the reaction is an attractive quality, it has not been fully exploited due to the toxicity of Cu(I) in these systems. An alternative reaction developed recently, is the strain-promoted azide-alkyne cycloaddition (SPAAC). First discovered by Bertozzi and coworkers[12], this reaction involves the use of a strained alkyne, typically strained within a ring, and an azide, as shown in Figure 1.2. The reaction works because of the ring strain that is released in the cycloalkyne upon reaction with an azide. In practice, cyclic structures containing less than eight atoms are avoided due to instability from polymerization. Cyclooctynes are generally used due to their stability while maintaining the reactivity required. There are, however, drawbacks to SPAAC. Firstly, building molecules that contain ring strain, about 18kcal/mol, into the system can be challenging. The strain needs to be introduced at a stage where its functionality won't be compromised by other side reactions, due to its reactive nature.[13] Furthermore, the synthetic complexity rises when parameters such as solubility or reaction rates come into play. Heteroatom-rich systems have been developed to increase solubility in water[14], or addition of fluorines to the ring for increase in reaction rate[15]. From a synthetic standpoint, these approaches are much more complex than utilizing readily available, stable terminal alkynes.

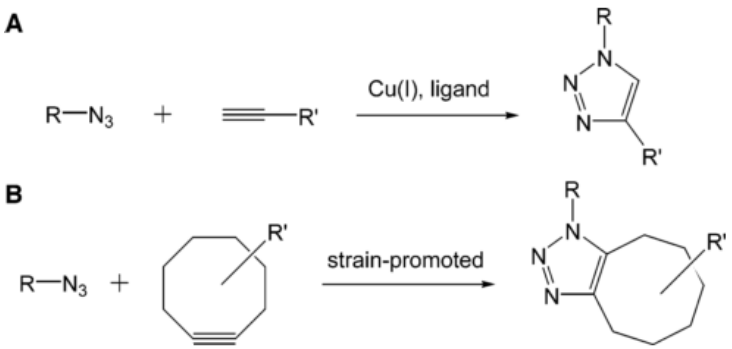

Figure 1.2. A) Comparison of Cu(I)-catalyzed azide-alkyne cycloaddition (CuAAC) of an organic azide and a terminal alkyne (top); and **B)** Strain-promoted azide-alkyne cycloaddition (SPAAC) of an organic azide and cyclooctyne (bottom). Image taken from Bertozzi and coworkers[12].

1.4 Use of nano-sized heterogeneous catalysts for CuAAC

We have discussed the issues of homogeneous CuAAC, and the idea that Cu(I) readily chelate to triazoles. If we could minimize the contact between the Cu-containing catalyst and the product, perhaps the amount of Cu contamination could be minimized. Since homogenous systems require the catalyst to be in the same phase as the reactants, where they are generally dissolved together in a solvent or neat conditions, one could imagine a heterogeneous system instead. The active catalyst would be in the solid phase and the reaction could therefore occur at the surface. Nanoparticles offer an opportunity for accessing active heterogeneous catalysts, as their surface area is higher compared to bulk or microparticulate systems. Nanoparticles are more amenable to separation, as larger ones can be directly filtered off and small ones supported. This avoids the need for lengthy Cu removal through methods such as scavenger columns, dialysis, precipitation or ultrafiltration. However nanoparticulate systems do also lead to leaching Cu ion and thus Cu-based toxicity. In the same study by Song and coworkers[11], it was found that the Cu NPs had the most Cu ion leaching in the first 24 hours. For example, the 25nm CuNPs had leached 70-80% of its total leached Cu in 24 hours. Therefore, the use of NPs as heterogeneous catalysts has not demonstrated yet it could Cu ion leaching.

This leads to the question of whether these nanoparticulate systems are truly heterogeneous or if leached molecular Cu species are responsible for catalyzing CuAAC.

A recent study published in the Scaiano group[7] proved a heterogeneous mechanism for CuNPs in CuAAC through single molecule fluorescent studies. They were able to show that the leached Cu from CuNPs was not responsible for catalysis. This is an important revelation in terms of reaction mechanics but does not address the issue of metal ion leaching. Since triazoles stabilize Cu(I), leaching would be difficult, if not impossible, to inhibit. The ideal situation would be to have the catalyst able to retrieve, or allow retention of its leached Cu. This concept has been probed, but in a completely different field, groundwater remediation, which will be discussed in the next section.

1.5 Nano-sized Fe NPs for metal remediation

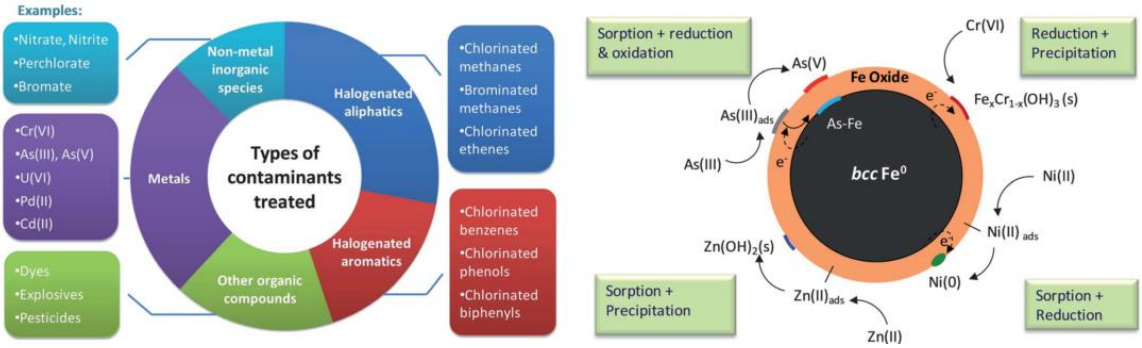

Figure 1.3a, 1.3b. a) Outline of the types of contaminants that can be treated with Fe NPs (left); **b)** The mechanism of possible methods of reduction of metal contaminations by Fe NPs (right). Image taken from Yan et al.[16]

Fe NPs are the most extensively used nanomaterial in groundwater remediation of heavy metals[16], as well as many other types of contaminants, as shown in Figure 1.3a. This process involves the surface adsorption of ions onto the iron oxide shell. Through this interaction, metal ions are reduced to their elemental form by electrons supplied from the iron core. Any metal that has a suitable reduction potential (e.g. Cu^{2+} has a reduction potential of +0.34V) can be reduced by Fe^0 but it is imperative there is a surface interaction between metals. This allows for adsorption of the metal of interest which can then be removed with the FeNPs, as opposed to simply reduced and left behind.[17] A schematic of the reduction of metals ions by Fe NPs is shown in Figure 1.3b.

As a simplistic example to probe how well these FeNPs work in removing heavy metals in water, work done by Sampaio et al[18] showed that using FeNPs to remove Cu^{2+} from a 50ppm solution was successful, where they measured 100% uptake of Cu from the solution after treatment with FeNPs. It should be noted that the pH needs to be basic because the OH groups on the surface of the FeNPs (in the form of FeOOH) need to be deprotonated to facilitate coordination of the metal ions[19]. Veinot et al[17] demonstrated that they were able to reduce the amount of Cu^{2+} in solution from 129ppm to 28.7ppb. Interestingly, they also used the same FeNPs to remove chelated Cu from the product of a click reaction. They found that it took two cycles but they were able to reduce the amount of Cu (found through ICP-MS) from 2026ppm to 15.5ppm, then down to 4.6ppm. These findings demonstrate that FeNPs are not only able to reduce Cu onto its surface, allowing for potential use as a heterogeneous catalyst for CuAAC but FeNPs are magnetic. In terms of catalyst removal, a magnet would simply be required to magnetically retrieve the catalyst after reaction. This concept, coupled with the inherent "greenness" of using a cheap, earth abundant metal as an anchor for another metal destined for catalysis, lead to the work done in our group using copper coated iron nanoparticles (Cu@Fe NPs) for CuAAC.

1.6 Previous work on copper coated iron nanoparticles in catalysis

In the Moores group, we have demonstrated that Cu@Fe NPs could be used as recyclable catalysts in CuAAC[20]. The key component for allowing the reaction to proceed is the presence of Cu(I), namely is the form of Cu_2O as seen by XPS. To contrast, work also published in our group[21] using $CuFe_2O_4$ NPs, where only Cu(II) is found, requires an electron donating ligand, 2,2'-bipyridine, to give full conversion to the triazole product. Attempts to use sodium ascorbate as a mild reductant dissolved the NPs into a homogenous mixture. The Cu@Fe NP catalyst contains a core-shell Fe/Fe_xO_y NPs coated with Cu at various oxidation states. Fe NPs are good supports because of their ability to seed, reduce and support Cu onto its surface. This allows for the generation of the active catalytic species, Cu(I), supported onto the surface of the Fe NPs. Due to the

magnetic nature of the Fe NPs, the removal and recovery of the catalyst is simply done with the use of a magnet without further purification required.

1.7 Copper coated iron particles as catalysts in biological systems

The reason we were interested in having a magnetically retrievable, heterogeneous catalyst for our system was twofold. The central theme of this project is to use CuAAC for biological purposes. Firstly, having a catalyst that can be magnetically retrievable without lengthy purification is ideal for *in vivo* testing where any purification step may be destructive. Secondly, for CuAAC, Cu(I) is the active catalytic species, which is known to be toxic to cells. Having a heterogeneous catalyst minimizes contact of the Cu(I) with the biological molecules because the catalyst is not dissolved or in the same phase as these molecules of interest. Instead, the reaction occurs at the surface of the NP.

The reaction we are interested in probing is the CuAAC between a rhodamine-based azide (**rhod-azide**) and ethisterone **(testo-alkyne)** to produce **rhod-*triazole*-testo**. Ethisterone is testosterone with an extra ethynyl group. Several bimetallic, magnetically retrievable catalysts (Cu@Fe NPs, Cu-Fe MPs, and C@Cu-Fe MPs), will be tested to catalyze this reaction, as shown in Scheme 1.1. The overall goal of this thesis is to produce rhod-triazole-testo using a magnetically retrievable, low leaching catalyst. These classes of catalysts would allow for easy separation of catalyst from product, no purification and low Cu content in the desired product to avoid toxicity problems. The rhod-triazole-testo product would be used for the purpose of developing a ratiometric, nanosensor-based assay for the real-time detection of aromatase activity that is based on FRET measurements. Aromatase and the development of this nanosensor are discussed in the next section.

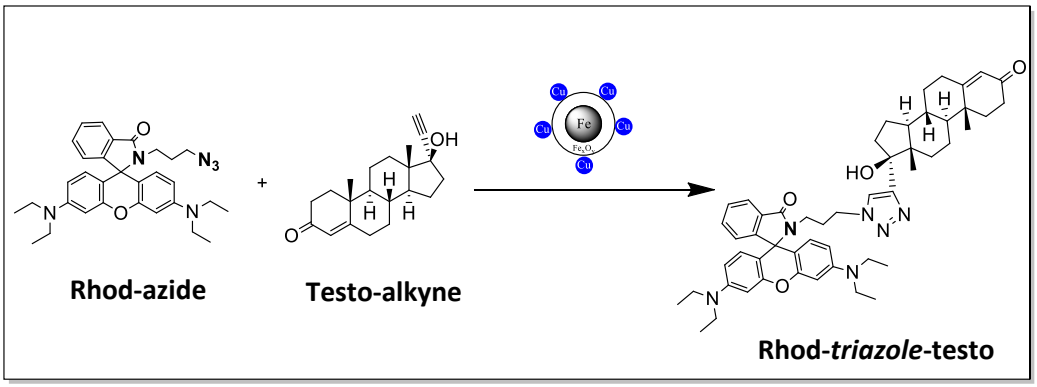

Scheme 1.1. Cu(I) azide-alkyne click reaction of **rhod-azide** and **testo-alkyne** and using our Cu-Fe catalyst.

1.8 Introduction to aromatase (written by Dr. Annie Castonguay)

Aromatase is an enzyme which plays an important role in sexual differentiation, fertility, and carcinogenesis[22] It is a particularly well-studied enzyme because of its key role in the biosynthesis of estrogens from androgens in peripheral tissues and in the central nervous system[23]. An X-ray structure of aromatase is shown in Figure 1.4. Developing an assay to measure the aromatase activity is of importance since it is the target of numerous drugs.

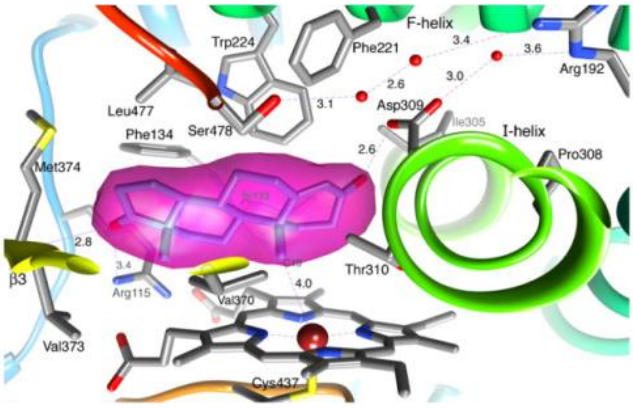

Figure 1.4. X-Ray structure of the aromatase enzyme, showing an androgen (pink) interacting with the catalytic iron site (in red).

1.8.1 Existing aromatase assays

Only a few types of aromatase assays are available and they all have considerable limitations. Briefly, they rely on either radioactive materials requiring

specialized equipment (tritiated-water assay[24]), or hard-to-prepare antibodies with reliable measurements only at low levels of enzyme (ELISA assay[25]) and overall inability to perform real-time analysis. The proposed nanosensor, described in the next section, avoids all of these limitations.

1.8.2 Proposal of fluorescence detected aromatase sensor

The measurement of the aromatase activity will be made possible due to the interaction of two major players: i) fluorescently-labeled estradiol molecules (estradiol*), produced by the action of aromatase on fluorescently labeled testosterone molecules (testosterone*), and ii) estradiol aptamers (nucleic acids or peptides that exhibit affinity and selectivity for estradiol), linked to gold nanoparticles (GNPs), but also coupled to fluorescently labeled complimentary oligonucleotide strands (oligonucleotides*) which emit at a different wavelength (Figure 1.4)[26]. In the absence of aromatase, upon excitation, testosterone* will emit at a specific wavelength, whereas the oligonucleotides* emission will be quenched by the GNPs (by fluorescence resonance energy transfer, FRET). In the presence of aromatase, estradiol* will be produced and will bind to the GNP-linked estradiol aptamers, such that the emission of the estradiol* will become quenched by FRET to the GNPs. Simultaneously, the oligonucleotides* will be released (due to the small changes in the conformation of the estradiol aptamers induced by their interaction with estradiol*) and their fluorescence will no longer be quenched by the GNPs (Figure 1.5). It was previously reported that small conformational changes in the structure of aptamers (e.g. adenosine triphosphate (ATP) and thrombin aptamers)[26-27], disrupt their Watson-Crick base-pairing with oligonucleotides. Monitoring the ratio between the emission peaks of different fluorophores will provide precise and accurate information on the rate of the enzyme activity (fluorescence intensity and lifetime). The efficiency of the nanosensor will depend on the greater affinity of the estradiol aptamers with estradiol*, compared to their affinity with the oligonucleotides*. This will first have to be experimentally

assessed using different amounts of the independently prepared estradiol* with the oligonucleotide*-aptamer-GNP system.

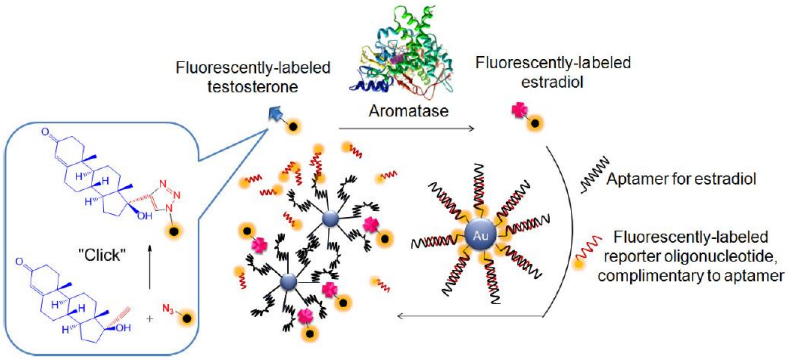

Figure 1.5. Proposed aromatase assay. Interaction between i) a fluorescently-labeled estradiol (produced by the aromatase enzyme from a fluorescently-labeled testosterone, prepared using "click" chemistry), and ii) aptamers for estradiol (linked to GNPs, but also coupled to fluorescently-labeled complimentary oligonucleotides). Release of the fluorescently-labeled oligonucleotides allows the quantification of aromatase activity.

This novel sensitive tool will be able to detect the aromatase activity in real time, in vitro and in vivo, using ratiometric and multiparametric fluorescence measurements (fluorescence intensity and lifetime). The assay does not involve radioactive components or antibodies. Instead, it is based on the modulation in FRET efficiency between fluorescent molecules as donors and gold nanoparticles (GNPs) as acceptors, and requires the use of estradiol aptamers[28], which are less expensive, more stable, more resistant to denaturation, and easier to prepare and purify than antibodies. Moreover, "click" chemistry[29] (Scheme 1.1) is suggested for the preparation of the assay precursor, a labeled testosterone, which makes the excitation/emission fluorescence wavelengths tunable for that assay, given the variety of different fluorescent molecules that can be used. This can be easily done by using ethisterone, a commercially available synthetic progestogen. It is a 17α-ethynyl analog of testosterone that has progestogenic effects similar to those of progesterone which is a steroid hormone involved in the menstrual cycle, pregnancy, and embryogenesis[30]. Since ethisterone already has an ethynyl group, CuAAC are an obvious choice for reaction. Furthermore, CuAAC reactions are considered biorthogonal, therefore, are preferred in reactions involving biological molecules. In terms of the fluorescent azide portion, a

multitude of molecules could be used, where; an azide group can be added. We chose to convert the carboxylic acid group in rhodamine B to an azide group through peptide coupling. The following chapters will outline our attempts to prepare the fluorescently-labelled testosterone (**rhod-*triazole*-testo**) by using copper coated iron particles by CuAAC of **rhod-azide** and **testo-alkyne**.

1.9 References

1. Meldal, M.; Tornøe, C. W., Cu-Catalyzed Azide−Alkyne Cycloaddition. *Chem. Rev. (Washington, DC, U. S.)* **2008,** *108* (8), 2952-3015.
2. Struthers, H.; Mindt, T. L.; Schibli, R., Metal chelating systems synthesized using the copper(i) catalyzed azide-alkyne cycloaddition. *Dalton Trans.* **2010,** *39* (3), 675-696.
3. Hein, J. E., Fokin, V. V., Copper-catalyzed azide-alkyne cycloaddition (CuAAC) and beyond: new reactivity of copper(i) acetylides. *Chem. Soc. Rev.* **2010,** *39* (4), 1302-1315.
4. Rostovtsev, V. V.; Green, L. G.; Fokin, V. V.; Sharpless, K. B., A Stepwise Huisgen Cycloaddition Process: Copper(I)-Catalyzed Regioselective "Ligation" of Azides and Terminal Alkynes. *Angewandte Chemie International Edition* **2002,** *41* (14), 2596-2599.
5. Chan, T. R.; Hilgraf, R.; Sharpless, K. B.; Fokin, V. V., Polytriazoles as Copper(I)-Stabilizing Ligands in Catalysis. *Org. Lett.* **2004,** *6* (17), 2853-2855.
6. Ahmad Fuaad, A.; Azmi, F.; Skwarczynski, M.; Toth, I., Peptide Conjugation via CuAAC 'Click' Chemistry. *Molecules* **2013,** *18* (11), 13148-13174.
7. Letelier, M. E.; Lepe, A. M.; Faúndez, M.; Salazar, J.; Marín, R.; Aracena, P.; Speisky, H., Possible mechanisms underlying copper-induced damage in biological membranes leading to cellular toxicity. *Chem.-Biol. Interact.* **2005,** *151* (2), 71-82.
8. Gaetke, L. M.; Chow, C. K., Copper toxicity, oxidative stress, and antioxidant nutrients. *Toxicology* **2003,** *189* (1–2), 147-163.
9. Song, L.; Connolly, M.; Fernández-Cruz, M. L.; Vijver, M. G.; Fernández, M.; Conde, E.; de Snoo, G. R.; Peijnenburg, W. J. G. M.; Navas, J. M., Species-specific toxicity of copper nanoparticles among mammalian and piscine cell lines. *Nanotoxicology* **2014,** *8* (4), 383-393.
10. Agard, N. J.; Prescher, J. A.; Bertozzi, C. R., A Strain-Promoted [3 + 2] Azide−Alkyne Cycloaddition for Covalent Modification of Biomolecules in Living Systems. *J. Am. Chem. Soc.* **2004,** *126* (46), 15046-15047.
11. Jewett, J. C.; Bertozzi, C. R., Cu-free click cycloaddition reactions in chemical biology. *Chem. Soc. Rev.* **2010,** *39* (4), 1272-1279.
12. Sletten, E. M.; Bertozzi, C. R., A Hydrophilic Azacyclooctyne for Cu-Free Click Chemistry. *Org. Lett.* **2008,** *10* (14), 3097-3099.
13. Agard, N. J.; Baskin, J. M.; Prescher, J. A.; Lo, A.; Bertozzi, C. R., A Comparative Study of Bioorthogonal Reactions with Azides. *ACS Chem. Biol.* **2006,** *1* (10), 644-648.
14. Decan, M. R.; Impellizzeri, S.; Marin, M. L.; Scaiano, J. C., Copper nanoparticle heterogeneous catalytic 'click' cycloaddition confirmed by single-molecule spectroscopy. *Nat Commun* **2014,** *5*.
15. Yan, W.; Lien, H.-L.; Koel, B. E.; Zhang, W.-x., Iron nanoparticles for environmental clean-up: recent developments and future outlook. *Environmental Science: Processes & Impacts* **2013,** *15* (1), 63-77.

16. Macdonald, J. E.; Kelly, J. A.; Veinot, J. G. C., Iron/Iron Oxide Nanoparticle Sequestration of Catalytic Metal Impurities from Aqueous Media and Organic Reaction Products. *Langmuir* **2007,** *23* (19), 9543-9545.
17. Liendo, M.; Navarro, G.; Sampaio, C., Nano and Micro ZVI in Aqueous Media: Copper Uptake and Solution Behavior. *Water, Air, Soil Pollut.* **2013,** *224* (5), 1-8.
18. Li, X.-q.; Zhang, W.-x., Iron Nanoparticles: the Core−Shell Structure and Unique Properties for Ni(II) Sequestration. *Langmuir* **2006,** *22* (10), 4638-4642.
19. Hudson, R.; Li, C.-J.; Moores, A., Magnetic copper-iron nanoparticles as simple heterogeneous catalysts for the azide-alkyne click reaction in water. *Green Chem.* **2012,** *14* (3), 622-624.
20. Ishikawa, S.; Hudson, R.; Moores, A.; Li, C. J., LIGAND MODIFIED CuFe2O4 NANOPARTICLES AS MAGNETICALLY RECOVERABLE AND REUSABLE CATALYST FOR AZIDE-ALKYNE CLICK CONDENSATION. *Heterocycles* **2012,** *86* (2), 1023-1030.
21. Simpson, E. R.; Clyne, C.; Rubin, G.; Boon, W. C.; Robertson, K.; Britt, K.; Speed, C.; Jones, M., AROMATASE—A BRIEF OVERVIEW. *Annu. Rev. Physiol.* **2002,** *64* (1), 93-127.
22. Simpson, E. R., Sources of estrogen and their importance. *The Journal of Steroid Biochemistry and Molecular Biology* **2003,** *86* (3–5), 225-230.
23. (a) Njar, V. C. O.; Grun, G.; Hartmann, R. W., Evaluation of 6,7-Aziridinyl Steroids and Related Compounds as Inhibitors of Aromatase (P-450arom). *J. Enzyme Inhib. Med. Chem.* **1995,** *9* (3), 195-202; (b) Vinggaard, A. M.; Hnida, C.; Breinholt, V.; Larsen, J. C., Screening of selected pesticides for inhibition of CYP19 aromatase activity in vitro. *Toxicol. in Vitro* **2000,** *14* (3), 227-234.
24. Ohno, K.; Araki, N.; Yanase, T.; Nawata, H.; Iida, M., A Novel Nonradioactive Method for Measuring Aromatase Activity Using a Human Ovarian Granulosa-Like Tumor Cell Line and an Estrone ELISA. *Toxicol. Sci.* **2004,** *82* (2), 443-450.
25. Zheng, D.; Seferos, D. S.; Giljohann, D. A.; Patel, P. C.; Mirkin, C. A., Aptamer Nano-flares for Molecular Detection in Living Cells. *Nano Lett.* **2009,** *9* (9), 3258-3261.
26. Nutiu, R.; Li, Y., Structure-Switching Signaling Aptamers. *J. Am. Chem. Soc.* **2003,** *125* (16), 4771-4778.
27. Yildirim, N.; Long, F.; Gao, C.; He, M.; Shi, H.-C.; Gu, A. Z., Aptamer-Based Optical Biosensor For Rapid and Sensitive Detection of 17β-Estradiol In Water Samples. *Environ. Sci. Technol.* **2012,** *46* (6), 3288-3294.
28. Kolb, H. C.; Finn, M. G.; Sharpless, K. B., Click Chemistry: Diverse Chemical Function from a Few Good Reactions. *Angewandte Chemie International Edition* **2001,** *40* (11), 2004-2021.
29. King, T. L.; Brucker, M. C., *Pharmacology for women's health*. Jones and Bartlett Publishers: Sudbury, Mass., 2011.

1.10 Appendix

1.10.1. Equipment used for all experimental in thesis

Particles were characterized by TEM and EDX (FEI CM200 and FEI Tecnai F20 equipped with EDAX detector and FEI Krios, McGill University) equipped with a field-emission gun operated at 200 kV. SEM (Hitachi SEM-S3000N, performed at 10 kV. X–ray Photoelectron Spectroscopy (XPS) was performed on a VG ESCALAB 3 MKII spectrometer (VG, Thermo Electron Corporation, UK) equipped with an Mg Kα source. Reaction product characterization was done by NMR. Nuclear magnetic resonance (NMR) spectra were recorded on a 300 or 400MHz Varian Mercury spectrometer (for ^{1}H). Spectra were calibrated using the residual solvent signal from $CDCl_3$. Cu content in the particles and the reaction product was determined by inductively coupled plasma optical emission spectrometry, ICP-OES (Thermo Scientific-iCAP 6500).

Chapter 2- Use of Copper Coated Nano-Sized Iron Particles (Cu@Fe NPs) for the Click Reaction between Rhod-azide and Testo-alkyne

2.1 Introduction

Previously in our group, Cu@Fe NPs were shown to be efficient and recyclable catalysts for CuAAC[20]. These Cu@Fe NPs were able to catalyze several azide and alkyne combinations with moderate to excellent yields. Moreover, the catalyst could be recycled at least five times under nitrogen atmosphere with no depreciation in yield. Recycling on the benchtop showed a steady decrease in yield after the second run, with a sharp decrease after the fifth run. This was due to the oxidation of the copper on the surface to Cu^{2+} and possibly loss of Cu upon recycling. These limitations were completely circumvented by inert condition recycling. An important advantage of the use of Cu@Fe NPs as a catalyst was the fact they could be used in water with no additives. This is an important consideration since the ideal solvent for biological applications is water. We were encouraged then, to use these particles in our system. This chapter will outline the use of Cu@Fe NPs for the CuAAC of rhodamine azide (**rhod-azide**) and ethisterone (**testo-alkyne**) to form the clicked product rhodamine-testosterone (**rhod-*triazole*-testo)**. This catalyst is composed of a core-shell Fe/Fe_xO_y nanoparticle further coated with Cu at various oxidation states. Fe NPs are good supports because of their ability to seed, reduce and support Cu onto its surface. This allows for the generation of the active catalytic species, Cu(I), supported onto the surface of the Fe NPs. Due to the magnetic nature of the Fe NPs, the removal and recovery of the catalyst is simply done with the use of a magnet without further purification required.

The reason we were interested in having a magnetically retrievable, heterogeneous catalyst for our system was twofold. The central theme of this project is to use CuAAC for biological purposes. Firstly, having a catalyst that can be magnetically retrievable without lengthy purification is ideal for *in vivo* testing where purification may not be ideal. Secondly, for CuAAC, Cu(I) is the active catalytic species, which is known to be toxic to cells[8]. Having a heterogeneous catalyst minimizes contact of the Cu(I) with

the biological molecules because the catalyst is not dissolved or in the same phase as these molecules of interest. Instead, the reaction occurs at the surface of the NP. Based on our need for a heterogeneous catalyst that could have minimal leaching of Cu due to toxicity concerns, we decided to start using Cu@Fe NPs to catalyze the click reaction between a **rhod-azide** (synthesized in our lab) and **testo-alkyne** to produce **rhod-*triazole*-testo**. The resulting coupled molecule is to be used to develop a ratiometric, nanosensor-based assay for the real-time detection of aromatase activity that is based on FRET.

In this chapter, I present the preparation and use of the Cu@Fe NPs for the CuAAC of **rhod-azide** and **testo-alkyne**. The first section describes the Cu@Fe NPs synthetic method, and the characterization of the resulting species. Secondly, basic reaction conditions were established to determine if these particles work for our system. Finally the system was optimized by varying several parameters such as solvent choice and catalyst loading. We will comment on the successes and failures based on the experimental results and couple these with characterization of the Cu@Fe NPs to further understand some of the issues we came across. Scheme 2.1 depicts the CuAAC reaction between **rhod-azide** and **testo-alkyne** to prepare (**rhod-*triazole*-testo**), using our Cu@Fe NPs. This transformation will be the central reaction of interest for this thesis.

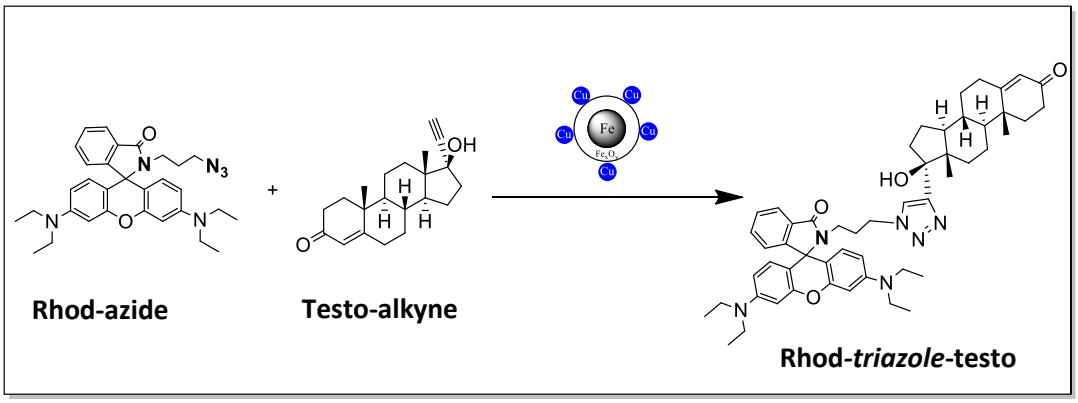

Scheme 2.1. Cu(I) azide-alkyne click reaction of **rhod-azide** and **testo-alkyne** using Cu@Fe NPs.

2.2 Synthesis of rhodamine azide (rhod-azide)

To begin, synthesis of the selected fluorescent azide was necessary. This was undertaken by Dr. Annie Castonguay. Detailed synthetic procedures are outlined in the appendix (Scheme 2.4). In short, there were two steps. The first step was the preparation of 3-azidopropan-1-amine from 3-bromopropan-1-aminium bromide. This azide was then reacted with rhodamine B to yield **rhod-azide**.

2.3 CuAAC of rhod-azide and testo-alkyne – homogenous

In this chapter, all %conversions for the product **rhod-*triazole*-testo** were calculated by NMR using an external standard. See Figure 2.4 and 2.5 in the appendix for details. To ensure that the click reaction was capable of proceeding, the CuAAC reaction was first tested homogenously using CuI/DIPEA in THF, described in Table 2.1.

Reactants	**MW**	**Qnt (mg)**	**mmol**	**eq**	**Mol%**
Rhod-azide	524.66	100	0.12	1	
Testo-alkyne	312.45	60	0.10	1	
CuI	190.45	2	0.01	0.05	**5mol%**
DIPEA	129.25	16.7µL		0.5	
THF		1mL			
%Conversions in 24h: 84% ± 5% (triplicate)					

Table 2.1. Testing the CuAAC between **rhod-azide** and **testo-alkyne**. Reaction conditions for homogenous reaction using 5mol% CuI/DIPEA.

The reaction between **rhod-azide** and **testo-alkyne** proceeded with 5mol% CuI/DIPEA in 24 hours with a yield of 84%± 5%. We could turn to Cu@Fe NPs.

2.4 CuAAC of rhod-azide and testo-alkyne – heterogeneous Cu@Fe NPs

In this section, the preparation of Cu@Fe NPs and its use as a catalyst in CuAAC of **rhod-azide** and **testo-alkyne** are presented. A number of solvents were tested, while noting that THF was mostly successful homogenously.

2.4.1 General Synthesis of Catalyst: Cu@Fe NPs

For the synthesis of Cu@Fe MPs, we used a method previously published in our group[20] with the exception of preparing the particles under Schlenk conditions versus in an anoxic glovebox. The method, in short, involved two parts: first, preparing the core-shell Fe/Fe_xO_y particles and second, addition of $CuSO_4$ to yield the Cu@Fe NPs.

2.4.1.1 Preparation of core-shell Fe/Fe_xO_y NPs

To prepare the core-shell Fe/Fe_xO_y NPs, $FeSO_4 \cdot 7H_2O$ was dissolved in degassed 30% MeOH in water with a stir bar. To this, a solution of $NaBH_4$ in water was added *via* syringe to produce a black precipitate containing Fe NPs. This solution was stirred for 30mins, then washed three times with degassed water and dried under vacuum. The dried Fe NPs were weighed and re-suspended in degassed water.

2.4.1.2 Preparation of copper coated FeNPs (Cu@Fe NPs)

To the re-suspended solution of FeNPs, a solution of $CuSO_4$ was added dropwise using a syringe while sonicating (see appendix for calculation of $CuSO_4$ used based on Fe NP mass). Once the addition of $CuSO_4$ was complete, the resulting Cu@Fe NPs were washed with 30% MeOH in water three times and dried under vacuum and were ready to be used in catalysis. The particles were dried to make weighing easier. The particles were kept in under anoxic conditions in a small glovebox. A complete list of all prepared batches, their %Cu from ICP, and molecular weights can be found in the appendix. A schematic of this synthesis, where a batch Cu@Fe NPs with a Cu-Fe ratio of 2:10 was prepared, is shown below in Scheme 2.2.

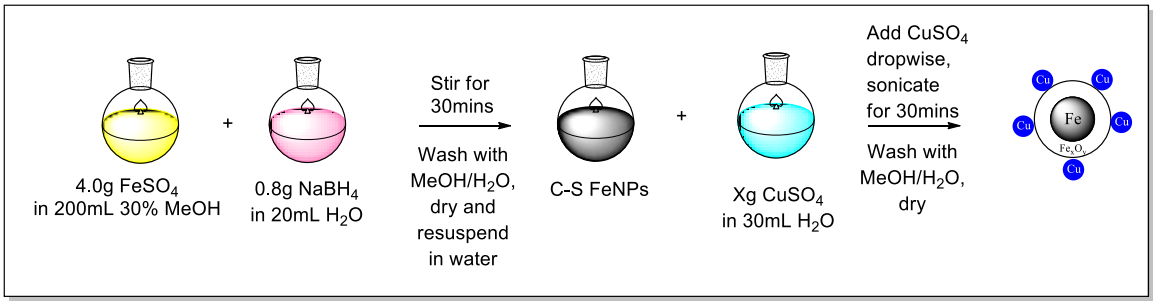

Scheme 2.2. Synthesis of Cu@Fe NPs. Note, this was done in Schlenk to avoid contact with oxygen. The amount of $CuSO_4$ added depends on the amount of FeNPs formed (has been found to vary despite using the same amount of starting material).

2.4.2 Catalysis using Cu@Fe NPs

In order to establish activity, Cu@Fe NPs were first tested as catalysts in large excess, about 500mol%. We began by preparing a batch of ratio 1:10 Cu@Fe NPs as described above. Several reaction parameters were probed: particle storage, particles used for reaction, copper plating ability, solvent, catalyst loading, and Cu/Fe ratio. The following table (Table 2.2) summarizes the options decided upon. Each parameter is discussed in the forthcoming sections of this chapter.

Parameters	Option A	Option B
Particle storage	Dried	Suspended in solvent
Age of Particles	Freshly made	Aged
Copper plating	Reproducible	Varies
Solvent	THF	DCM
Catalyst loading	Stoichiometric	Sub-stoichiometric
Cu/Fe ratio	1:10	2:10, 5:10

Table 2.2. Parameters probed during reaction optimization.

Upon testing several reaction parameters, we rapidly realized that we were faced with major reproducibility issues. Perhaps, some batches had more or less copper than others. We decided to quantitatively measure the Cu/Fe ratio through ICP-MS measurements and use this amount to accurately calculate the amount of Cu we introducing into the reaction. The next section, copper plating, outlines the differences we saw in the amount of Cu from batch to batch.

2.4.2.1 Cu plating reproducibility

Several batches of Cu@Fe NPs were prepared. Their true Cu contents were measured by ICP-MS to determine if 1) there was a drastic variation in the amount of Cu plated from batch to batch and 2) if this difference affects the catalytic ability of the Cu@Fe NPs. To allow for straightforward comparison, the reactions set up using each batch were not changed. Each reaction used the same amount of particles even if there was a variation in the %Cu. We tested the particles fresh in reaction as well as after one day. The following graph, Graph 2.1, outlines the catalytic activity obtained from three batches of Cu@Fe NPs and illustrates reproducibility concerns.

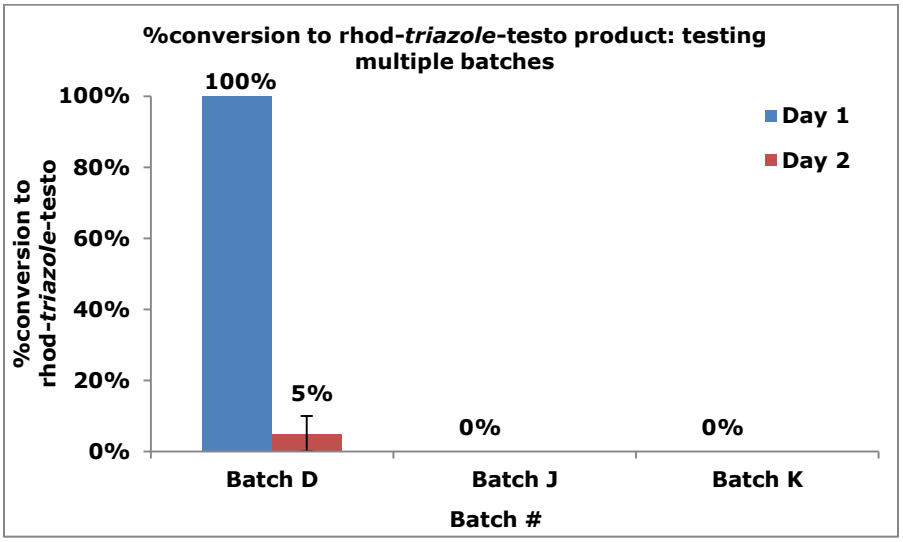

Graph 2.1. Testing three batches of Cu@Fe NPs for catalytic activity in terms of %conversion to **rhod-triazole-testo**. The particles were tested freshly made, Day 1 (in blue) and the day after preparation, Day 2 (in red). This graph demonstrates the lack of reproducibility between batches. Reaction conditions: 0.015mmol **rhod-azide**, 0.06mmol **testo-alkyne** (1:4 ratio), 1.5mL THF (0.010M), 47mg catalyst (Batch D: 930mol%; Batch J: 625mol%, Batch K: 1000mol%), 24h.

Batch D worked well to achieve 100% yield when the particles were used the same day as preparation (Day 1, in blue). However, the same batch of particles used the second day gave an average yield of 5% ± 5%. Furthermore, Batch J and K did not work at all despite attempts to catalyze the reaction the same day and the day after. Based on the %Cu found by ICP, each of the three batches varied in Cu content thus yielding a variety of mol% for each reaction. This did not affect reaction. These results forced us to

reevaluate the reaction conditions and find possible solutions, such as solvent selection, where the interaction of the solvent with the surface of the particle could have some effect on reactivity and Cu/Fe ratio of the particles, where, based on our findings, the Cu content can vary drastically from batch to batch. ICP-MS will be used to determine exact Cu content.

2.4.2.2 Solvent Selection

Under homogeneous conditions, solvent selection in CuAAC is usually simple because solvent polarity has little effect on the cycloaddition rate. Solvents are generally selected based on their ability to solubilize the chosen catalyst, such as non-aqueous solvents with CuI and aqueous solvents with $CuSO_4$/reductant. However, for heterogeneous catalysts, questions about solvents interacting with the surface, especially in the case of high surface area catalysts which rely heavily on the surface for reactivity, need to be taken into consideration. Chanda et al briefly touched on this subject while describing solvent effects on their Cu_2O nanocatalysts. They observed that, while solvents such as EtOH, water and mixtures of the two had no adverse effect on catalysis, solvents such as THF and CH_3CN did not allow for the click reaction to occur. Characterization by SEM of the Cu_2O NPs after reaction in THF and CH_3CN respectively, showed the THF-treated particles were coated in a thick layer of substance, which appeared to block catalytic sites. CH_3CN-treated particles appeared to be highly etched, possibly due to coordination of CH_3CN to the surface Cu atoms due to its affinity to cationic sites. This suggests that solvent choice is very important when doing CuAAC reactions heterogeneously, especially when employing nano-sized catalysts that are dependent on their surface for reactivity. A review written by Dervaux et al[31] suggests the use of CH_2Cl_2, a non-chelating solvent which is a weakly coordinating solvent as an option. As a result, we decided to test CH_2Cl_2 as a solvent for our click reaction.

2.4.2.3 Catalytic tests with CH_2Cl_2

Three freshly-prepared batches (Batch M, Batch N, Batch O), in addition to Batch K were used to test CH_2Cl_2 as the solvent for the reaction between **rhod-azide** and

testo-alkyne. First, a test reaction was done with a decrease in catalyst loading from 1000mol% to 100mol%. Graph 2.2 summarizes the results of these tests.

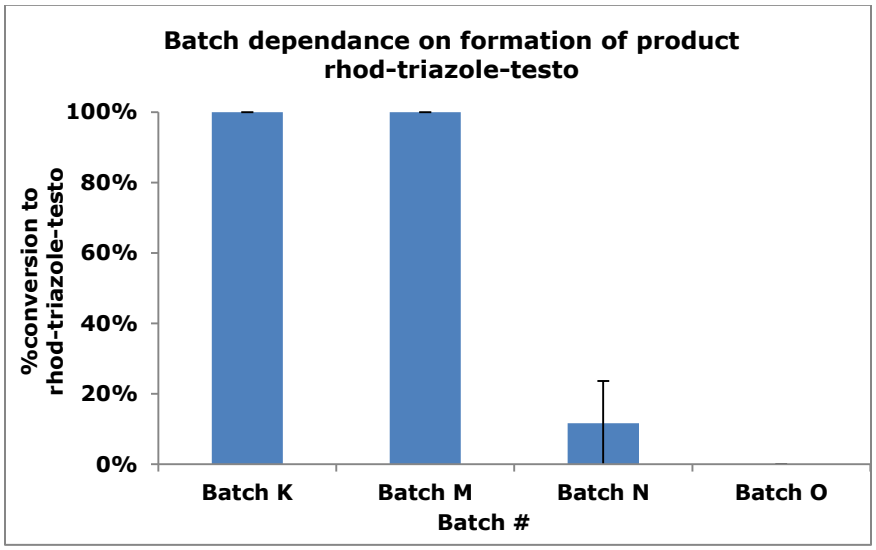

Graph 2.2. Reproducibility of multiple batches prepared for CuAAC to produce product **rhod-*triazole*-testo** using CH_2Cl_2 as a solvent. Reaction conditions: 0.019mmol **rhod-azide**, 0.016mmol **testo-alkyne** (1.2:1 ratio), 1.5mL CH_2Cl_2 (0.010M), 5mg catalyst (Batch K: 100mol% (18.7% Cu); Batch M: 100mol% (19.4% Cu); Batch N: 68mol% (12.3% Cu); Batch O: No ICP was done. Reaction for 24h.

The use of CH_2Cl_2 appeared to be promising, where both Batch K and M of Cu@Fe NPs gave full conversions to the product **rhod-*triazole*-testo** (Graph 2.2). However, two more batches were prepared and gave poor results. Batch N, done in triplicate, gave a maximum conversion of 30% and a minimum of 0%. Batch O showed no conversion at all. This suggests that, although perhaps CH_2Cl_2 was not detrimental to the reaction, there are other factors contributing to the inconsistencies in reaction. In the next section we analyze the possible effects of Cu/Fe ratios in our catalyst preparation and determine if copper coating has an effect on catalytic efficiency.

2.4.2.4 Preparation of Cu@Fe NPs – Cu/Fe ratio during synthesis

Next, we explored the impact of Cu/Fe ratio on catalysis in hope to find the proper conditions to optimize coating efficiency. In this section, we used a different reaction model, with reactants easier to access, in order to probe more rapidly catalytic activity. We used benzyl azide (Bn-N_3) and phenyl acetylene (Ph-CH), affording the

product, 1-benzyl-4-phenyl-1*H*-1,2,3-triazole, called herein **Bn-*triazole*-Ph** (Scheme 2.3). Benzyl azide was prepared from benzyl bromide and sodium azide (see appendix for synthesis) and phenyl acetylene was purchased commercially from Sigma Aldrich.

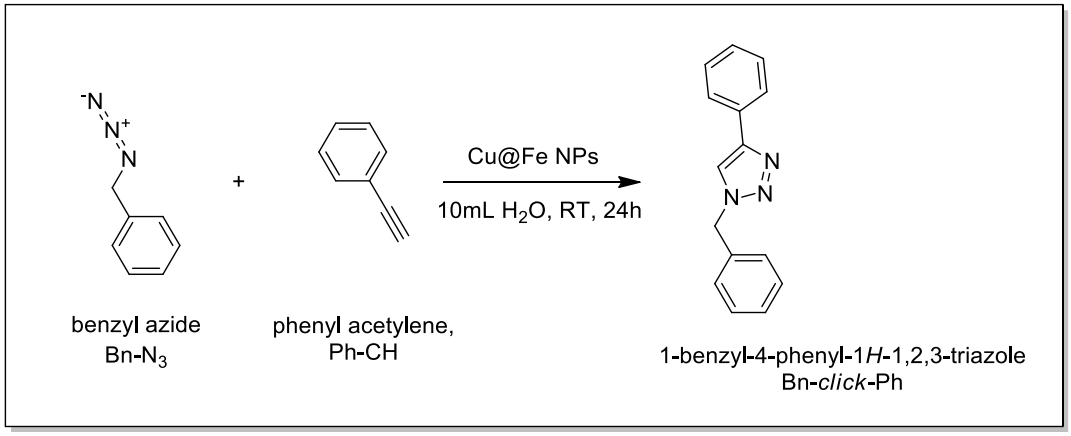

Scheme 2.3. CuAAC reaction between benzyl azide (Bn-N_3) and phenyl acetylene (Ph-CH) for the product **Bn-*triazole*-Ph**.

Preparation of the Cu@Fe NPs with varying Cu/Fe ratios is described in the Appendix. Briefly, the amount of $CuSO_4$ was varied based on the amount of FeNPs used, to obtain three Cu:Fe ratios: 1:10, 2:10 and 5:10. In total, six batches were prepared, with two of each ratio. CuAAC reactions with Bn-N_3 and Ph-CH to form **Bn-*triazole*-Ph** were done and their yields determined by isolation and confirmed by NMR using an internal standard (see the Appendix for method of %yield determination by NMR). The following graph, Graph 2.3, tabulates the results of the reaction yields based on Cu/Fe ratio. There were two batches per ratio (three ratios total) and each reaction was done in duplicate, therefore presented results were an average of four reaction yields.

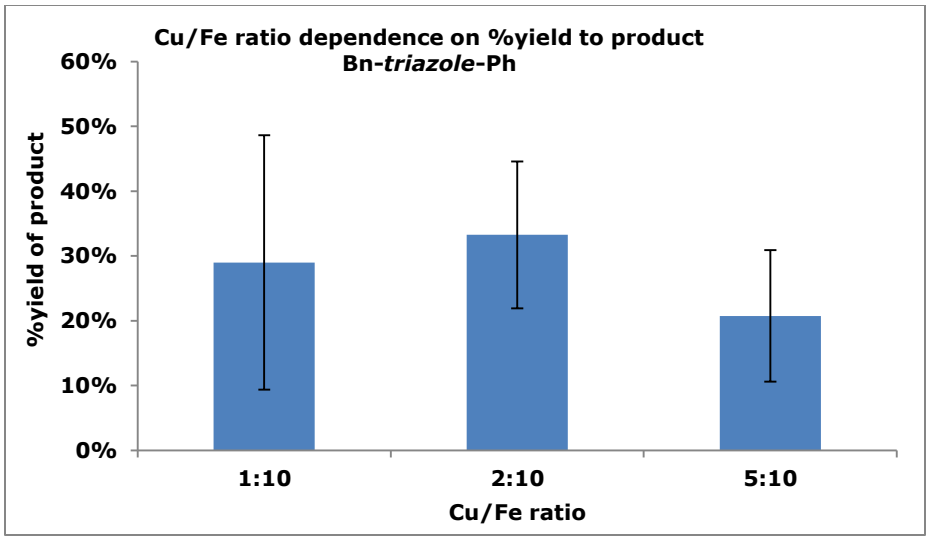

Graph 2.3. Catalytic activity of Cu@Fe NPs Cu/Fe ratios of 1:10, 2:10 and 5:10 in terms of yield. Each ratio represents two batches of Cu@Fe NPs which were used for reactions in duplicate, therefore four an average of four reactions per ratio. Reaction conditions: 1.2mmol benzyl azide, 1.0mmol phenyl acetylene (1.2:1 ratio), 10mL water (0.10M), 5mg catalyst (Cu/Fe 1:10 average 2.5mol% Cu; 2:10 average 4.5mol% Cu; 5:10 average 3.5mol% Cu), RT for 24h. Isolated yields.

Graph 2.3 shows that despite testing several Cu/Fe ratios, this did not appear to aid with increasing catalytic activity for formation of **Bn-*triazole*-Ph**. There was a large variation in %yields for each ratio of catalyst and no real trend for ideal Cu/Fe ratio of catalyst.

After having disappointing results that were difficult to reproduce despite our attempts, we decided to spend time fully characterizing our Cu@Fe NPs. An article published by our group in 2015 on these particles[20] presents a characterization study of these nanomaterials , gives insight into their structure and composition and proposes a growth mechanism to the formation of the Cu@Fe NP. The next section outlines selected results from this publication.

2.5 Characterization of Cu@Fe NPs

Characterization of the Cu@Fe NPs was done using several techniques. Transmission and scanning electron microscopy (TEM), coupled with Energy-dispersive X-ray spectroscopy (EDX), electron energy loss spectroscopy (EELS) spectroscopy and X-ray Photoelectron Spectroscopy (XPS), and ICP-OES (Inductively Coupled Plasma- Optical Emission Spectroscopy) were used. These techniques allowed probing of size, structure,

composition and morphology. Before exposure to copper, a TEM analysis revealed that the individual iron-based particles were approximately 100-150nm in diameter, and were composed of a core of iron zero and a shell of iron oxide. Due to the magnetic nature of these particles, they tend to form chain-like structures. After exposure to copper, there were two major structures observed by TEM: chains decorated with small (around 5nm) copper rich particles and/or hollow tubes. The hollow tubes were found by EDX and EELS to be rich in Cu, whereas the decorated chains were mostly Fe rich, as seen in Figure 2.2b. The hollow nature of the tubes is explained by iron depletion caused by reduction of copper onto the surface and diffusion of Fe cation out. Both these structures can be explained through a growth mechanism shown in Figure 2.3.

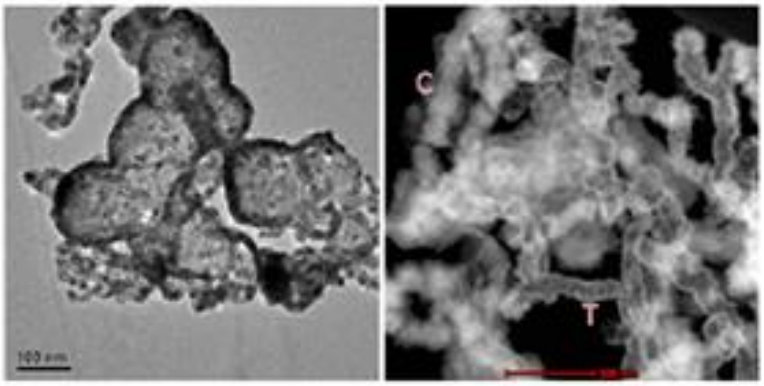

Figure 2.1. TEM (left) and STEM (right) images of Cu@Fe NPs. The "C" indicates portions unreacted chains and the "T" indicates the hollow, tubular structures. Images taken from Masnadi et al[32].

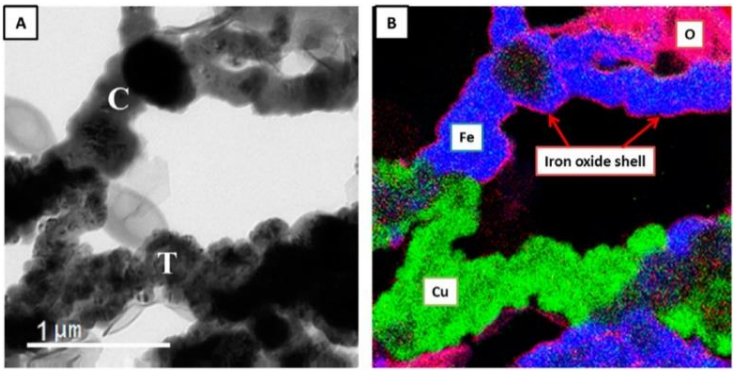

Figure 2.2a, 2.2b. a) Bright-field TEM image of Cu@Fe NPs. The "C" indicates portions unreacted chains and the "T" indicates the hollow, tubular structures; **b)** Corresponding EFTEM analysis: O in red (K edge, [540−560] eV,), Fe in blue (L23, [707−737] eV), and Cu in green (L23, [933−963] eV). Images taken from Masnadi et al[32].

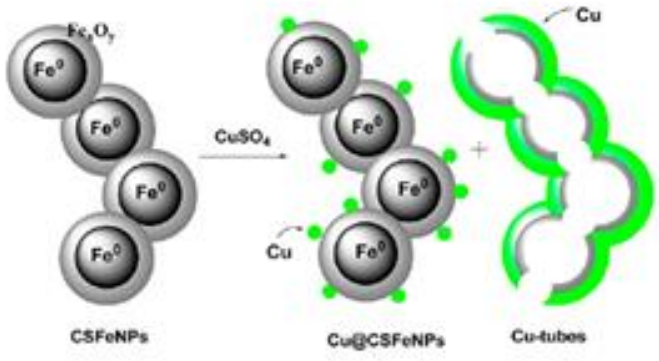

Figure 2.3. Growth mechanism of Cu onto the Fe NPs, where there is first, adsorption of Cu^{2+} followed by reduction of Cu^{2+} at low Cu/Fe, then further reduction of Cu^{2+} and depletion of oxidized Fe at high Cu/Fe ratios. Image taken from Masnadi et al[32]

Both structures were seen regardless of Cu/Fe ratios, but in general an increase in copper led to the presence of more tubes. For this work, XPS was only used to determine the percentage of Cu at the surface of the Cu@Fe NPs. This was compared to the bulk Cu obtained through ICP after complete sample digestion. The general trend was, the %Cu at the surface was higher than the bulk, which is expected since XPS only probes the first 5 to 10nm of the studied sample.

2.5.1 Links between characterization and catalytic activity of Cu@FeNPs

Based on the characterization described above and the observations made during catalysis, there are some conclusions that can be drawn about why there were so many reproducibility issues from batch to batch and within the same batch. The addition of $CuSO_4$ afforded two different structures, the Fe-rich decorated chain-like structure and the Fe-poor hollow tubes, but in proportions that are not easy to predict. The first structure may be more or less Cu covered, and thus more or less catalytically active. Importantly it retained good magnetic properties and thus is likely to be effectively retained upon washings and recycling. However the second structure is Fe-poor and thus was easily lost during these processes. In being discarded, it entrains most of the catalytic copper. Because one cannot control the proportion of copper entering each structure, even samples taken from the same batch may lead to wildly

different Cu amounts in the catalysts. This would also be true from batch to batch. Since the %Cu was calculated based on one aliquot of catalyst digested for ICP, it may not be an accurate representation of the entire sample. Based on these conclusions, we decided to switch to a larger iron particle size that, in theory, should make Fe depletion more difficult and thus lead to structures remaining magnetic. The switch hence was made to commercially available Fe powder which had particle sizes in the micrometer range. The next chapter will outline the use of these micro –sized Fe (Fe MPs) to prepare copper coated iron particles (Cu-Fe MPs) for the use in copper catalyzed click reaction.

2.6 Conclusions

The use of Cu@Fe NPs was successful in some instances but proved to not be reproducible when attempting to catalyze the click reaction between **rhod-azide** and **testo-alkyne** to produce **rhod-*triazole*-testo**. Several parameters such as particle storage, age of particles, copper plating, solvent, catalyst loading and Cu/Fe ratio were investigated. It was found that despite testing these parameters, there were still reproducibility issues not only from batch to batch but within the same batch. Based on the characterization, the conclusion was the addition of $CuSO_4$ may have been causing issues because of the randomness of the Cu plating. This led to certain portions of the catalyst being Cu-rich and Cu-poor and made reproducibility very challenging. Our next step was to use a larger iron particle in hopes of reducing some of this randomness and bringing more reproducibility to the click reaction of interest.

2.7 References

1. Hudson, R.; Li, C.-J.; Moores, A., Magnetic copper-iron nanoparticles as simple heterogeneous catalysts for the azide-alkyne click reaction in water. *Green Chem.* **2012,** *14* (3), 622-624.
2. Ahmad Fuaad, A.; Azmi, F.; Skwarczynski, M.; Toth, I., Peptide Conjugation via CuAAC 'Click' Chemistry. *Molecules* **2013,** *18* (11), 13148-13174.
3. Dervaux, B.; Du Prez, F. E., Heterogeneous azide-alkyne click chemistry: towards metal-free end products. *Chemical Science* **2012,** *3* (4), 959-966.
4. Masnadi, M.; Yao, N.; Braidy, N.; Moores, A., Cu(II) Galvanic Reduction and Deposition onto Iron Nano- and Microparticles: Resulting Morphologies and Growth Mechanisms. *Langmuir* **2014**.

2.8 Appendix

2.8.1 Materials and Reagents

All reactants were purchased from Sigma Aldrich and used as received. Organic azides (benzyl azide and 3-azidopropan-1-amine) were synthesized from the corresponding bromides via previously reported procedures[33]. Rhodamine azide was synthesized by peptide coupling of Rhodamine B and 3-azidopropan-1-amine[34]. All reactions were carried out in an oxygen-free glovebox, except where noted, and all solvents were de-gassed for 20 minutes prior to use.

2.8.2 FeNPs and Cu@Fe NPs synthesis

FeNPs were synthesized following a procedure similar to what had been reported before, where the following quantities can be scaled to produce more or less NPs. In 200mL of 30% MeOH– H_2O, 4g of FeSO4 was dissolved. This solution was reduced with aqueous $NaBH_4$ (0.8 g in 20 mL H_2O) to yield core-shell Fe/Fe_xO_y NPs. These NPs are washed three times with 50mL of 30% MeOH– H_2O then dried under vacuum. The particles are weighed an oxygen-free glovebox and generally yields approximately 800mg FeNPs. As an example, to prepare a batch of 1:10 Cu@Fe NPs, 350mg of FeNPs are suspended in 35mL of water in a Schlenk flask. To this FeNPs suspension, 100mg of $CuSO_4$ was weighed into a Schlenk flask and dissolved in water then added dropwise via canula. The resulting slurry was left to sonicate for 30 minutes after addition of $CuSO_4$. These nanoparticles were then washed three times with 30 mL water, then dried under vacuum. The catalyst is used as a dried powder and weighed directly into the reaction vial.

2.8.3 Reaction set-up

A typical reaction generally uses 1.2 equiv rhodamine azide (rhod-azide) and 1 equiv ethisterone (testo-alkyne) in its respective reaction solvent (THF, DCM etc) at varying concentrations. In general, 1 dram vials are used with or without a stir bar. Reactions are left to stir on a magnetic stir plate for 24 hours unless otherwise noted. To work-up the reaction, a supermagnet is used to separate the Cu@FeNPs from the reaction mixture. Via Pasteur pipette, the reaction mixture is removed from the vial and the particles are washed approximately three times with the same solvent as the reaction and combined with the reaction mixture. The solvent was evaporated under vacuum and analyzed by NMR for %conversion.

2.8.4 List of Cu@Fe NPs batches

Name of Batch	Ratio Cu:Fe	Cu_XFe_{10} by ICP	Cu_1Fe_X (X=) by ICP	MW of Cu_1Fe_X	%Cu
A-susp	1:10	1	10	622.00	9.1%
B-susp	1:10	0.69	14.5	872.89	6.5%
D-susp	1:10	6.5	1.5	149.46	39.4%
D-dried	1:10	2.1	4.8	329.47	17.4%
F	1:10	0.64	15.6	936.12	6.0%
J	1:10	1.3	7.7	493.12	11.5%
K	1:10	2.3	4.3	306.35	18.7%
M	1:10	2.4	4.2	296.23	19.4%
N	1:10	1.4	7.1	462.44	12.3%
T	2:10	2.8	3.6	262.99	21.9%
U	5:10	5.8	1.7	159.83	36.7%
V	1:10	46.8	0.2	75.48	82.4%
W	1:10	15.3	0.7	100.05	60.5%
X	1:10	39.6	0.3	77.65	79.8%
Y	1:10	3.5	2.9	223.10	25.9%
Z	2:10	5.6	1.8	163.27	35.9%
AA	5:10	35.4	0.3	79.32	78.0%
AB	1:10	4.2	2.4	196.51	29.6%
AC	2:10	22.3	0.4	88.59	69.0%
AD	5:10	1.8	5.6	373.80	15.3%

Table 2.3. ICP data for Cu-Fe nano-sized particles. The ratios of Cu:Fe are indicated, along with their ICP data and calculated molecular weight. Note, the batches A, B and D were suspended in water therefore an aliquot was syringed out, water evaporated then digested for ICP. All other batches were used dried

2.8.5 Rhodamine Azide synthesis

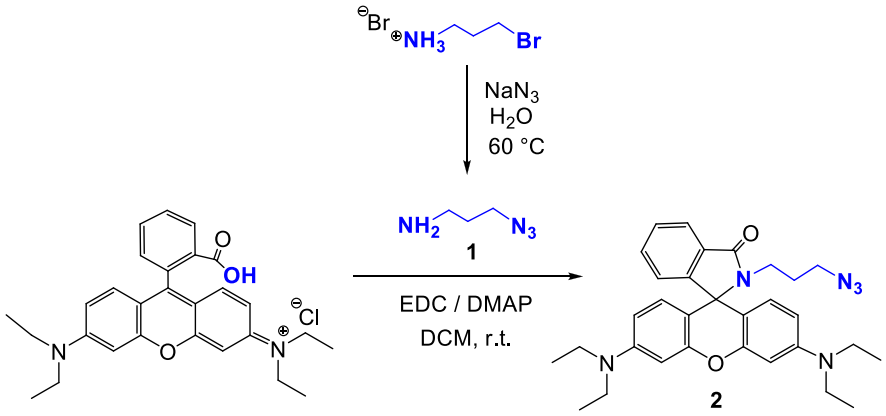

Scheme 2.4. Synthetic route for the preparation of rhodamine azide (**rhod-azide**). All reactions are conducted under nitrogen flow in Schlenk flasks.

Step 1: Synthesis of 3-Azidopropylamine (**1**)

- Commercially available 3-bromopropylamine hydrobromide and NaN_3 (excessive) are dissolved in water and degased under N2 flow
- Heating under N_2 flow at 60°C overnight
- Neutralization of the product with KOH
- Extracted with 100mL ether for 3 times (300 ml in total)
- Dried with $MgSO_4$ and filtered, obtained colorless oil after rotovap

Step 2: Synthesis of Rhodamine-azide (**2**)

- 3-azidopropylamine and Rhodamine B (1:1) are dissolved in DCM then the solution is degased
- Adding 1 eq. DMAP and stir for at least 5 min
- Adding 1.8 eq. EDC
- Reaction mixture stirred at r.t. for overnight
- Product mixture is purified by flash column chromatography with silica gel:
  - After wetting the column with DCM, add the mixture and wait until it enters the gel
  - Pure DCM is used as eluent and only the non-fluorescent form of rhodamine-azide comes out (takes quite long time) → no extraction needed
  - At the final stage, 1:9 acetone:DCM mixture is used to accelerate the elution and both fluorescent and non-fluorescent product will come out simultaneously → extraction needed
  - After rotovap, the non-fluo mixture is extracted by ethyl ether and then filtered

- The solvent is rotovaped and white (sometimes with very light pink color) solid is the final product

2.8.6 Calculation of %conversion and %yield of reaction

To quantify both **rhod-*triazole*-testo** and **Bn-*triazole*-Ph**, NMR yields were used. An detailed outline is given for both products.

2.8.6.1 Calculation for rhod-triazole-testo

To calculate %conversion and %yield of **rhod-*triazole*-testo**, 1H NMR was used. A typical spectrum looks like the following.

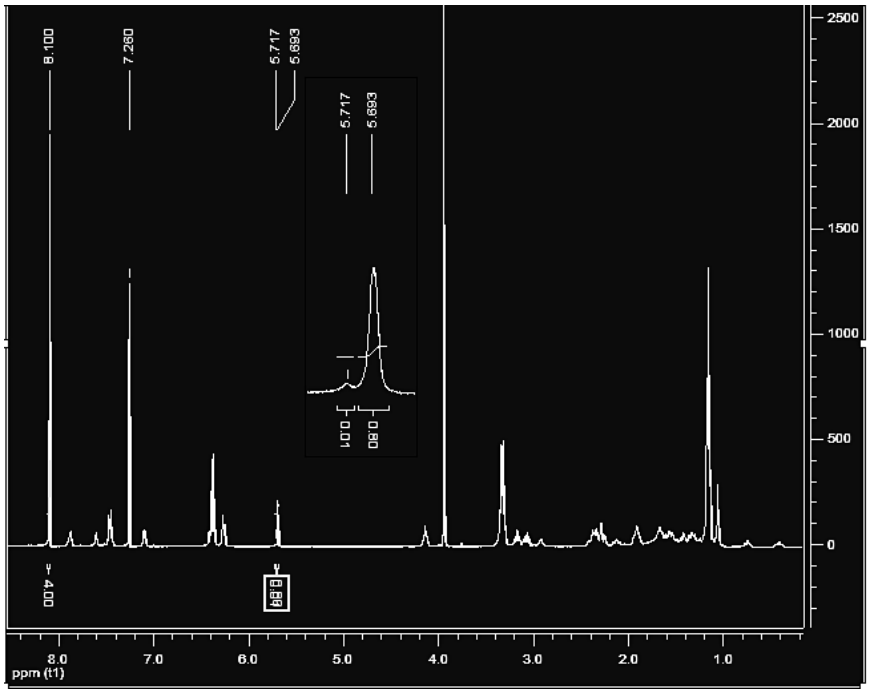

Figure 2.4. NMR of **rhod-*triazole*-testo** containing external standard dimethyl terephthlate.

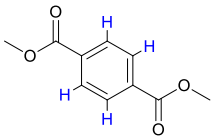

Dimethyl terephthalate
Peak at 8.11ppm
corresponds to 4 protons (highlighted)

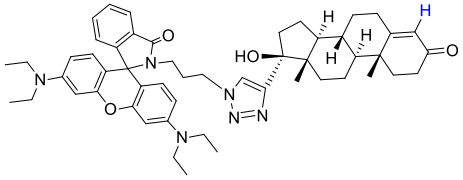

Product of click reaction
rhodamine-testosterone
Peak at 5.69ppm corresponds to allylic proton (highlighted)

Figure 2.5. Structure of external standard dimethyl terephthalate and product rhodamine-testosterone (**rhod-*triazole*-testo**).

NMR spectra were taken using $CDCl_3$ as a solvent on the 200Mz Varian. To calculate %yield of reaction, an external standard was used. In this case, dimethyl terephthalate was added and the peak at 8.11ppm was integrated to four protons and compared to the integrated peak at 5.69ppm corresponding to the one allylic proton from the product **rhod-*triazole*-testo**. A calibration curve was built at various amounts of **rhod-*triazole*-testo** and used to determine the yield of reaction. For calculating %conversion, the peak at 5.69ppm was integrated and compared to the integrated peak at 5.73ppm which corresponds to the same proton as the **rhod-*triazole*-testo** without the **rhod-azide** attached. The integrated area of the product peak divided by the total area occupied by both peaks gives the %conversion of the product. Since **testo-alkyne** is the limiting reagent, it is assumed when the peak at 5.73ppm is not present the conversion is 100% to the **rhod-*triazole*-testo**. A second check is to determine if the peak which corresponds to the alkynyl proton from **testo-alkyne** is present. This peak is located at 2.57ppm and its disappearance also implies the complete reaction of **testo-alkyne**.

2.8.6.2 Calculation for Bn-triazole-Ph

To calculate %conversion and %yield of **rhod-*triazole*-testo**, 1H NMR was used. A typical spectrum looks like the following.

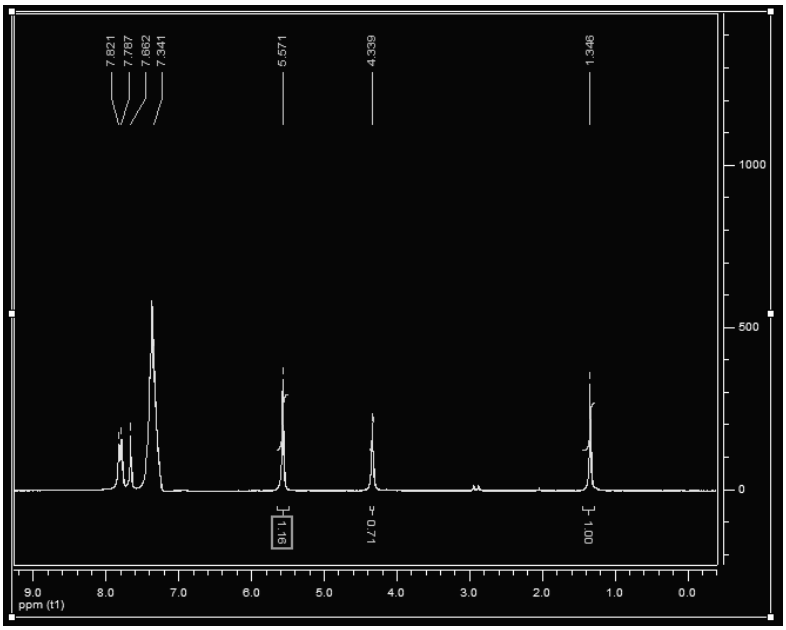

Figure 2.6. NMR of **Bn-*triazole*-Ph** containing external standard 1,3,5-tri-tert-butylbenzene.

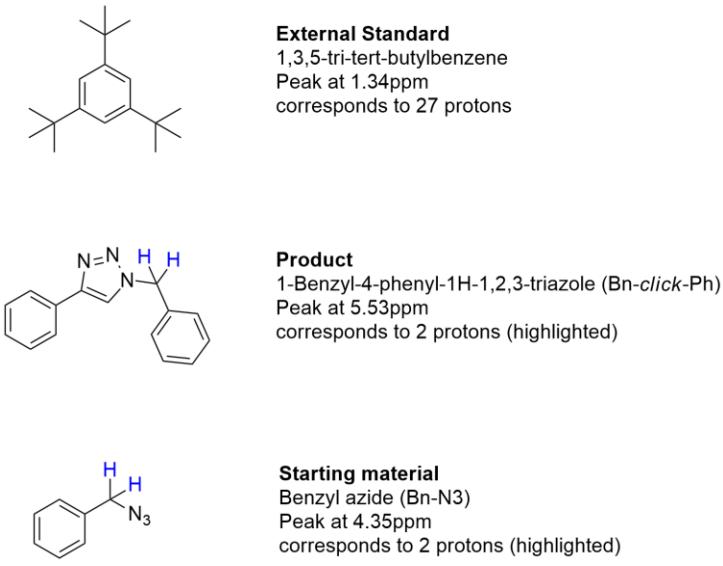

Figure 2.7. Structure of external standard 1,3,5-tri-tert-butylbenzene, product **Bn-*triazole*-Ph**, and starting material benzyl azide (Bn-N_3), found in NMR spectrum.

For calculating %yield of reaction, both crude yields and NMR yields with an external standard were used. The crude yield for this reaction was 160mg. To the reaction mixture, 8mg of external standard was added. The NMR spectrum was taken in $CDCl_3$ on the 200Mz Varian. The peak at 1.34ppm corresponding to the external standard (1,3,5-tri-tert-butylbenzene) was integrated to 1, which corresponded to 27 protons. The peak at 5.33ppm corresponding to the CH_2 group of the product (**Bn-*triazole*-Ph**) was integrated, and gave a value of 1.16 with corresponded to 2 protons. The following calculations were done, as an example, where the isolated yield was 170mg:

$$\frac{\mathbf{8}\boldsymbol{mg}\ (\boldsymbol{external\ standard})}{\mathbf{246.43}\frac{\boldsymbol{g}}{\boldsymbol{mol}}}\ \boldsymbol{x}\ \frac{\mathbf{2}}{\mathbf{27}}\ \boldsymbol{x}\ \frac{\mathbf{1}}{\mathbf{1.16}}\ \boldsymbol{x}\ \mathbf{236.28}\frac{\boldsymbol{g}}{\boldsymbol{mol}}$$

$$= \mathbf{116}\boldsymbol{mg\ product}$$

Scheme 2.5 Calculation of **Bn-*triazole*-Ph** product yield after reaction (by NMR)

In this case, where there was not full conversion and to account for the difference in mass of the isolated product and the NMR yield, a mass was also calculated from the remaining benzyl azide.

$$\frac{\mathbf{8}\boldsymbol{mg}\ (\boldsymbol{external\ standard})}{\mathbf{246.43}\frac{\boldsymbol{g}}{\boldsymbol{mol}}}\ \boldsymbol{x}\ \frac{\mathbf{2}}{\mathbf{27}}\ \boldsymbol{x}\ \frac{\mathbf{1}}{\mathbf{0.71}}\ \boldsymbol{x}\ \mathbf{133.15}\frac{\boldsymbol{g}}{\boldsymbol{mol}}$$

$$= \mathbf{45}\boldsymbol{mg\ \ benzyl\ azide}$$

Scheme 2.6 Calculation of benzyl azide remaining after reaction (by NMR)

The total weight of the product and benzyl azide was 161mg, which is in agreement with the crude yield. To calculate the %conversion, 116mg divided by 161mg is 72% conversion, with a yield of 68% (161mg/236mg), where the theoretical mass was 236mg (based on a 1mmol reaction).

Chapter 3- Use of Copper Coated Micron-Sized Iron Particles (Cu-Fe MPs) for the Click Reaction between Rhod-azide and Testo-alkyne

3.1 Introduction

In the last chapter, Cu@Fe NPs were used for the click reaction of **rhod-azide** and **testo-alkyne** to form the product **rhod-*triazole*-testo**. There were difficulties in reproducing the results from batch to batch as well as within the same batch. In this chapter, Fe NPs were replaced with Fe MPs as a support for copper. These MPs are larger in size therefore the addition of copper should be more homogeneous during galvanic reduction, where it takes more Cu^{2+} to deplete each particle. This would imply more reproducible reactions not only batch to batch but within the same batch. Therefore, each aliquot taken for a reaction should have a more similar composition than in the case of the NPs.

Fe MPs were expected to be great catalyst support because, like their NP counterparts, they are magnetically retrievable, heterogeneous copper-containing catalysts. After the reaction, these particles could be recovered with the simple use of a magnet, and recycled many times. A similar catalyst had been prepared by Kovacs et al[35] and had great success in low leaching CuAAC reactions. These types of catalysts are also of interest because they were active under mild conditions, easily removable from reaction mixtures, and their heterogeneous nature limited the concentration of toxic metal species in solution. By limiting the amount of copper in solution, scavenger columns, dialysis, precipitation or ultrafiltration techniques, commonly used in homogeneous catalysis, may no longer be needed. This is advantageous in biological systems where Cu(I) is toxic to cells and its limited presence is crucial if copper catalysts are to be used.

In this chapter, we outline three different aspects of the click reaction for conversion of **rhod-azide** and **testo-alkyne** to the **rhod-*triazole*-testo** product, catalyzed by the Cu-Fe MPs. First, the synthesis of Cu-Fe MPs is described with full characterization of these particles[32]. Second, the reaction parameters, which affect the

rate and reactivity of the reaction, are probed. These include, solvent choice, catalyst loading in high and low concentration of reactants, use of stir bar and reaction atmosphere. Finally, calculation of Cu content leached into the product **rhod-*triazole*-testo** from the catalyst was performed and compared to a traditional homogenous reaction.

3.2. General Synthesis of Catalyst: Cu-Fe MPs

For the synthesis of Cu-Fe MPs, we used our group's Cu@Fe NPs synthetic method, which utilized Fe NPs instead of MPs to prepare this catalyst. We were encouraged that the switch to MPs would be catalytically active based on the article by Kovacs et al.[35], where they used Fe powder of size 3-6µm in diameter as supports onto which $CuSO_4$ was plated. Our method, in short, involved adding a solution of degassed $CuSO_4$ to a suspension of Fe MPs in degassed water, while sonicating. This solution was then washed and dried under reduced pressure. A complete list of all prepared batches, their %Cu from ICP, and molecular weights can be found in the appendix (section 3.9.4). A schematic of this synthesis, where a batch Cu-Fe MPs with a Cu-Fe ratio of 2:10 wasj prepared, is shown below in Scheme 3.1.

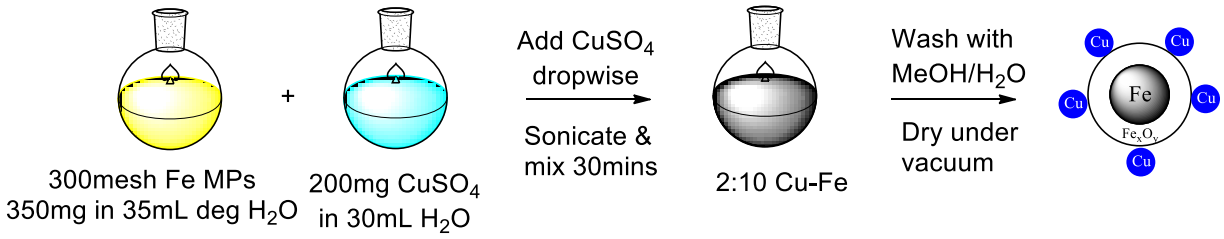

Scheme 3.1. Synthesis of Cu-Fe MPs. Note, this is done in Schlenk to avoid contact with oxygen.

3.2.1 Varying the Cu:Fe Ratio

The Cu:Fe ratio during catalyst preparation was probed to determine if the ratio of Cu added to Fe would affect the catalytic ability of the particles. This parameter was briefly analyzed in the previous chapter with the Cu@Fe NPs. Three ratios were tested: 1:10, 2:10 and 5:10, which describes the amount of $CuSO_4$ added to the Fe MPs. ICP-OES measurements were done to calculate the true %Cu after synthesis of the particles. This

value was used when calculating catalyst loading. Details about how the following parameters were determined can be found in the following sections of the appendix: detailed ratio calculations (section 3.9.1); ICP-OES methodologies (section 3.9.2 for digestions and 3.9.3 for operation) and batch details (section 3.9.4).

3.3. Characterization of Cu-Fe MPs

Full characterization of these Cu-Fe MPs were recently published in our group[36] including mechanisms of growth of Cu onto the Fe MPs. The images were taken by Dr. Mitra Masnadi and used with permission.

Characterization of the Cu-Fe MPs was done using several techniques. Therein, transmission and scanning electron microscopy (TEM and SEM), coupled with Energy-dispersive X-ray spectroscopy (EDX), electron energy loss spectroscopy (EELS) spectroscopy and X-ray Photoelectron Spectroscopy (XPS), and ICP-OES were used. These techniques allowed probing of the size, structure, composition and morphology of the Cu-Fe MPs. Figure 3.1a is an image of what these particles look like together and 3.1b is the EDX mapping of one particle which contains Fe and Cu. Through TEM and SEM, three structures were identified: decorated, microspheres and fern structures. Decorated refers to nanosized copper decorating the surface of iron MPs. Microspheres refer to a nearly-depleted iron core with larger copper particles at the surface. Fern structures refer to large appendages of copper growing from the depleted iron particles. Figure 3.2 summarizes the three structures with images taken from TEM and SEM.

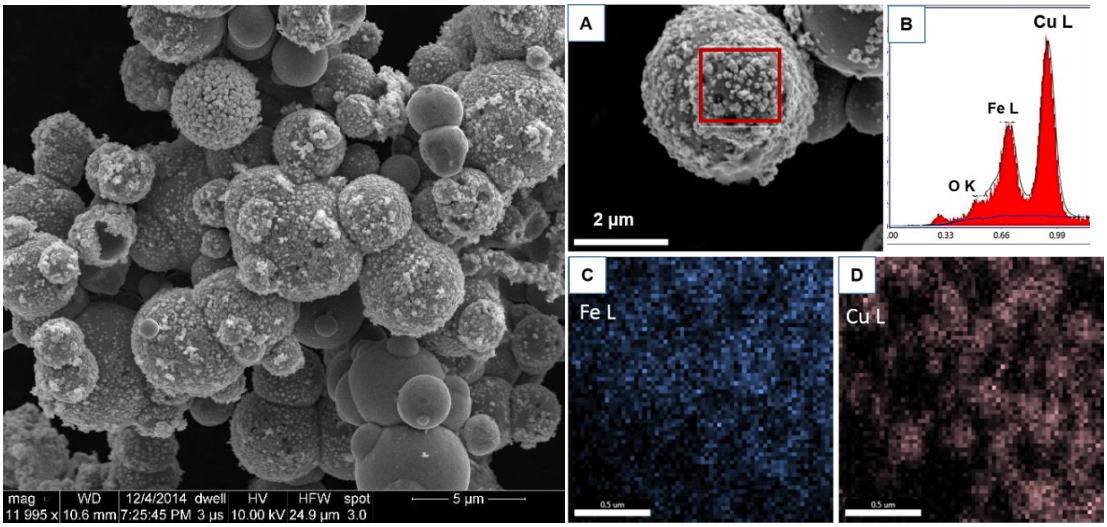

Figure 3.1a, 3.1b. **a)** SEM image of 1:10 Cu-Fe MPs encompassing all of the potential structures (left) and **b)** EDX mapping of one particle (right).

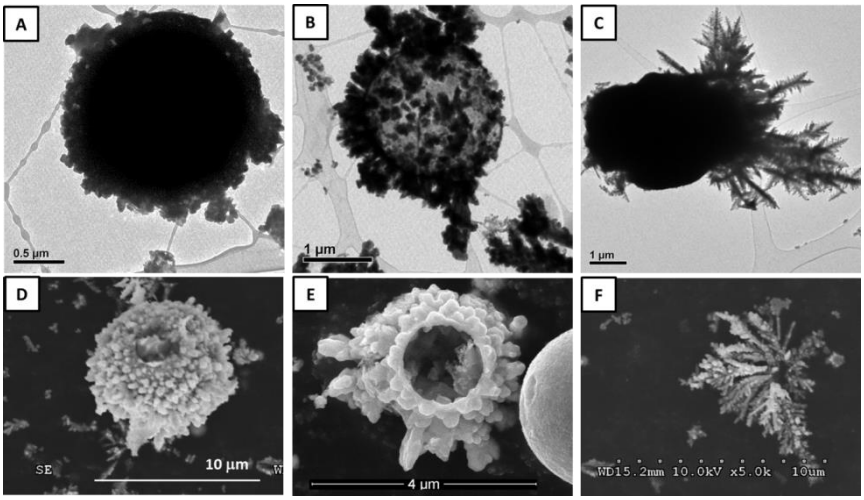

Figure 3.2. TEM (top row) and SEM (bottom row) images from Cu-Fe MPs (Cu:Fe=1:10) show different morphologies present simultaneously for the Cu-Fe MPs. The structures are referred to as **a.)** and **d.)** Cu-Fe MPs; **b.)** and **e.)** Cu-microshell; **c.)** and **f.)** Cu-fern. Image taken from Masnadi et al[32].

All structures were found in all samples, regardless of Cu:Fe ratios, but in general an increase in copper corresponded to an increase in fern structures. The latter structure was expected to follow a different growth mechanism from the decorated or microshells. Moreover, an increase in copper would also show an increase in microshells versus decorated particles, but it would be difficult to properly quantify the proportion of each structure based on the ratio of Cu to Fe.

XPS (X-ray photoelectron spectroscopy) was used to understand the oxidation

states of our copper species. XPS is a surface technique which probes the first 5-10nm of a material. Through sputtering experiments, layers of the surface can be removed to reveal subsurface as well. By analyzing the Cu2p region, we could begin to understand the states of copper at the surface of Cu-Fe MPs. Based on the literature, we discovered that the copper oxidation states of interest, namely Cu^0, Cu^{1+} (as Cu_2O), and Cu^{2+} (as CuO) lead to generation of photoelectrons which are very close in kinetic energies[37]. Specifically, both $2p_{2/3}$ lines in Cu^0 and Cu^{1+} were too close to be differentiated, with kinetic energies of 932.7eV and 932.6eV respectively. $2p_{2/3}$ in Cu^{2+} has a kinetic energy of 933.1eV. Cu^{2+} features a distinct, broad satellite peak, typically called a "shake-up" peak found between the $Cu2p^{3/2}$ and $Cu2p^{1/2}$ peaks, which can be unambiguously attributed. To differentiate between Cu^0 and Cu^{1+}, we had to analyze the Auger region of Cu. The literature gave kinetic energy values of 918.6eV for Cu^0, 916.8eV for Cu^{1+} and 917.7eV for Cu^{2+}. Table 3.1 summarizes the XPS and Auger energies for each oxidation state of Cu. Figure 3.3a, and 3.3b show the XPS of the Cu2p region and an Auger spectrum of Cu, respectively, for a batch of Cu-Fe MPs. Both spectra were recorded by Peng Zhao from the Bruce Koel group in Princeton University.

Cu species	Cu $2p_{3/2}$ binding energy (eV) – XPS	Cu LMM kinetic energy (eV) – Auger
Metallic (Cu^0)	932.7	918.6
Cu_2O (Cu^{1+})	932.6	916.8
CuO (Cu^{2+})	933.1	917.7

Table 3.1. Binding and kinetic energies of Cu^0, Cu^{1+} and Cu^{2+}. Energy values used from Thermo Scientific XPS Knowledge Base (http://xpssimplified.com/elements/copper.php)

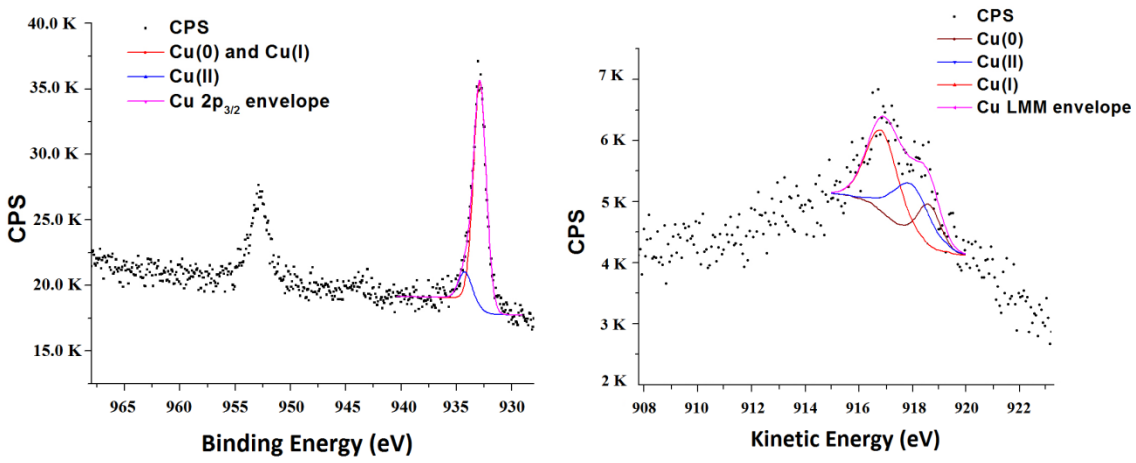

Figure 3.3a, 3.3b. a) XPS spectrum of Cu2p region. **b)** Auger spectrum for Cu.

3.4 Catalytic Tests – Reaction condition optimization

As stated in the introduction and in chapter 2, the reaction we were interested in probing was that of rhodamine azide (**Rhod-azide**) and ethisterone (**testo-alkyne**) to prepare rhodamine-testosterone (**Rhod-*triazole*-testo**), using our Cu-Fe MPs (Scheme 3.2).

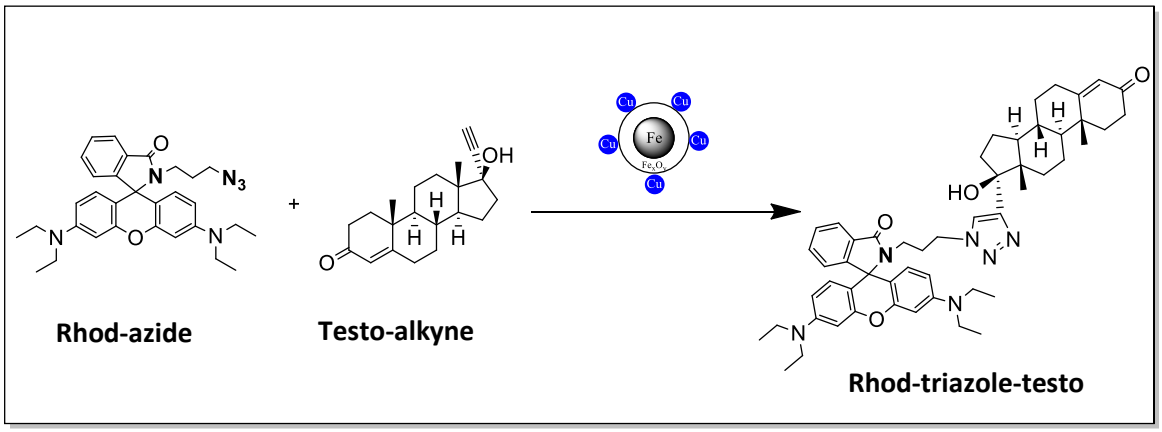

Scheme 3.2. Cu(I) azide-alkyne click reaction of **rhod-azide** and **testo-alkyne** using Cu-Fe MPs to produce **rhod-*triazole*-testo**.

3.4.1 Click Reaction Parameters – Rate of Reaction

To determine if the reaction worked with these Cu-Fe MPs, a reaction was set up where, a near-stoichiometric amount of catalyst was used. A 90mol% reaction was set up using 5mg of Cu-Fe MPs in DCM and the formation of the product, **rhod-*triazole*-testo**, was monitored over time. The following graph, Graph 3.1, shows the %conversion in terms of time of reaction.

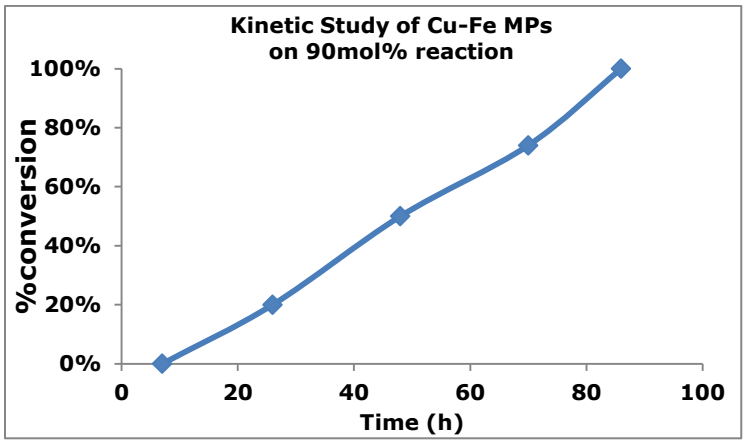

Graph 3.1. Kinetic Study of 90mol% reaction to produce **rhod-*triazole*-testo**. Reaction conditions: 0.023mmol **rhod-azide**, 0.019mmol **testo-alkyne**, 2mL DCM (0.0095M) 5mg Cu-FeMPs containing 17% Cu (90mol%).

Aliquots of approximately 0.2mL were taken over the course of several days until 100% conversion was obtained after 86h in DCM. Graph 3.1 also suggests there is an induction period, where, it takes at least 7 hours for product formation. An extensive study was not conducted to determine the mechanism of catalysis or the nature of the catalyst at the time of reaction. It can be hypothesized that both a homogeneous and heterogeneous mechanism is taking place and that perhaps this induction period potentially involves Cu ion leaching (homogeneous) and/or a change in oxidation state of Cu at the surface (heterogeneous). Further mechanistic studies would need to be conducted to fully understand the nature of this induction period.

Although the reaction worked, reaction conditions optimization was required to reduce the reaction time. The following parameters were tested: Cu/Fe ratio in catalyst,

solvent, concentration of reactants, mol% of catalyst, stir bar and atmosphere. The following sections outline attempts for each parameter.

3.4.2 Ratio of Cu/Fe in catalyst

Based on the characterization of the Cu-Fe MPs, we knew that higher Cu:Fe ratios (such as 1:1) favor more Fe depleted structures in the form of nearly-depleted microshells and fern structures[32]. These structures could thus lead to more copper leaching and less efficient catalyst recovery, either because of they were overall less magnetic or because heavily copper coated systems may be mechanically strained and break apart. Using a low Cu:Fe ratio, such as 1:100 would mean more decorated particles, thus more magnetically active particles . The drawback here was that low loading implied larger amounts of catalyst were needed for our tests. We decided that either a 1:10 or 2:10 ratio would be optimal, because it is in a range where we would still have more iron-rich structures (decorated and partially depleted microshells) while using a manageable amount of catalyst for each reaction. For this project, we have used exclusively the 2:10 particles.

3.4.3 Solvent Choice

Based on literature of heterogeneous catalysts for click reactions, non-chelating and less polar solvents were selected to minimize leaching of copper[31]. We tested two solvents that fit into this category: CH_2Cl_2 and $CHCl_3$, where the latter is a more non-polar solvent with a lower dielectric constant. Both solvents were tested in reactions, where aliquots of the reaction mixture were taken at specific time intervals at analyzed by NMR. The following graph, Graph 3.2, outlines the results.

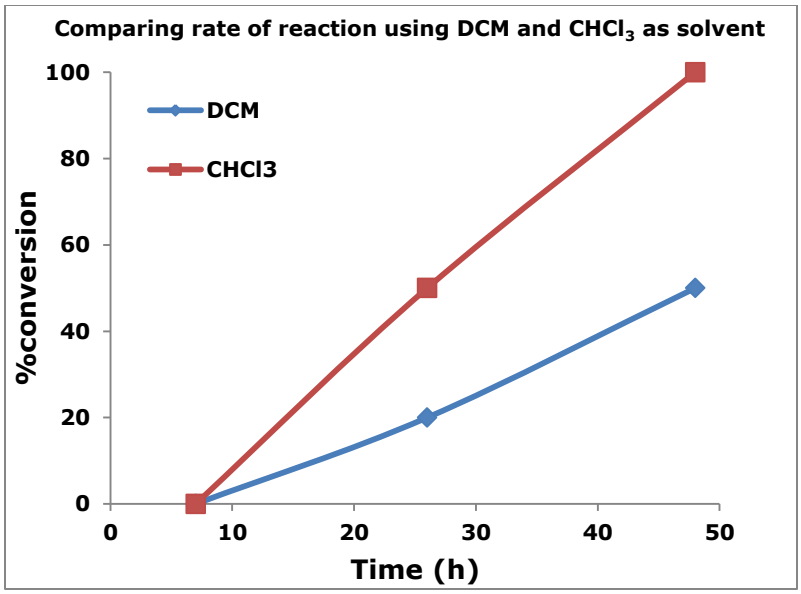

Graph 3.2. Comparing rate of reaction using DCM and $CHCl_3$ as solvent. Reaction conditions (90mol%): 0.023mmol **rhod-azide**, 0.019mmol **testo-alkyne**, 2mL DCM or $CHCl_3$ (0.0095M), 5mg Cu-FeMPs (17% Cu)

It can be seen that the reaction fully converted to the **rhod-*triazole*-testo** product after 48h using $CHCl_3$, whereas after the same amount of time, DCM only converted 50%. While both solvents are chlorinated, $CHCl_3$ is more non-polar with a lower dielectric constant. Furthermore, $CHCl_3$ is slightly more acidic and could interact with the surface making it more active for catalysis. Thus, $CHCl_3$ was selected as the solvent for the reaction.

3.4.4 Effect of Concentration of Reactants and Mol% catalyst on reaction rate

To determine if the concentration of reactant played a role in reaction rate, two types of reactions were compared: “low concentration” where the concentration between 0.040M-0.08M and “high concentration” being a concentration of 0.25M. All low concentration reactions were conducted without a stir bar, simply using the magnetic nature of the Cu-Fe MPs to stir the reaction. For all “high concentrated” reactions however, a stir bar needed to be used.

3.4.4.1 High vs Low Concentration – Time of Reaction

To compare rate of reactions in high and low concentration reactions, four "low" concentration reactions of decreasing mol% were set up and monitored by NMR to completion. Likewise, two "high" concentration reactions were also set up and monitored by NMR. The following graph, Graph 3.3, plots the mol% of catalyst versus time of reaction, where each point is 100% conversion to **rhod-*triazole*-testo**.

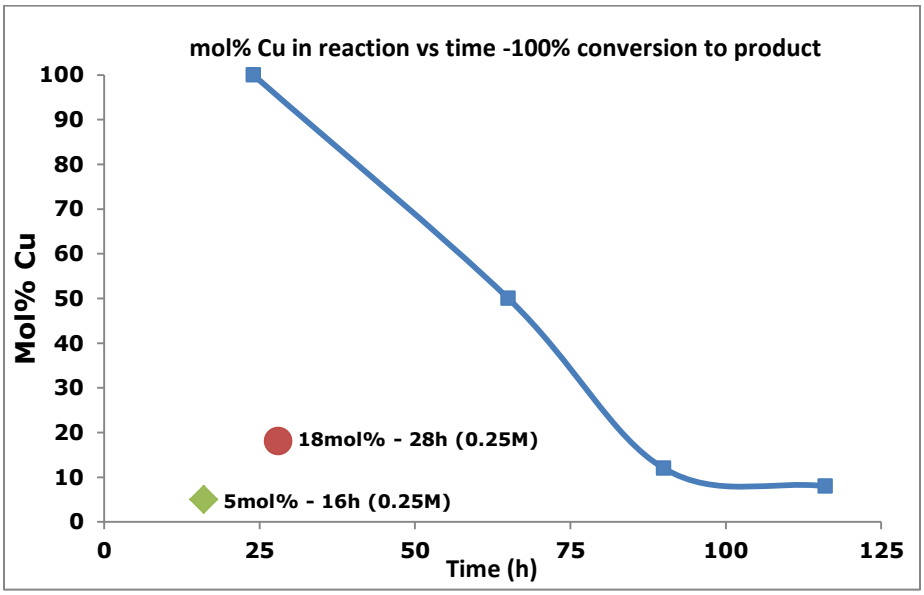

Graph 3.3. Effect of mol% Cu-Fe MPs on time of reaction, probing low vs high concentration of reactants. Reaction conditions for low concentration reactions (blue line): 0.12mmol **rhod-azide**, 0.10mmol **testo-alkyne**, 1mL $CHCl_3$. Reaction time varies based on catalyst loading. *Note: the 8mol% reaction only achieved a 92% conversion. Reaction conditions of 18mol% reaction (high concentration, red dot): 1.20mmol **rhod-azide**, 1.00mmol **testo-alkyne**, 4mL $CHCl_3$, (0.25M), 60mg Cu-Fe MPs (16.7% Cu). %Conversion: 97%±1%; Yield: 100% in 28h. Reaction conditions of 5mol% reaction (high concentration, green square): 0.076mmol **rhod-azide**, 0.064mmol **testo-alkyne**, 0.25mL $CHCl_3$ (0.25M), 4mg Cu-Fe MPs (4.5% Cu). %Conversion: 93%±4%; Yield: 100% in 16h.

It can be seen for the low concentration reactions (0.05M) that, a decrease in mol% Cu was proportional to an increase in reaction completion time. At high concentration (0.250M), however, we did not observe this trend. In fact, the best result was the 5mol% reaction reaching completion after 16h. This can be explained by the fact that there were more azide and alkyne molecules in direct contact with the catalyst which allowed for the reaction to occur much more rapidly.

It should be noted, since a stir bar was used for the "high" concentration reactions and not the "low" concentration, we tested the effect of using a stir bar for a

low concentration reaction. We found only a 20% increase in rate using a stir bar vs no stir bar. This was not sufficient enough to explain the drastic difference between high and low concentration, therefore we could conclude that using a high concentration reaction was ideal and preferred for further catalytic tests.

3.4.5. Atmosphere of reaction

We wanted to test the recyclability of the Cu-Fe MPs with our substrates, as well as the effect of N_2 vs air on the ability of the particles to be recycled. From the previous work done in our group with core-shell Fe-Fe_3O_4 NPs and Cu@Fe NPs, it was known that the presence of air and/or undegassed solvents would quickly deactivate the catalyst and inhibit multiple catalyst recycling runs. We wanted to test this parameter for the Cu-Fe MPs as well. The following graph, (Graph 3.4), demonstrates the %conversions after each recycling run (four recyclings) under an atmosphere of N_2 and degassed solvent and air with undegassed solvent.

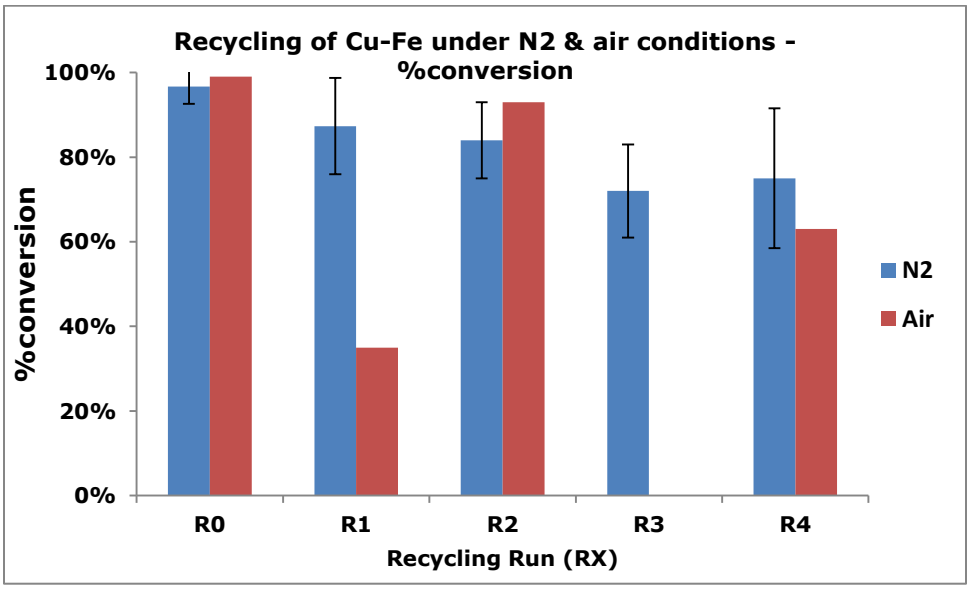

Graph 3.4. Effect of N_2 and air atmosphere in %conversion. Reaction conditions: 0.050mmol **rhod-azide**, 0.042mmol **testo-alkyne**, 1mL $CHCl_3$, (0.042M), 40mg Cu-Fe MPs. Note reactions under N_2 were done in triplicate; reactions in air only once.

Under N_2 atmosphere, recycling four times led to a modest and progressive loss of activity, from 97% at R0 to 75% at R4. Possibly, the drop in activity can be due to loss

of Cu from the catalyst upon recycling. This will be probed more closely in the next section. The reactions under air, however, were very sporadic and didn't follow any sort of trend. Again, analysis of the Cu content leached into **rhod-*triazole*-testo** will be probed in the next section. Based on the %conversions alone, we could conclude that, indeed, the reactions should be set up and recycled under N_2 atmosphere and degassed solvent should be used.

3.4.6. Conclusions: Best reaction conditions for %conversion

To summarize, we have shown the best conditions for the Cu(I) catalyzed click reaction between **rhod-azide** and **testo-alkyne** were a high concentration (0.25M), 5mol% reaction using $CHCl_3$ under N_2 which has a %conversion of 93% ± 5% after 16h. These parameters were found by testing the following parameters: 1) solvent, where $CHCl_3$ afforded reaction rates twice as fast as DCM; 2) concentration of reactants, where a high concentration (0.25M) allowed for lower mol% of catalyst to achieve full conversion faster than if done under a lower concentration. By consequence of doing a high concentration reaction, a stir bar was required to better mix the particles with the reactants. Finally 3) reactions set up under anoxic conditions, where N_2 atmosphere and degassed solvents allowed for more consistent results after several recycling runs.

After optimizing these parameters to obtain a good conversion in a reasonable time, we wanted to turn our attention to the findings in Graph 3.4 which showed a decrease in Cu during recycling under both N_2 and air conditions. We concluded that despite having a heterogeneous catalyst there was still leaching occurring. Section 3.5 of this chapter follows our attempts to understand more about this leaching and find the best conditions limit Cu leaching.

3.5 Click Reaction Parameters – Leaching tests

We hypothesized that despite having a heterogeneous catalyst, there was still leaching of Cu occurring in two ways: 1) Cu ions could leach directly from the catalyst into **rhod-*triazole*-testo**, notably via the triazole ring, which is known to chelate Cu(I)[5, 38] or 2) Cu nanomaterials could either physically detach from the catalyst or be lost during

washings or recovery, due to lack of magnetic properties upon Fe depletion. We used two methods of determining Cu leaching into **rhod-*triazole*-testo**: 1) ICP-OES measurements of **rhod-*triazole*-testo** to determine the exact copper content and 2) blank catalytic tests, where the supernatant of reaction was used as catalyst itself. The success of each catalyst was assessed by both its activity and its limited leaching. Scheme 3.3 outlines the two types of leaching and how we intend on distinguishing between the two through ICP-OES measurements.

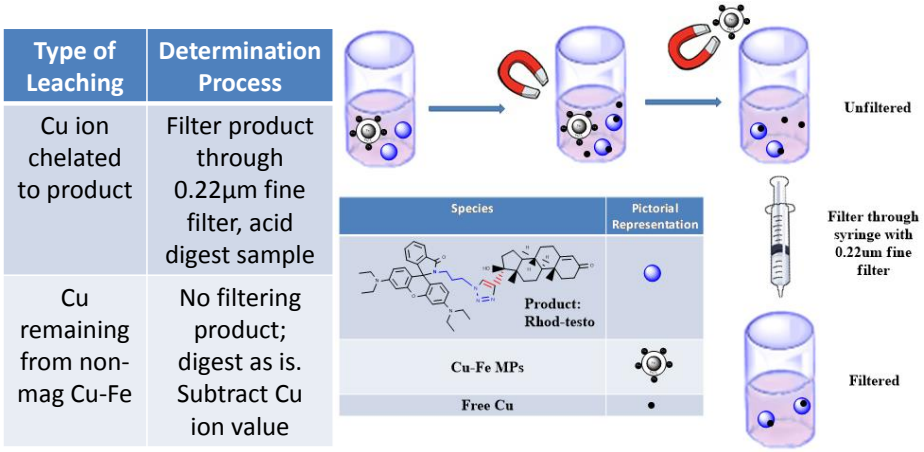

Scheme 3.3. Method used to distinguish between two types of leaching; chemical leaching of Cu ions (filtered) and physical leaching of catalyst containing Cu (unfiltered).

The total amount of leaching was determined by digesting **rhod-*triazole*-testo** directly and subjecting the resulting solution to ICP-OES analysis. This total Cu content was the result of both physical detachment of the Cu from the Fe NP or possibly from loss of magnetism of the Cu-Fe, and Cu ion leaching by chelation to **rhod-*triazole*-testo**. To distinguish the latter phenomenon, the **rhod-*triazole*-testo** (after quantification of %conversion) was dissolved in $CHCl_3$. The solution was then filtered through a 0.22µm fine filter, the solvent evaporated and the remaining **rhod-*triazole*-testo** digested for ICP-OES analysis. The value found for the Cu in the filtered **rhod-*triazole*-testo** was then subtracted from the unfiltered to take into account only one type of Cu leaching.

It should be noted that one of our initial concerns when we decided to further investigate this leaching was the possibility that the leached copper from the catalyst

was catalyzing the click reaction instead of a truly heterogeneous reaction at the surface of the Cu-Fe particles. There are very few articles in the literature that address Cu leaching from a heterogeneous reaction into the supernatant of a reaction.[20] Just recently, an article from the Scaiano group[7] confirmed that Cu NPs catalyzed azide-alkyne click reactions heterogeneously through single-molecule fluorescent experiments and showed the reaction indeed occurred at the surface of the Cu NP. While their system was not identical to ours, we believe this is a good first step to understanding how our particles behave in reaction.

There were some initial questions we had before starting. Based on the Scaiano article, we postulated that there would be more leaching of Cu ions from the Cu-Fe MPs in the presence of the **rhod-*triazole*-testo** and/or **rhod-azide**, **testo-alkyne** in the solvent than just the solvent. If this was true, was the Cu leached either into **rhod-*triazole*-testo** or solvent enough to catalyze a reaction? We thus devised a secondary Cu leaching test, whereby we extracted **rhod-*triazole*-testo** or the supernatant of a reaction and used it as a catalyst in a subsequent one. Conversion served as a probe for the presence of catalytically active copper species and would give also mechanistic indications. This complements the quantitative ICP-OES method.

Furthermore in this section, we investigated leaching of Cu-Fe MPs in the presence of the reactants individually, under N_2 and air conditions, and the effect particle storage had. The overall goal was to determine the optimal reaction conditions that reduced the amount of Cu loss while maintaining high activity.

3.5.1. Cu Leaching into solvent alone, in absence of reagents or products

For this test, we wanted to see how much Cu leached naturally into the solvent without the presence of reactants. As a secondary test, we would use this supernatant to attempt to catalyze another reaction. To do this, we set up three vials, where 5mg of particles were placed into 2mL $CHCl_3$ each. The solvent + particles were stirred on a stir plate (no stir bar) for 90h, and then an ICP was taken of the supernatants of two vials.

The supernatant of the third vial was isolated and used as an attempt to catalyze a reaction. Scheme 3.4 shows an overview of this experiment.

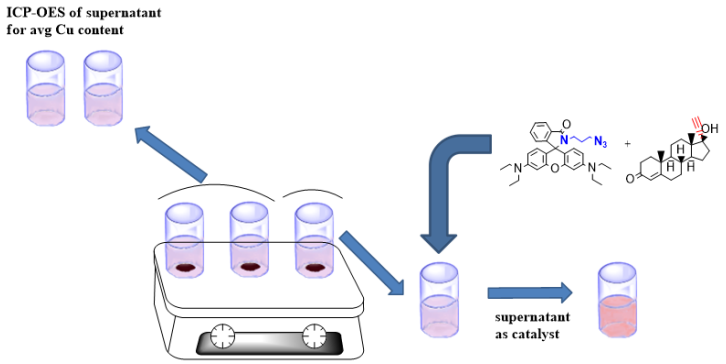

Scheme 3.4. Overview of blank test, where each vial contained 5mg of catalyst + 2mL of $CHCl_3$. Two supernatants were isolated from the particles and analyzed for Cu by ICP-OES, while the third had its supernatant isolated and used as a catalyst for another reaction. The reaction conditions were 0.12mmol **rhod-azide**, 0.10mmol **testo-alkyne**, 2mL of Cu-containing supernatant, reacted for 90h.

The following table (Table 3.2) outlines the amount of Cu found on average in the two supernatants, the subsequent mol% of Cu based on the amount of reactants added and the %conversion.

AVG Cu content in two supernatants	Mol% of Cu in subsequent reaction	%Conversion (by NMR)
59.9±23.0 µg	0.92mol%	0% (<5% by ESI-MS)

Table 3.2. Content of Cu in supernatant, corresponding loading in the secondary reaction and %conversion obtained. The loading is obtained calculated as the molar ratio of total quantity of copper leached on the reagent. The reaction conditions for the secondary reaction were 0.12mmol **rhod-azide**, 0.10mmol **testo-alkyne**, 2mL of Cu-containing supernatant, reacted for 90h.

It was found that by NMR, the supernatant from the blank reaction was unsuccessful in catalyzing the reaction, where the mol% of Cu from the blank leaching was 0.92mol%. As a second check, ESI-MS was done and confirmed this. In the absence of any chelating species, the solvent only led to leaching in the form of solid copper pieces, either detached from the magnetic iron core, or copper from iron depleted particles.

3.5.2 Initial tests for Cu content in rhod-triazole-testo product

In addition to spontaneous leaching observed in the solvent, we wanted to quantify how much leaching could be attributed to **rhod-*triazole*-testo** chelation since it is known that triazole rings chelate well to Cu species.[5, 38b] Two reactions were set up, where one had the **rhod-*triazole*-testo** filtered and the other unfiltered. Half of each was digested for ICP-OES to obtain its Cu content, while the other halves were used for secondary reactions. Table 3.3 gives the amount of Cu in μg/g for the filtered and unfiltered **rhod-*triazole*-testo** product.

Cu content in filtered rhod-*triazole*-testo (μg/g)	**Cu content in unfiltered rhod-*triazole*-testo (μg/g)**
3243.6 *126.5±8.5% (μg)	16217.9 *632.5 (μg)

Table 3.3. Copper content in **rhod-*triazole*-testo** (filtered and unfiltered). Reaction conditions of original reaction: 0.050mmol **rhod-azide**, 0.042mmol **testo-alkyne**, 1mL $CHCl_3$ (0.042M), 40mg Cu-Fe MPs (500mol%). *Actual amount of Cu in μg without regard to mass of **rhod-*triazole*-testo**.

Based on the ICP-OES results, the product **rhod-*triazole*-testo** contained 3243.6 μg Cu per gram of product in the case of the filtered product and 16217.9 μg Cu per gram of product in the unfiltered **rhod-*triazole*-testo**. Therefore, despite having a heterogeneous catalyst, we did observe loss of copper from the catalyst due to the presence of the **rhod-*triazole*-testo**. The leaching was greatly enhanced compared to the leaching due to the solvent alone, thus showing the effect of the triazole ring in increasing the total copper leached by liberation of ions. The majority of the leaching happened in the form of solid pieces that could be filtered off. The fact it happened via a mechanism extracting ions, reveals that ion liberation led to catalyst depletion and eventually fragility, inducing more solid copper to detach from their corresponding magnetic core.

As a secondary test, we used the isolated **rhod-*triazole*-testo** as a catalyst to probe if the Cu species it contained could catalyze the reaction. We compared the catalytic ability of both the Cu ions chelated, seen in the filtered **rhod-*triazole*-testo** and the Cu from Cu-Fe MPs that became detached or lost magnetism (seen in the unfiltered product). The following table (Table 3.4) illustrates the amount of Cu in both filtered and

unfiltered **rhod-*triazole*-testo** and the %conversions obtained during the secondary test reactions.

Entry	Sample	Cu content (μg)	%Conversion (by NMR) of secondary reaction
1	Supernatant of Cu-Fe MPs with solvent	59.9±23.0 (0.92mol% of Cu)	0% (<5% by ESI-MS)
2	Filtered supernatant of Cu-Fe MPs exposed to **rhod-*triazole*-testo**	126.5±8.5 (8.8mol% of Cu)	98.5%±2.2%
3	Unfiltered supernatant of Cu-Fe MPs exposed to **rhod-*triazole*-testo**	632.5 (47.9mol% of Cu)	100%

Table 3.4. Copper content and %conversion of reaction when using supernatant as a catalyst (entry 1), filtered **rhod-*triazole*-testo** as catalyst (entry 2) and unfiltered **rhod-*triazole*-testo** (entry 3). Reaction conditions for each secondary reactions: 0.025mmol **rhod-azide**, 0.021mmol **testo-alkyne**, 0.5mL $CHCl_3$ (0.04M). The value in brackets is the corresponding mol% of Cu used in the secondary reaction. Reactions were done in duplicate in the case of the filtered **rhod-*triazole*-testo** catalysis only.

The amount of Cu in the blank supernatant secondary reaction was close to 1mol% with respect to the reagents (entry 1), which was not enough to catalyze a reaction in 90h, whereas both the filtered and unfiltered **rhod-*triazole*-testo**, which correspond to Cu ion leached and Cu from the catalyst, respectively, were both able to catalyze the subsequent reaction at 9mol% (entry 2) and 50mol% (entry 3). This indicates to us that the leaching from just the particles into the supernatant without the presence of the reactants and/or product is very low and that the majority of the leaching occurs during the actual click reaction. The next step, naturally was to determine how much each reactant contributes to the leaching landscape.

3.5.3. Leaching from starting materials

Thus far, we established that the triazole ring from **rhod-*triazole*-testo** was a major contributor to Cu leaching. To have a better understanding and confirm this hypothesis, we decided to mix each of the starting substrates with Cu-Fe MPs and solvent and determine the Cu content after allowing the particles to be in contact with the individual substrates for a typical reaction time. A blank reaction with only Cu-Fe

MPs and $CHCl_3$ was also run and the leaching from this blank was subtracted from each reaction so as to only take into account leaching from the individual substrates and of **rhod-*triazole*-testo**. Graph 3.5 outlines the Cu leaching contributions from the when Cu-Fe MPs and $CHCl_3$ was mixed with **rhod-azide**, **testo-alkyne**, and both reactants (typical reaction). The percentages above each bar showed the amount of Cu lost from the initial catalyst loading.

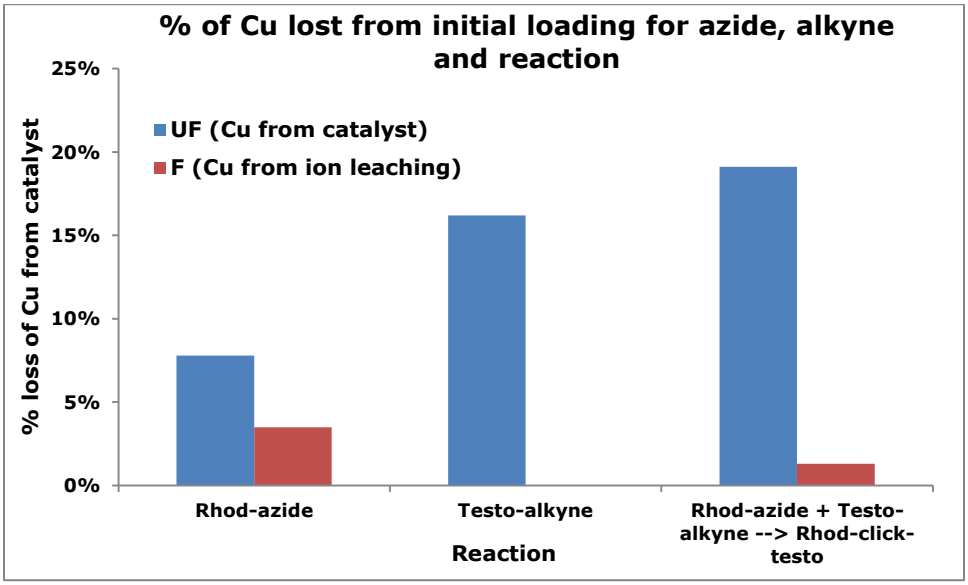

Graph 3.5. %loss of Cu from initial catalyst loading in **rhod-azide**, **testo-alkyne** and both together (**rhod-*triazole*-testo**), respectively, when mixed with Cu-Fe MPs and $CHCl_3$. The following amounts of reagent were used with 72mg Cu-Fe MPs and 1mL $CHCl_3$: 50mg **rhod-azide**; 25mg testo-alkyne; 50mg **rhod-azide** + 25mg **testo-alkyne**. As a blank, 50mg **rhod-azide** + 25mg **testo-alkyne** were only mixed with 1mL $CHCl_3$ and no catalyst. This mixture was tested for Cu content and contained 1.2µg Cu, which corresponded to <0.01% Cu.

This graph shows an interesting trend. In all cases, the majority of the leaching occurred in the form of solid leaching that could be filtered off. The interpretation of these results was thus based on the unfiltered results. First, upon comparing the two reagents individually with the catalyst, we observed that the **testo-alkyne** afforded more leaching than the **rhod-azide**. This is consistent with the literature where the Fokin group[39] reported that alkynes coordinated more to Cu(I) than azides. This also makes sense due to the mechanism of the reaction involving Cu-acetylide formation. When comparing reagents with an actual reaction setting (**rhod-azide** + **testo-alkyne** -> **rhod-*triazole*-testo** with Cu-Fe MPs), we observed slightly more leaching than with

testo-alkyne alone, but less than the sum of the effect of both **rhod-azide** and **testo-alkyne**. Of course, as the reaction proceeded, both the **rhod-azide** and **testo-alkyne** were consumed and transformed into **rhod-*triazole*-testo**. **Rhod-*triazole*-testo**, a triazole molecule, also has the capacity of coordinating Cu[5, 38a]. Schematically, if one assumed that each Cu-coordinated **testo-alkyne** converted into 1 Cu-coordinated **Rhod-*triazole*-testo**, we would have observed a leaching of 16%. The extra 3% to get to the 19% we measured could be attributed to the effect of coordination by **rhod-azide**.

3.5.4. Catalyst leaching under N_2 and air conditions

In section 3.4.5, we probed the effect that an N_2 and air atmosphere had on the reaction recycled over several cycles to have an appreciation of a trend. The N_2, degassed solvent reactions seemed to slowly decrease in yield after four cycles whereas the air, undegassed reactions were very sporadic in their yields with no general trend. We wanted to have an idea of what sort of Cu loss we could expect after each recycling for each atmosphere. Below, in Graph 3.6a and 3.6b, are the %conversions originally shown in as Graph 3.4 alongside the Cu content loss for each recycling run for the respective atmosphere.

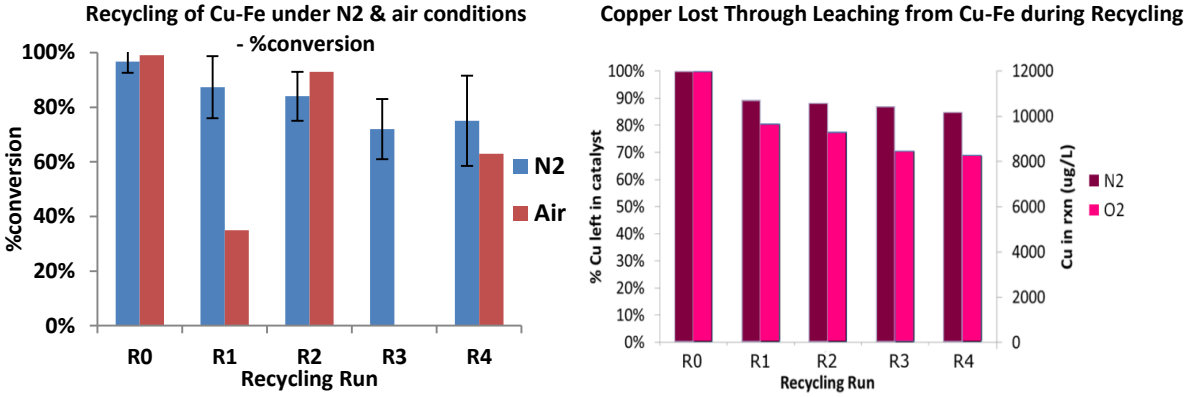

Graph 3.6a, 3.6b. a) Graph of %conversion of reactions under N_2 and air atmosphere after four recycles. **b)** Cu content lost through each recycling run. Reaction conditions: 0.050mmol **rhod-azide**, 0.042mmol **testo-alkyne**, 1mL $CHCl_3$, (0.042M), 40mg Cu-Fe MPs. Note reactions under N_2 were done in triplicate; reactions in air only once.

Another graph (Graph 3.7) was made to illustrate the leaching profile Cu-Fe particles in 500mol% reactions under N_2. The red line denotes Cu content in the unfiltered **rhod-*triazole*-testo** (physical detachment of Cu from catalyst) and the blue line is the filtered **rhod-*triazole*-testo** which shows the Cu ion leaching. It can be seen that the Cu ion leaching remained consistent throughout each recycling but the amount of Cu from the catalyst detachment was significantly reduced.

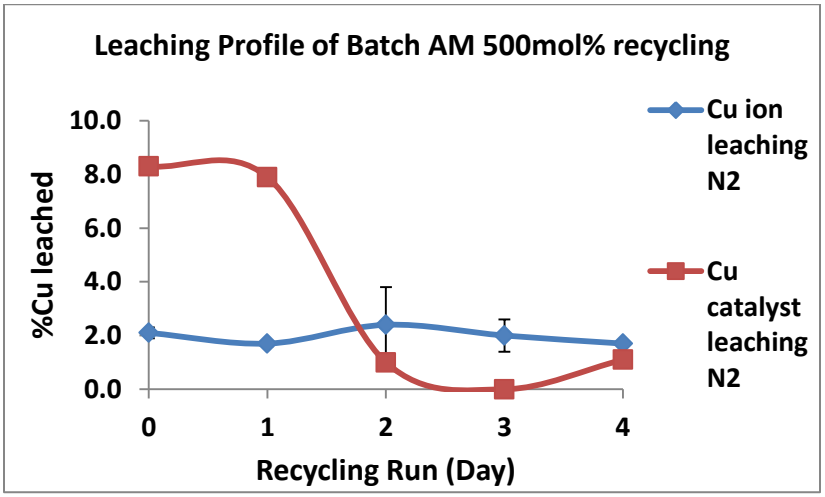

Graph 3.7. Leaching profile of recycled Cu-Fe MPs at 500mol% over four runs.

It also appears that the majority of the physical catalyst leaching occurred within the first two recycling runs (R0 and R1) then there is a steady decline. In terms of Cu ion leaching into **rhod-*triazole*-testo**, the values were pretty consistent throughout the recycling run which implied a similar amount of Cu leaches into the **rhod-*triazole*-testo** regardless of how many times the catalyst was recycled.

3.5.5 Leaching into rhod-triazole-testo

From graph 3.3, the best conditions for complete conversion in the least amount of time were 5mol% completed in 16h (%conversion 93% ± 5%) in $CHCl_3$. A catalyst loading of 20mol% could also catalyze the reaction in 28h (%conversion 97% ± 1%). To determine if the resulting Cu content in **rhod-*triazole*-testo** was affected by this difference in loading and rate, we compared the filtered and unfiltered rhod-*triazole*-

testo products, shown in Graph 3.8.

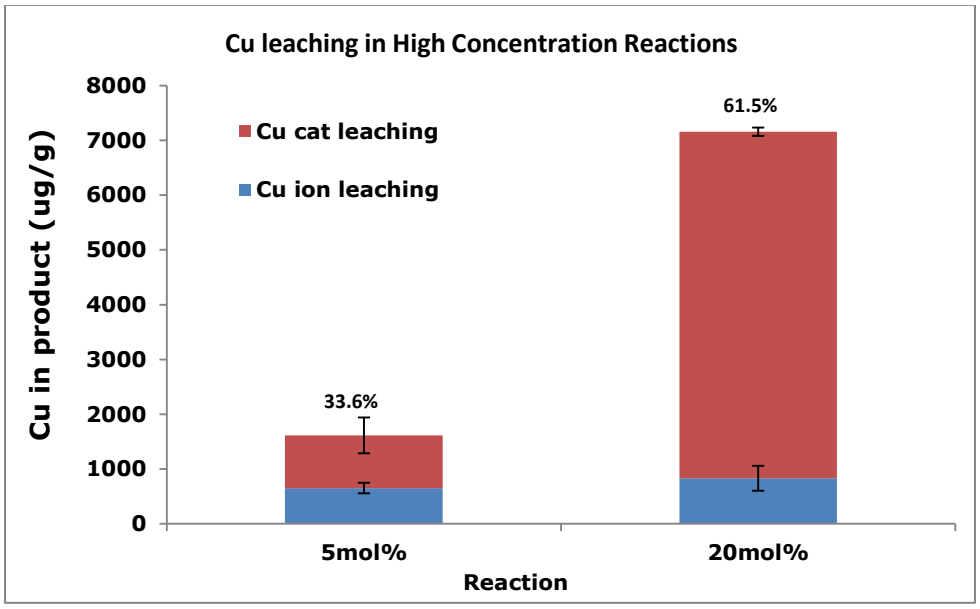

Graph 3.8. Comparison of Cu leaching in "high" concentration 5mol% and 20mol% reactions. Reaction Conditions: Reaction conditions: 5mol%: 0.30mmol **rhod-azide**, 0.25mmol **testo-alkyne**, 1mL $CHCl_3$ (0.25M), 4mg Cu-Fe MPs. 20mol%: 1.20mmol **rhod-azide**, 1.00mmol **testo-alkyne**, 4mL $CHCl_3$,(0.25M), 60mg Cu-Fe MPs. The values in brackets show the %Cu lost with respect to the original catalyst loading.

Based on both the Cu content from ion leaching and the physical catalyst leaching, the 5mol% loading had a total of 961.2µg/g Cu in **rhod-*triazole*-testo** translating to a 33.6% loss based on the initial amount in the catalyst. The 20mol% loading gave 6323.42µg/g Cu in **rhod-*triazole*-testo** with a loss of 61.5% Cu. This was a promising finding since, this result shows that the lower mol% and faster reaction time did not translate to an increase in leaching.

3.5.6 Leaching in homogeneous reaction

To establish the low leaching ability of the Cu-Fe MPs, catalysis using the homogenous counterpart, CuI/DIPEA was used and the Cu content in rhod-*triazole*-testo was compared. Graph 3.9 shows the difference in Cu content, where, the Cu-Fe MPs were simply magnetically removed from the reaction with no further purification. The CuI/DIPEA reaction was filtered through Celite to remove the excess catalyst.

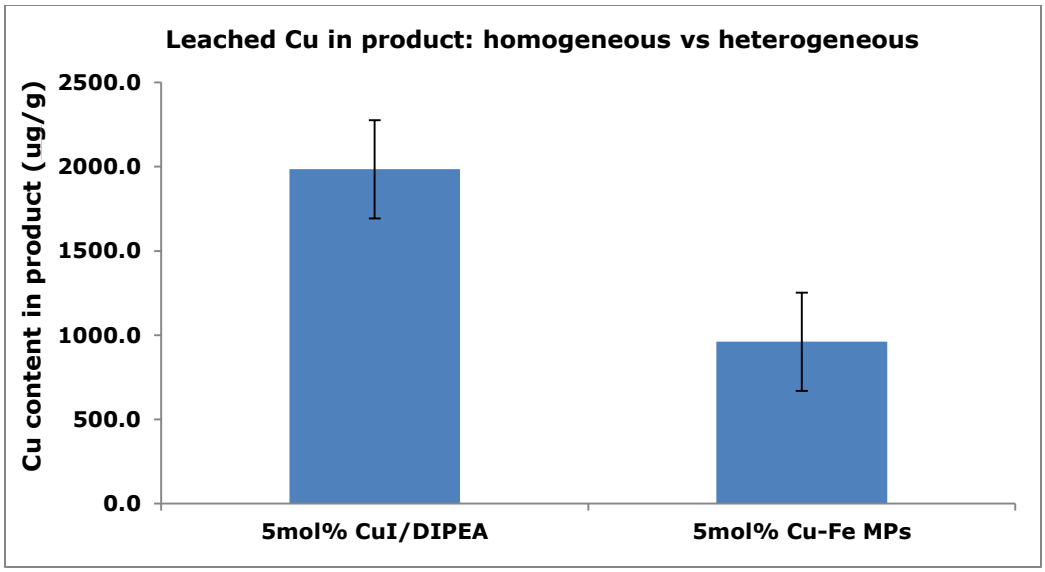

Graph 3.9. Cu content in **rhod-*triazole*-testo** after reaction (homogeneous and heterogeneous reactions). The CuI/DIPEA was filtered through Celite after reaction; the Cu-Fe MPs were simply magnetically removed with no further purification. Reaction conditions (homogeneous – CuI/DIPEA): 0.19mmol **rhod-azide**, 0.19mmol **testo-alkyne**, 1mL THF (0.20M), 0.01mmol CuI (5mol%), 0.5eq DIPEA (16.7µL), 24 hours; %conversion 84±5% (triplicate). Reaction conditions (heterogeneous – Cu-Fe MPs): 0.30mmol **rhod-azide**, 0.25mmol **testo-alkyne**, 1mL $CHCl_3$ (0.25M), 4mg Cu-Fe MPs, 23 hours; %conversion 98±2% (duplicate).

Graph 3.9 shows that the amount of Cu in **rhod-*triazole*-testo** using CuI/DIPEA was 1985µg/g, whereas using the Cu-Fe MPs the copper content was 961.2µg/g, about half. The reactions both took about the same amount of time, but the Cu-Fe MPs had a %conversion of 98±2% whereas the CuI/DIPEA had 84±5%. The Cu-Fe MPs were more efficient in converting to **rhod-*triazole*-testo** with less Cu content.

3.5.7 Conclusions for leaching tests

As in the previous section on rate of reaction, the optimal conditions for the click reaction was a high concentration of reagents at a low mol% of Cu-Fe MPs. Using a lower mol% of catalyst (5mol%) was an ideal balance of rate of reaction with leaching. This product containing 961.2µg/g Cu was then tested in an actual breast cancer cell to determine if this leached Cu was toxic.

3.6 Toxicity Testing

Since the product of our click reaction, **rhod-*triazole*-testo**, had a desired application *in vivo*, it was important that we tested it's toxicity within a cell that expressed aromatase. Human breast cells, MCF-7 was chosen. An MTT assay was used (3-(4,5-dimethylthiazol-2-yl)-2,5-diphenyltetrazolium bromide), where the cell's metabolic activity, more specifically, the activity of NAD(P)H-dependent oxidoreductase enzymes was probed. This enzyme could reduce the MTT reagent to purple formazan which was measured by absorbance. The metabolic activity of the mitochondria was therefore linked to cell viability. A decrease in metabolic activity implies death of cells due to the toxic nature of the foreign substance introduced into the cell. This toxicity testing was conducted in the group of Dr. Dusica Maysinger. The product of the 5mol% reaction containing 961.2µg/g Cu (shown in Graphs 3.8 and 3.9) was sent for toxicity testing, along with the same batch of Cu-Fe MPs used in this reaction. The results are presented in Figure 3.4a and 3.4b.

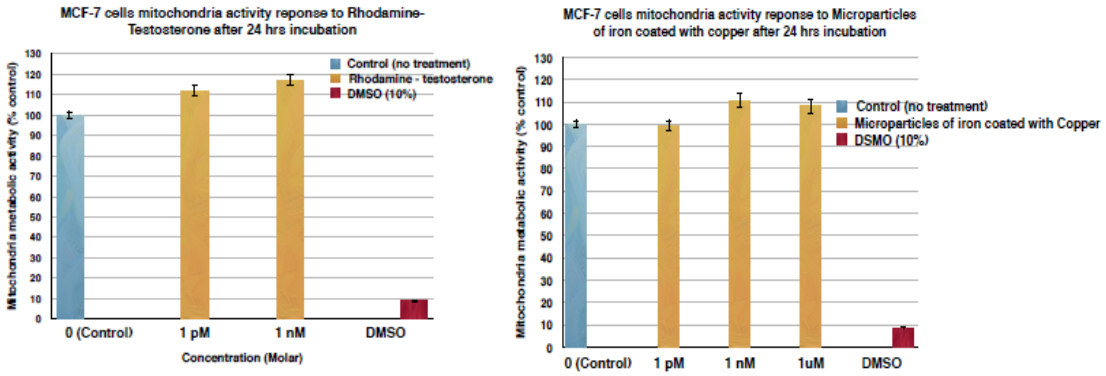

Figure 3.4a, 3.4b. Mitochondrial activity response to **a) rhod-*triazole*-testo** and **b)** Cu-Fe MPs after 24 hour incubation in MCF-7 human breast cancer cells. The control, set at 100%, was the response with no treatment.

In Figure 3.4a, which shows the mitochondria activity response to the **rhod-*triazole*-testo** product after 24 hour incubation, there is no toxicity at the 1pM and 1nM range based on the control. Figure 3.4b demonstrates no toxicity to the cells when subjected to 1pM, 1nm and 1µM of Cu-Fe MPs. It should be noted the slight increase in metabolic activity can be linked to the metabolism of the cells rapidly dividing which

reduce the MTT faster therefore exhibiting a slightly higher than 100% mitochondrial metabolic activity. To compare, using 10% DMSO was toxic to the cells since there was a decrease to 10% metabolic activity after 24 hours.

Through this toxicity study, we were able to confirm that both the Cu contained in the product of a 5mol% reaction (961.2μg/g Cu) and the catalyst Cu-Fe MPs were not found to be toxic when incubated for 24 hours in MCF-7 human breast cells up to the nM and μM range respectively. These results that showed our Cu-Fe MPs were promising CuAAC catalysts for biological applications and could be used in real-time sensing applications.

3.7 Conclusions

Overall, the click reaction of **rhod-azide** and **testo-alkyne** was successful using the Cu-Fe MPs. These particles had three major morphologies: decorated, microspheres and fern structures which varied in copper content. Several reaction parameters, such as solvent, concentration of reactants, catalyst loading and atmosphere were probed. The best conditions for both reaction rate and minimal Cu loss were a catalyst loading of 5mol% with completion in 16 hours and a copper content of 961.2μg/g by simply removing the catalyst magnetically with no further purification. These conditions also led to a reduced reaction time and less copper in **rhod-*triazole*-testo** than the homogenous counterpart of CuI/DIPEA. Both the Cu-Fe MPs and **rhod-*triazole*-testo** were also found to be not toxic towards the MCF-7 breast cancer cells. This will allow for further development of the aromatase sensor in the future.

Using these pristine Cu-Fe MPs, it was found copper loss was inevitable. While in our case, this was not an issue for toxicity, we wondered if modifications of the Cu-Fe MPs could lead to a decrease in Cu loss. This would be advantageous from a cost perspective, where perpetual catalyst loss could be costly and inconvenient but furthermore decreasing leaching could allow for the Cu-Fe MPs to be used in other biological applications that are more sensitive to Cu contamination. Chapter 4 will be

investigating the use of carbon coatings and heat treatments of the Cu-Fe MPs to decrease Cu loss.

3.8 References

1. Kovacs, S.; Zih-Perenyi, K.; Revesz, A.; Novak, Z., Copper on Iron: Catalyst and Scavenger for Azide-Alkyne Cycloaddition. *Synthesis-Stuttgart* **2012,** *44* (24), 3722-3730.
2. Masnadi, M.; Yao, N.; Braidy, N.; Moores, A., Cu(II) Galvanic Reduction and Deposition onto Iron Nano- and Microparticles: Resulting Morphologies and Growth Mechanisms. *Langmuir* **2014**.
3. Masnadi, M.; Yao, N.; Braidy, N.; Moores, A., Cu(II) Galvanic Reduction and Deposition onto Iron Nano- and Micro-Particles: Resulting Morphologies and growth Mechanisms. *Langmuir* **2014**.
4. Poulston, S.; Parlett, P. M.; Stone, P.; Bowker, M., Surface Oxidation and Reduction of CuO and Cu2O Studied Using XPS and XAES. *Surf. Interface Anal.* **1996,** *24* (12), 811-820.
5. Dervaux, B.; Du Prez, F. E., Heterogeneous azide-alkyne click chemistry: towards metal-free end products. *Chemical Science* **2012,** *3* (4), 959-966.
6. (a) Rodionov, V. O.; Presolski, S. I.; Diaz, D. D.; Fokin, V. V.; Finn, M. G., Ligand-Accelerated Cu-Catalyzed Azide-Alkyne Cycloaddition: A Mechanistic Report. *J. Am. Chem. Soc.* **2007,** *129* (42), 12705-12712; (b) Aromí, G.; Barrios, L. A.; Roubeau, O.; Gamez, P., Triazoles and tetrazoles: Prime ligands to generate remarkable coordination materials. *Coord. Chem. Rev.* **2011,** *255* (5–6), 485-546; (c) Chan, T. R.; Hilgraf, R.; Sharpless, K. B.; Fokin, V. V., Polytriazoles as Copper(I)-Stabilizing Ligands in Catalysis. *Org. Lett.* **2004,** *6* (17), 2853-2855.
7. Hudson, R.; Li, C.-J.; Moores, A., Magnetic copper-iron nanoparticles as simple heterogeneous catalysts for the azide-alkyne click reaction in water. *Green Chem.* **2012,** *14* (3), 622-624.
8. Decan, M. R.; Impellizzeri, S.; Marin, M. L.; Scaiano, J. C., Copper nanoparticle heterogeneous catalytic 'click' cycloaddition confirmed by single-molecule spectroscopy. *Nat Commun* **2014,** *5*.
9. Rodionov, V. O.; Fokin, V. V.; Finn, M. G., Mechanism of the Ligand-Free CuI-Catalyzed Azide–Alkyne Cycloaddition Reaction. *Angew. Chem.* **2005,** *117* (15), 2250-2255.

3.9 Appendix

3.9.1 Materials and Reagents

All reactants were purchased from Sigma Aldrich and used as received unless otherwise noted. Organic azides (benzyl azide and 3-azidopropan-1-amine) were synthesized from the corresponding bromides via previously reported procedures[33]. Rhodamine azide was synthesized by peptide coupling of Rhodamine B and 3-azidopropan-1-amine[34]. All reactions were carried out in an oxygen-free glovebox, except where noted, and all solvents were de-gassed for 20 minutes prior to use.

3.9.2 Cu-Fe MPs synthesis

FeMPs were purchased from Alfa Aesar and used as received. In a Schlenk flask, 350mg of FeMPs were weighed and suspended in 35mL of water. To this Fe MP suspension, 100mg of $CuSO_4$ was weighed into a Schlenk flask and dissolved in water then added dropwise via canula. The resulting slurry was left to sonicate for 30 minutes after addition of $CuSO_4$. These microparticles were then washed three times with 30 mL water, and then dried under vacuum. The catalyst is used as a dried powder and weighed directly into the reaction vial.

3.9.3 Reaction set-up

A typical reaction generally uses 1.2 equiv rhodamine azide (rhod-azide) and 1 equiv ethisterone (testo-alkyne) in $CHCl_3$ at varying concentrations. In general, 1 dram vials are used with or without a stir bar or 10mL microwave vials with a stir bar for the larger scale reactions. Reactions are left to stir on a magnetic stir plate until completion (time varies based on conditions). To work-up the reaction, a supermagnet is used to separate the Cu@FeNPs from the reaction mixture. Via Pasteur pipette, the reaction mixture is removed from the vial and the particles are washed approximately three times with $CHCl_3$ and combined with the reaction mixture. This $CHCl_3$ was evaporated under

vacuum and analyzed by NMR for %conversion. For recycling runs, after washing the particles with $CHCl_3$, another aliquot of rhod-azide and testo-alkyne was weighed into the same vials and dissolved in $CHCl_3$ to commence another reaction.

3.9.4 Sample Calculation for mass of $CuSO_4$ added to Fe to prepare Cu-Fe MPs

$$mass\ of\ Cu\ in\ 200mg\ of\ CuSO_4 = 200mg\ CuSO_4\ x\ \frac{63.546\frac{g}{mol}}{159.62\frac{g}{mol}} = 79.6mg\ Cu$$

$$Cu: \frac{0.0796g}{63.546\frac{g}{mol}} = 0.00125mol = 1$$

$$Fe: \frac{0.350g}{55.845\frac{g}{mol}} = 0.00628mol = 5$$

$$\therefore 1 : 5 = 2 : 10$$

Scheme 3.5. Calculation of mass of $CuSO_4$ required for a 2:10 Cu:Fe particles.

3.9.5 Sample preparation for ICP-OES or ICP-MS analysis – Cu and Fe

Unless otherwise noted, all samples were analyzed using ICP-OES

3.9.5.1 Types of samples tested for ICP

In terms of samples tested for ICP, we demonstrate Cu ion leaching into the product by filtering the sample before digestion and the physical catalyst leaching without filtering the sample before digestion. The filter used, unless otherwise specified, was a 0.2µm, PTFE membrane which is small enough to remove 2µm sized Cu-Fe MP. It was important to make this distinction since we are using a magnetically retrievable catalyst that can lose some of its magnetic ability and thus not be completely retrieved. This opens up the possibility of having high Cu contents based on loss of catalyst into the product which does not represent the Cu ion leaching into the product. Cu ion leaching contents can be achieved by filtering the product to remove any non-magnetic catalyst from the

product and get a better idea of the Cu ion leaching. It should be mentioned though, that the values for physical leaching can drastically change simply by having less or more loss of magnetism which would lead a wide range for copper content found in the product. This appears to be hard to control as slight oxidation or mixing during the reaction can affect the particles. It was found even the positioning of the vials on the stir plate could be enough to skew otherwise duplicate reactions in terms of yield or physical catalyst leaching.

3.9.5.2 %Cu in Cu-Fe MPs

For determination of Cu and Fe content of prepared Cu-Fe microparticles, weigh a few milligrams into a 10mL pyrex digestion tube. Add 1mL of conc HNO_3 (68%) and heat at 100^{o}C for 1 hour. Include a blank digestion, where 1mL of HNO_3 is digested in the same way. After the sample has cooled, dilute the sample to give a 1% HNO_3 content in 10mL (by weight).

3.9.5.3 %Cu in product of reaction

For determination of Cu and Fe content in the product of the click reaction, **rhod-*triazole*-testo**, weigh approximately 20mg into a 10mL pyrex digestion tube. Add 1mL of conc HNO_3 (68%) and heat at 100^{o}C for 1 hour. Remove from heat and add 1mL of milliQ water, followed by 1mL of Trace Analysis Grade hydrogen peroxide. Heat for another hour at 100^{o}C. Include a blank digestion, where 1mL of HNO_3, followed by 1mL water and 1mL hydrogen peroxide is digested in the same way. After the sample has cooled, dilute to give a 1% HNO_3 content in 10mL (by weight).

3.9.6. ICP-OES operation

The ICP-OES (Inductively Coupled Plasma Optical Emission Spectrometry) used was a Thermo Scientific-iCAP 6500 . The method used to analyze the samples was developed by Ranjan Roy and Andrew Golsztajn from Engineering. This method selects the Cu 324.7nm and Cu 327.3nm line for Cu analysis and the Fe 238.2nm and Fe 259.9nm for Fe analysis. Based on the calibration curve, background signal and %RSD,

we select the line that gives the most reliable data. Generally, the Cu 324.7nm and Fe 259.9nm are selected. Calibration curve solution concentrations of Cu and Fe are the following (in 1% HNO3): 0.05ppm, 0.5ppm, 5ppm and 50ppm.

Note: ICP-MS samples were sent to UdeM and were analyzed by Madjid Hadioui.

3.9.7 ICP data for Cu-Fe micron-sized particles

The ratios of Cu:Fe are indicated, along with their ICP data and calculated molecular weight.

Name of Batch	Ratio Cu:Fe	Cu_XFe_{10} by ICP	Cu_1Fe_X (X=) by ICP	MW of Cu_1Fe_X	%Cu
*Batch AF	1:10	1.7	5.8	387.447	14.7
Batch AG	2:10	1.7	5.8	387.447	14.7
Batch AH	2:10	2.4	4.2	298.095	19.2
Batch AI	1:10	1.6	6.3	415.370	14.0
Batch AJ	2:10	4.8	2.1	180.821	32.3
Batch AK	5:10	14	0.7	102.638	58.8
Batch AL	1:10	1.8	5.6	376.278	15.2
Batch AM	2:10	4.3	2.3	191.99	30.3
Batch AN	5:10	10	1	119.39	50.0
***Batch AO	2:10	1.1	9.1	571.228	9.9
Batch AP	2:10	1.8	5.6	376.278	15.2
Batch AQ	2:10	2.0	5.0	342.771	16.7
Batch AR	2:10	2.0	5.0	342.771	16.7
**Batch AS	2:10	1.85	5.4	365.109	15.6
***Batch AT	2:10	1.73	5.8	386.349	14.7
Batch AU	2:10	1.97	5.1	347.020	16.4

Table 3.5. ICP data for each batch of Cu-Fe MPs prepared, including initial ratio, molecular weight & %Cu.
*Batch AF was not hand mixed; blue colour of Cu^{2+} remained in supernatant therefore less Cu plating
**Batch AS was stored in the vacuum oven at 50°C as opposed to the glovebox.
***Batch AO and AT were made in twice the quantity from the usual preparation of particles (700mg Fe, 400mg $CuSO_4$).

3.9.7.1 Replicating batch preparation to determine Cu content

The following batches were prepared to determine the reproducibility of the different types of particles (1:10, 2:10 and 5:10). The following table shows the amounts of Cu contained in each batch based on type.

Batch Name	Ratio	%Cu	AVG %Cu	Std Dev %Cu
Batch AI	1:10	14.0	14.60	0.85
Batch AL	1:10	15.2		
Batch AM	2:10	30.3	31.30	1.41
Batch AJ	2:10	32.3		
Batch AK	5:10	58.8	54.40	6.22
Batch AN	5:10	50.0		

Table 3.6. Preparation of multiple batches of Cu-Fe MPs of the same ratio for %Cu comparison.

In general, these batches follow a trend, where, the average %Cu approximately doubles from 1:10 to 2:10 from 14.60% to 31.30%. However, there appears to be a decrease proportionally in copper when reaching 5:10. This is due to the fact that at higher ratios of Cu, such as 5:10, it has been observed that the Cu undertakes a more "fern-like" structure which has shown to lead to more leaching of Cu. In the 1:10 and 2:10 particles, there is more of a hollow structure and surface coated structure which is the ideal type of catalyst it terms of not leaching too much Cu. This ruled out using the 5:10 particles. Since both the 1:10 and 2:10 had similar Cu plating ability, we decided to use the 2:10 since it contained more Cu than the 1:10 therefore we could conduct more experiments per batch of particles.

Chapter 4: Use of carbon coated Cu-Fe micron-sized particles (C@Cu-Fe MPs) for the click reaction of benzyl azide and phenyl acetylene –probing the reactivity of this novel catalyst and its leaching effect

4.1 Introduction

In Chapter 3, CuAAC was successfully used to produce **rhod-*triazole*-testo**, from **rhod-azide** and **testo-alkyne**. The focus was on having successful catalysis with reproducibility while finding conditions to improve reaction rates. By varying the conditions, it was possible to speed up or decrease the rate of reaction, as well as affect the amount of Cu leaching found in **rhod-*triazole*-testo**. The optimal conditions were 5mol% Cu-Fe MPs in 0.25M of $CHCl_3$, under N_2 atmosphere leading to 961.2 μg/g Cu in **rhod-*triazole*-testo** after simply magnetically removing the catalyst and no further purification. Both the **rhod-*triazole*-testo** product of this reaction and the Cu-Fe MPs were tested in vivo in MCF-7 breast cells. It was found not to be toxic at the pM and nM levels for the **rhod-*triazole*-testo** product and pM, nM and μM level for the Cu-Fe MPs. In this chapter, we chose to focus on decreasing the loss of Cu through catalyst modification. We had hypothesized that there were two methods in which Cu was lost from the catalyst: 1) chemical leaching of Cu ions from the surface and 2) physical detachment of Cu particles from the surface either mechanically or through loss of magnetization from portions of the catalyst containing copper. Both types of copper loss could be quantified together by ICP-OES by simply magnetically removing the catalyst with no further workup, and acid digesting. Ion loss could be was quantified separately by filtering the product before acid digestion.

In the literature, many recent accounts have reported interesting catalytic results using heterogeneous catalysts, which, among other benefit, help decrease metal species leaching into the product[40]. The issue became proper quantification of leached metal into the product that was going to inadvertently happen even with a heterogeneous system. What was found was, either no quantification of metal species in the product was done or this quantification was done after filtration, columns or other methods used to remove metal species typically done in homogeneous reactions.

In some ways, this defeats one of the purposes of heterogeneous catalysts, which is having the ease of separation leading to not requiring further purification. If heterogenizing a catalyst only leads to having to use similar techniques for catalyst removal as homogenous reactions, it doesn't appear worth the effort of synthesizing them, especially when heterogeneous reactions have a tendency to take longer than homogenous reactions.

The approach was to take the existing Cu-Fe MPs and try to modify them to decrease Cu loss during CuAAC reactions. Since the application of interest would be for biological molecules, the modifications made needed to be biocompatible. We choose to add a carbon layer at the surface of the particles to create a barrier over the copper for two reasons: 1) to decrease the direct and continuous contact between the substrates and product with copper, which we believe leads to more leaching and 2) prepare a more robust catalyst that contains the copper within the catalyst and leads to less physical detachment.

4.2 Introduction to carbon coated particles

The idea of coating the surface of a material with carbon for purposes such as increasing battery performance[41] and enhancing heavy metal remediation for wastewater[16, 42] has been well documented. Nanomaterials also benefit from carbon coating to stabilize smaller particles from agglomeration[43]. In the case of magnetic nanoparticles, such as Fe, Co and Ni, to achieve optimal magnetization, reduced metal nanoparticles are preferred over metal oxides. The issue with reduced metal NPs is that they are highly air sensitive and can be pyrophoric. By coating the surface with carbon, very small, reduced metal nanoparticles can be achieved, which can withstand oxidation[44]. These stabilized particles could also be used directly in catalysis, where the reduced metal is required for organic transformations.

Carbon coating for catalytic purposes, specifically for decreasing leaching has been less studied. In 2009, Huang et al[45] synthesized nanosized Cu, Ag, Pd, Ni, CuPd alloy and Cu-Ag bimetallic particles and was able to control the sizes of the particles

using a carbon shell. The carbon shell was formed during the synthesis of the particles using cyclodextrin annealed at 300-400^{o}C. Characterization was done to determine the particle sizes based on the ratio of cyclodextrin to metal precursor. This article mentioned potential applications, such as enhancing electrolyte conductivity electro-optical devices but otherwise only particle synthesis and characterization was done. Finally, two recent articles by Baig et al prepared iron oxide NPs coated with carbon from glucose, then coated with Pd for use in hydrogenation, oxidation, coupling reactions. The authors claimed the coating helped the Pd NPs adhere better to the entire NP, via Pd chelation to the hydroxide groups of the glucose, before calcination to form the amorphous carbon with embedded Pd NPs. Despite several examples of carbon coatings being employed for improving performance, their use in catalysis as a method to decrease leaching or catalyst detachment is scarce. Our approach was slightly different than that of Baig, where instead of the carbon coating being between the iron core and palladium particles, our coating would be at the surface, acting as a barrier between direct and prolonged contact of the substrates and product with the copper.

4.3 Synthesis of carbon coated Cu-Fe MPs

The general synthesis of the carbon coated Cu-Fe MPs (C@Cu-Fe MPs) used 125mg of Cu-Fe MPs placed into a degassed solution of dissolved glucose (250mg in 20mL H_2O) and autoclaved at 160^{o}C for 4 hours. This resulted in crystallized glucose at the surface of the Cu-Fe MPs (glucose@Cu-Fe MPs). The glucose@Cu-Fe MPs were then annealed under argon at 800^{o}C to calcinate the organics and leave behind an amorphous carbon layer. Details of this synthetic process can be found in the appendix (section 4.8.1). ICP-OES measurements for the %Cu in the catalysts are in Table 4.4 in the appendix.

4.3.1 Synthesis of annealed Cu-Fe MPs

To probe the effect of a simple heat treatment on the catalysts without carbon-coating, Cu-Fe MPs were only annealed under argon at 800^{o}C. Details of this synthetic

process can be found in the appendix (section 4.8.2). ICP-OES measurements for the %Cu in the catalysts are in Table 4.4 in the appendix.

4.4 Catalytic tests and leaching

In this section, we were interested in seeing how well our carbon-coated Cu-Fe MPs (C@Cu-Fe MPs) could catalyze a click reaction and if the amount of Cu contained in the product of reaction could be reduced compared to the original Cu-Fe MPs. Several tests were done, where, reaction time was probed in each instance, and ICP-OES measurements were done to determine Cu content in the product. We determined the Cu contents in filtered and unfiltered samples to distinguish between the two types of leaching we observed, as was done in the previous chapter. The two types of leaching were: 1) Cu ion leaching from the Cu particles on the surface of the Fe MPs, 2) physical detachment of the catalyst containing Cu, either in the form of structural breakage or loss of magnetism resulting in Cu not being recovered during recycling.

This new study required to access large quantities of starting materials, and we chose to move away from the difficult to synthesis biologically relevant molecules, to focus on catalyst optimization. We picked the classic click reaction reagents, benzyl azide (Bn-N_3) and phenyl acetylene (Ph-CH). Benzyl azide was prepared based on an existing methodology; see section 4.83 of the appendix for details. A reaction scheme is shown in Scheme 4.1. The reaction parameters such as solvent (DCM), catalyst loading (~3mol%), concentration (1M) and atmosphere were not varied, as they were in Chapter 3. We used a low mol% catalyst loading, high concentration reactants under N_2 atmosphere since these were ideal conditions for the rhod-azide and ethisterone system from Chapter 3. The method of calculating yields, by weight and with NMR, for this click reaction shown in the appendix of Chapter 2 (section 2.8.6.2).

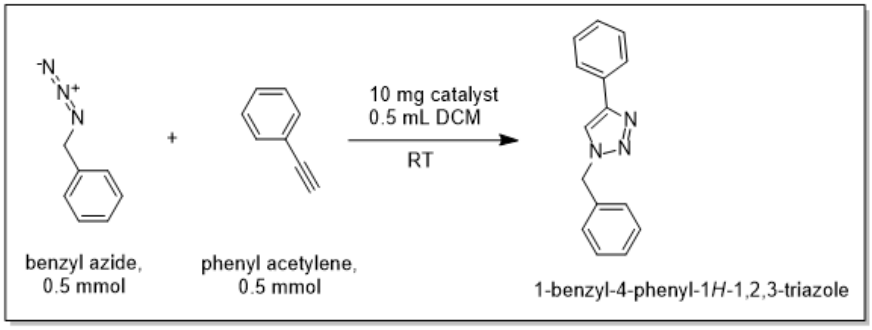

Scheme 4.1. Reaction conditions for click reaction between benzyl azide and phenyl acetylene to form 1-benzyl-4-phenyl-1H-1,2,3-triazole (**Bn-triazole-Ph**).

4.4.1 Cu-Fe MPs vs C@Cu-Fe MPs –initial tests

As a starting point to compare the catalytic abilities of both Cu-Fe MPs and C@Cu-Fe MPs for the reaction between benzyl azide and phenyl acetylene to form the product **Bn-*triazole*-Ph**, we set up two reactions where each set of particles were recycled four times, every 24h. This was to determine if the C@Cu-Fe MPs were capable of catalyzing the reaction, how well they could be recycled and the amount of Cu that was in the product, **Bn-*triazole*-Ph**, after each run. Graph 4.1 explores the %yields of during recycling of the carbon coated and uncoated (pristine) Cu-Fe MPs.

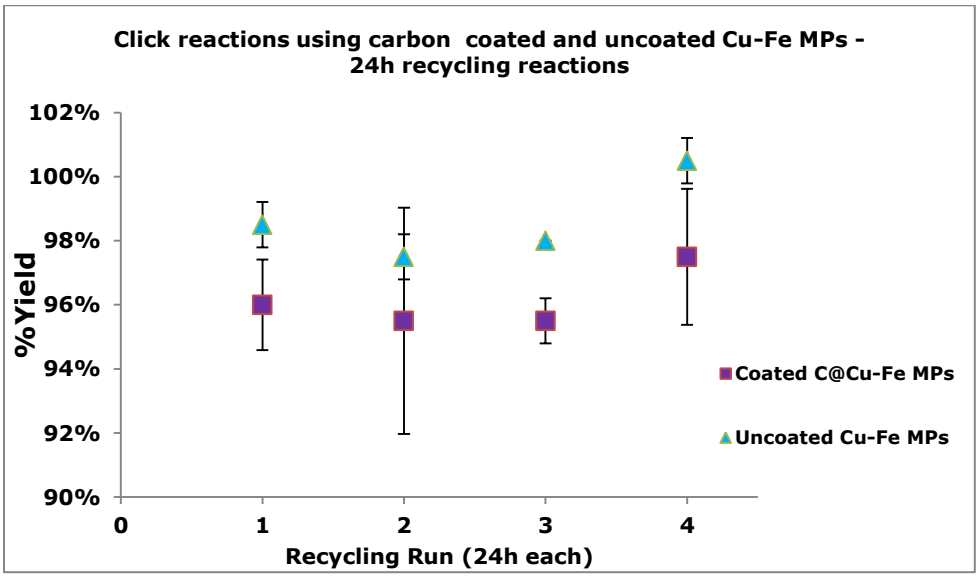

Graph 4.1. %yield of reaction using carbon coated C@Cu-Fe MPs (purple points) and uncoated (pristine) Cu-Fe MPs (blue points). Reaction conditions for uncoated Cu-Fe MPs: 0.5mmol benzyl azide, 0.5mmol phenyl acetylene, 10mg catalyst (2.6mol% Cu), 0.5mL DCM, RT.

Based on the recycling tests that were done both particles have similar activity and can be recycled multiple times without a decrease in yield. The Cu content of the product, **Bn-*triazole*-Ph,** was also measured at each recycling run. These results are shown in Graph 4.2a and 4.2b.

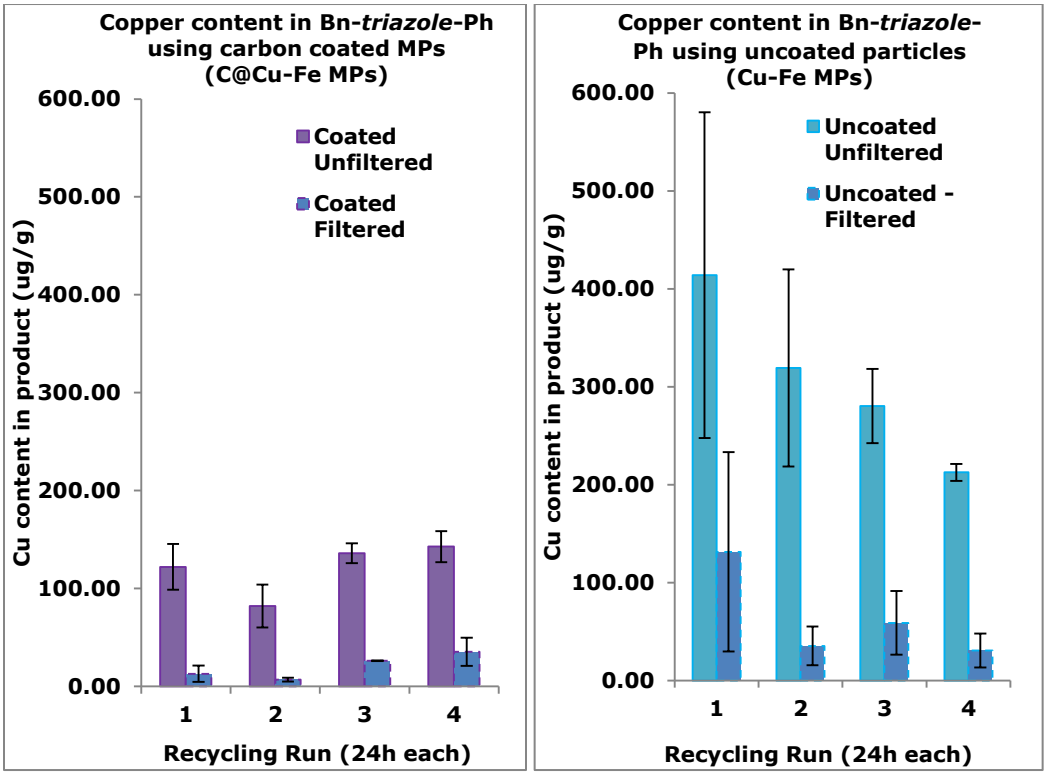

Graph 4.2a, 4.2b. a) Cu content in **Bn-*triazole*-Ph** using C@Cu-Fe MPs shown (left, in purple) and **b)** Cu content in **Bn-*triazole*-Ph** using uncoated (pristine) Cu-Fe MPs (Cu-Fe MPs) (right, blue). The solid line represents unfiltered and the dashed line represents the filtered **Bn-*triazole*-Ph**.

Based on the Cu content found in the filtered (Cu ion leaching) and unfiltered **Bn-*triazole*-Ph,** (catalyst detachment), it can be seen that there is a 2-3X decrease in Cu content from physical detachment and 2-5X decrease in leached Cu into **Bn-*triazole*-Ph**. This was a promising result and therefore we decided to further pursue the use of these carbon coated particles. We decided to probe reaction times to determine how long it actually took to obtain full conversion to the product **Bn-*triazole*-Ph** using both pristine Cu-Fe MPs and carbon coated C@Cu-Fe MPs. To do this, we did a time study, where aliquots of the reaction mixture were taken at specific time intervals and their yields were probed. Furthermore, the Cu content was also determined at each time.

4.4.2 Time study of Cu-Fe MPs in reaction

We did a reaction time study for the coated and uncoated particles to gauge what the actual reaction time was for these particles. Graph 4.3a demonstrates the %yields after several time intervals and Graph 4.3b is the Cu content of the product, **Bn-*triazole*-Ph,** at these time intervals.

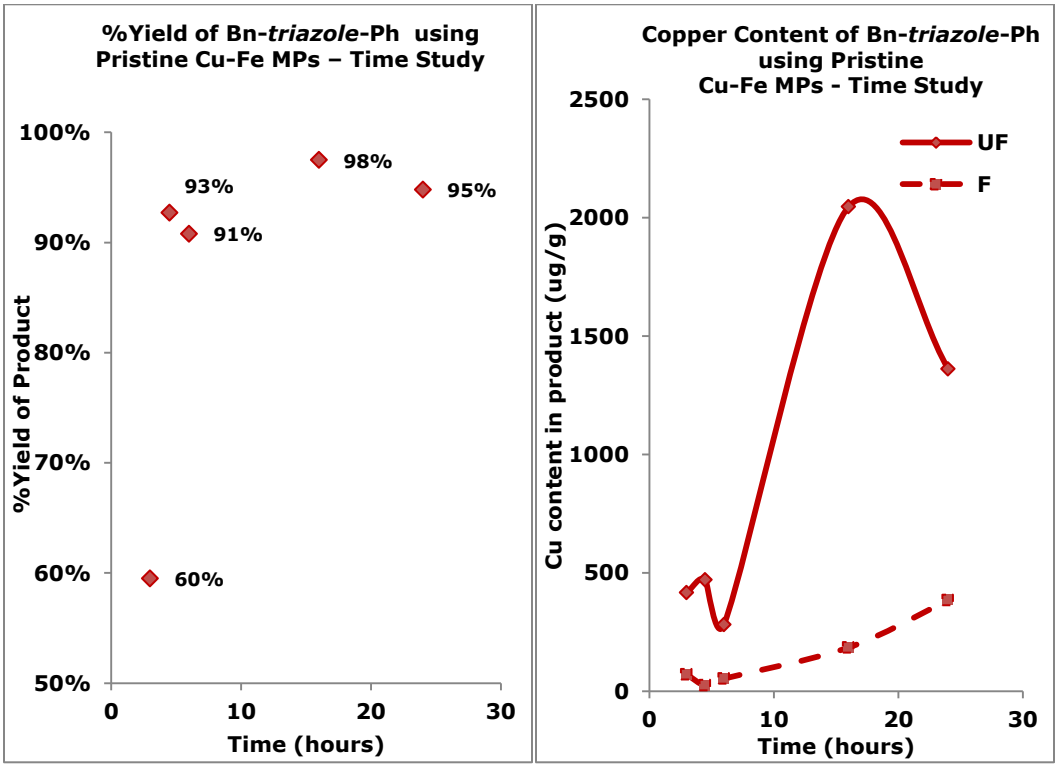

Graph 4.3a, 4.3b. Time study of **a)** %yield of **Bn-*triazole*-Ph** after 3h, 4.5h, 6h, 16h, 24h; and **b)** Cu content (ug/g) in **Bn-*triazole*-Ph** at same time intervals, where the solid line corresponds to the unfiltered product and the dashed line the filtered **Bn-*triazole*-Ph**. Reaction conditions for uncoated Cu-Fe MPs: 0.5mmol benzyl azide, 0.5mmol phenyl acetylene, 10mg catalyst (2.6mol% Cu), 0.5mL DCM, RT.

It can be seen from the time study that the reaction was almost at completion after about 5 hours. Correlating time of reaction to the Cu content in the product revealed that leaving the reaction for longer than needed led to more Cu from catalyst detachment, as seen in the solid line denoting the unfiltered product. This implied that Cu ion leaching did not increase very much by leaving the product **Bn-*triazole*-Ph** in contact with the catalyst, contrary to Cu detachment from the pristine Cu-Fe MPs.

4.4.2.1 Cu-Fe MPs –5h recycling reactions

To minimize the potential of excess leaching due to the prolonged contact of the catalyst with the substrates in reaction, we decided to do the recycling runs again but in 5h intervals for the pristine Cu-Fe MPs. We were able to run two runs per day, store the particles in the freezer in 0.5mL DCM overnight, and restart the recycling again the next day. We found this to be the best and safest way to store the particles. Other methods considered for storing the particles overnight were also probed and can be found in the appendix (section 4.8.4). Below is a summary of the results obtained in terms of %yield and Cu content (Graph 4.4a, 4.4b)

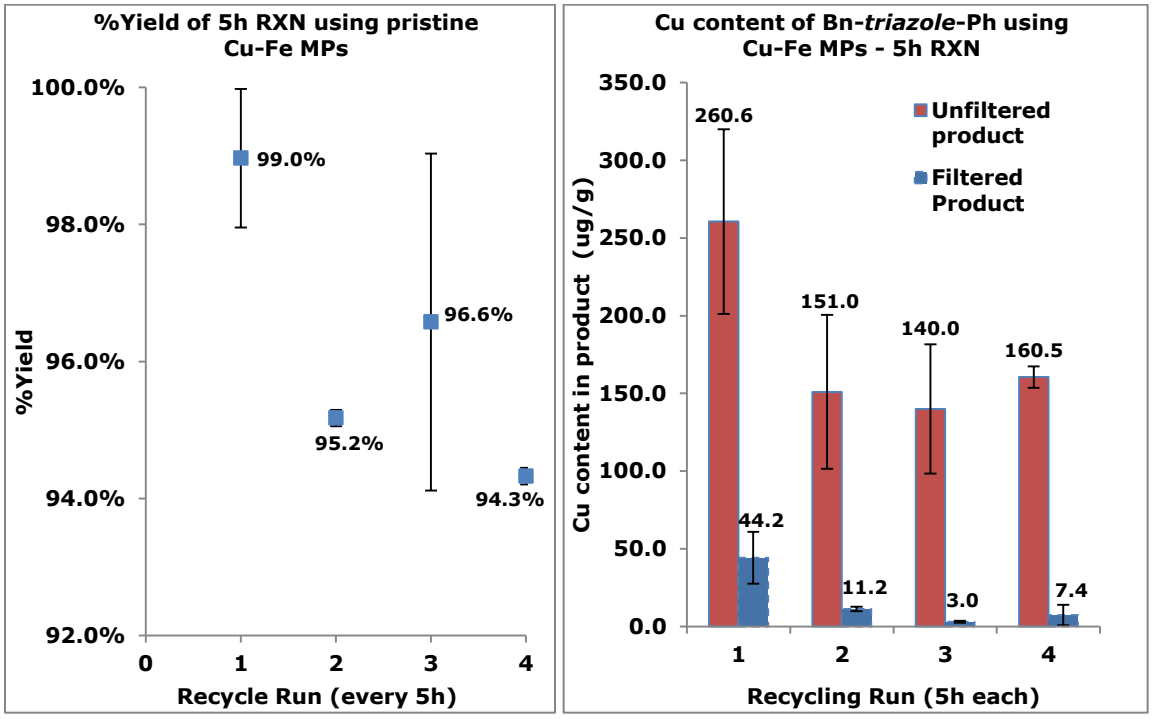

Graph 4.4a, 4.4b. Graph of **a)** %yield of **Bn-*triazole*-Ph** after each recycling run of 5h (left); **b)** Cu content in **Bn-*triazole*-Ph**, unfiltered (solid line) and filtered (dashed line) after 4 recycling runs in 5h intervals (right). Reaction conditions for Cu-Fe MPs reaction: 0.5mmol benzyl azide, 0.5mmol phenyl acetylene, 10mg catalyst (2.6mol% Cu), 0.5mL DCM, RT.

In terms of %yield, each recycling had a consistent yield, with the overall trend showing a slight decrease but still maintaining a close to full conversion. It can be seen that the leaching profile of the 5h reaction started high but slowly decreased as the recycling runs increased. It should be noted that by decreasing the reaction time from

24h to 5h, we maintained the yield while decreasing the amount of Cu in **Bn-*triazole*-Ph** by over half. This was an important point since prolonged exposure of **Bn-*triazole*-Ph** to the catalyst suggested continuous and unnecessary loss of Cu. We suggest the reaction should be stopped as soon as the product is completely formed to remove stop further Cu loss. Graph 4.5 is a plot of the 24h reaction vs the 5h reaction to visualize this Cu content difference.

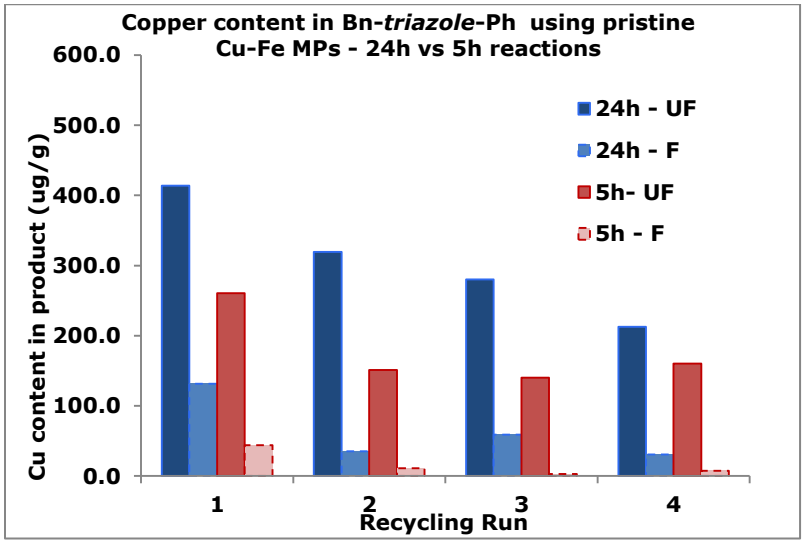

Graph 4.5. Comparison of Cu content in **Bn-*triazole*-Ph** after four recycling runs using Cu-Fe MPs reacting for 24h versus 5h. The Cu content can be decreased by over half by reducing the reaction time to the minimum required for full conversion.

4.4.3 Time study of carbon coated C@Cu-Fe MPs in reaction

The carbon coated Cu-Fe MPs were tested in catalysis to determine exact reaction time. Table 4.1 outlines the %yield and Cu content results.

Reaction Time	%Yield	Cu content (ug/g) - unfiltered	Cu content (ug/g) - filtered
3h	>5%	---	---
5h	>5%	---	---
10h	10%	---	---
18h	95.4	71.1	4.2
24h	99.6	86.0	8.8

Table 4.1. Time study of C@Cu-Fe MPs in the click reaction of benzyl azide and phenyl acetylene, with the Cu content in the unfiltered and filtered product, **Bn-*triazole*-Ph**. Reaction conditions: 0.5mmol benzyl azide, 0.5mmol phenyl acetylene, 10mg catalyst (2.0mol% Cu), 0.5mL DCM, RT.

It was found that the reaction was complete after 18h, where the reaction was stopped after 3h, 5h, 10h, 18h and 24h. Since the yields of the first three reactions were so low, ICP was only done on the 18h and 24h reactions. Both values, around 80ug/g were greatly lower than the values found for the uncoated particles at the time of completion (between 300 and 500 ug/g). Of course this came at the cost of a slower reaction. The next step was to set up recycling runs every 18h to determine recyclability and leaching profile of these carbon coated particles. The next section outlines these efforts.

4.4.4 Carbon coated C@Cu-Fe MPs – 18h recycling reactions

Next, we set up recycling runs using the C@Cu-Fe MPs for 18h runs. The following %yields and Cu contents were found (Graph 4.6a, 4.6b).

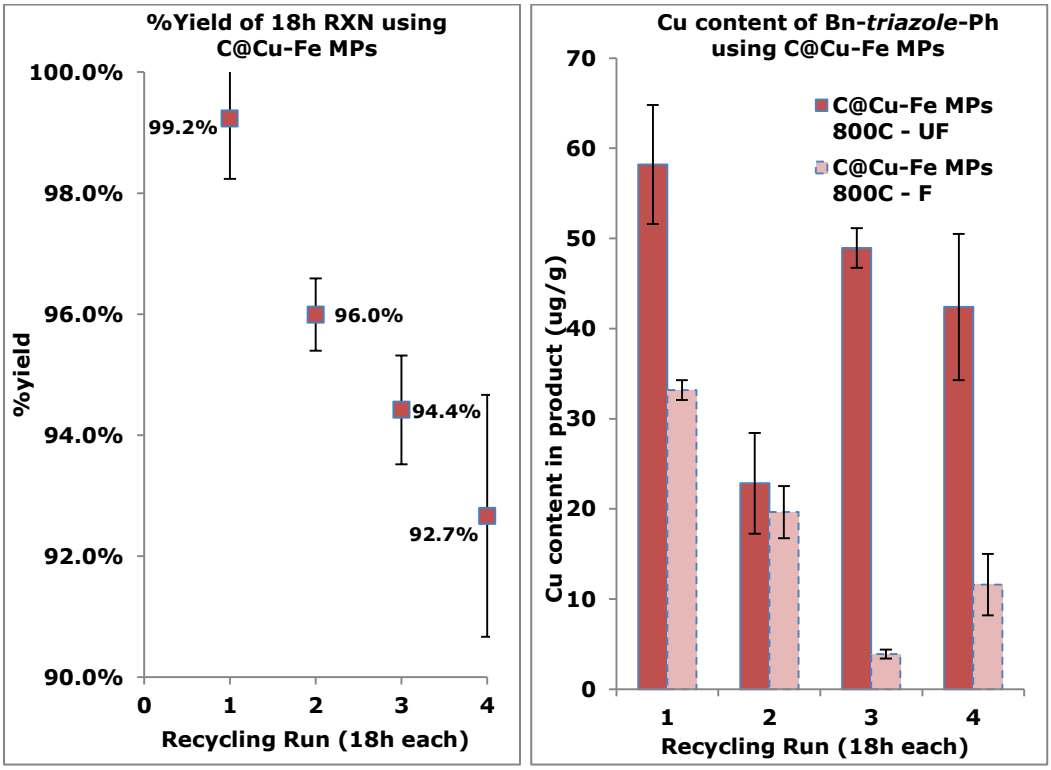

Graph 4.6a, 4.6b. **a)** %yield of **Bn-*triazole*-Ph** using carbon coated particles (left); **b)** Cu content of **Bn-*triazole*-Ph** unfiltered, UF (solid lines) and filtered, F (dashed lines) during each recycling run (right). Reaction conditions for C@Cu-Fe MPs-800^{0}C: 0.5mmol benzyl azide, 0.5mmol phenyl acetylene, 10mg catalyst (2.7mol% Cu), 0.5mL DCM, RT.

The yields for both these reaction recycled over four runs followed the same trend in general, where, the %yield decreased slowly run after run. The Cu content for the physically detached (unfiltered) Cu in both cases followed a similar profile with the carbon coating having less Cu overall.

4.4.5 Time study of annealed only (ann-Cu-Fe MPs) in reaction

Since the carbon coated particles prepared required an annealing step, we were interested to study the effect of a simple annealing step, with no carbon exposure, on both catalytic activity and Cu loss. We thus took Cu-Fe MPs and only annealed them at 800^{o}C, without coating with glucose. We performed a time study to find the time of reaction (Graph 4.7a) and Cu loss profile (Graph 4.7b).

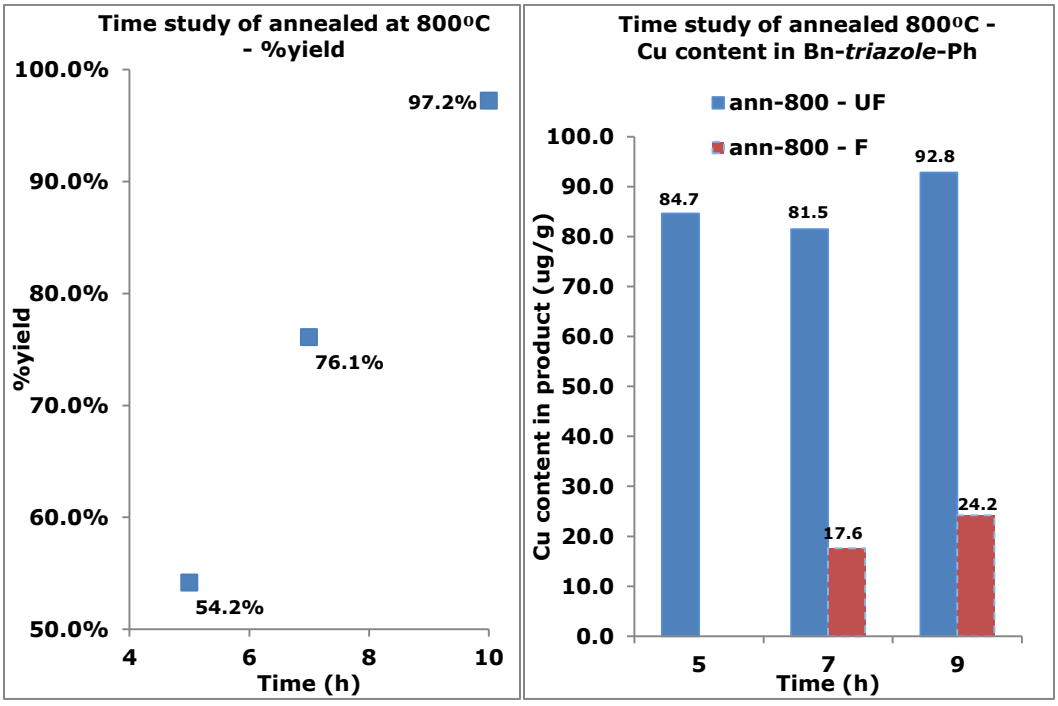

Graph 4.7a, 4.7b. Time study of **a)** %yield of **Bn-*triazole*-Ph** (left) **b)** Cu content (ug/g) in **Bn-*triazole*-Ph** at same time intervals, where the solid line corresponds to the unfiltered product and the dashed line the filtered **Bn-*triazole*-Ph** (right). Reaction conditions for annealed-800^{o}C Cu-Fe MPs: 0.5mmol benzyl azide, 0.5mmol phenyl acetylene, 7.5mg catalyst (3.0mol% Cu), 0.5mL DCM, RT.

Based on the time study done on the annealed particles at 800^{o}C, it was found that the reaction completion time was 10h. Correlating this to the Cu content in **Bn-**

***triazole*-Ph**, it was found that the Cu from catalyst detachment (solid line) was about 85µg/g or five times more than the Cu ion leaching (dotted lines), which was about 20 µg/g. To better understand the structure and morphology of these particles, full characterization was required and will be discussed in section 4.5.

4.4.5.1 Annealed-only Cu-Fe MPs --10h Recycling

After finding the optimal reaction time for the ann-Cu-Fe MPs (10h), recycling runs were set up and the Cu content of **Bn-*triazole*-Ph** measured (unfiltered and filtered). Graph 8a, 8b show the results of this recycling.

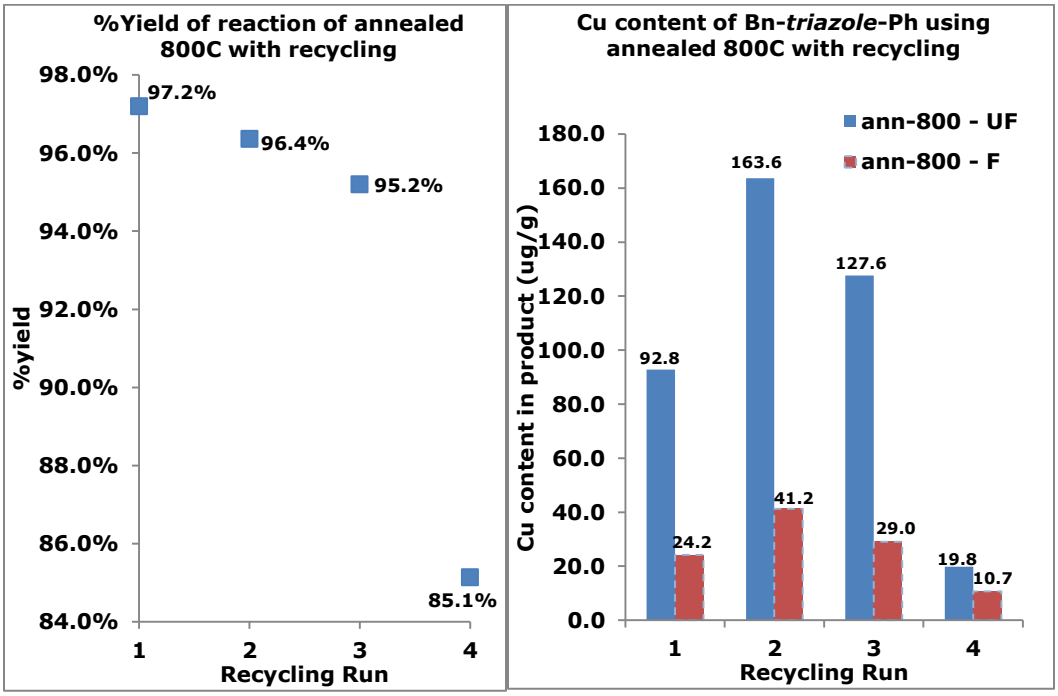

Graph 4.8a, 4.8b. **a)** %yield of **Bn-*triazole*-Ph** using ann-Cu-Fe MPs (left); **b)** Cu content of **Bn-*triazole*-Ph** unfiltered (solid lines) and filtered (dashed lines) (right). Reaction conditions for ann-Cu-Fe MPs: 0.5mmol benzyl azide, 0.5mmol phenyl acetylene, 7.5mg catalyst (3.0mol% Cu), 0.5mL DCM, RT.

Surprisingly and contrary to the results obtained with both uncoated and carbon coated Cu-Fe MPs, the reaction %yield at the 4th recycle dropped dramatically by 10%. This drop in %yield could be correlated to a decrease in copper content in **Bn-*triazole*-Ph**. This could be explained by a loss of Cu from the surface of the catalyst.

4.4.6 Comparison of Cu-Fe MPs vs C@Cu-Fe MPs vs ann-Cu-Fe MPs

To determine the best particles in terms of Cu leaching, we compared the uncoated Cu-Fe MPs, C@Cu-Fe MPs and ann-Cu-Fe MPs in terms of yield (Graph 4.9a) and Cu content in the unfiltered **Bn-*triazole*-Ph** (Graph 4.9b).

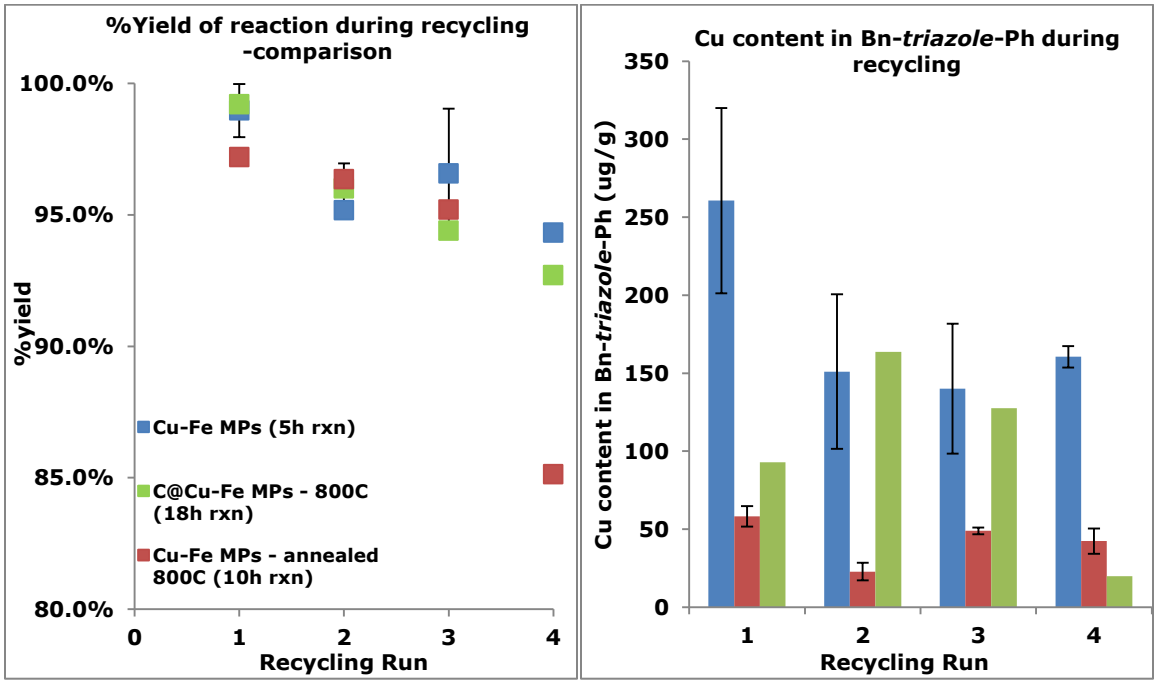

Graph 4.9a, 4.9b. a) Comparison of %yield of **Bn-*triazole*-Ph** using Cu-Fe MPs, carbon coated C@Cu-Fe MPs and ann-Cu-Fe MPs (left); **b)** Cu content in **Bn-*triazole*-Ph** using Cu-Fe MPs, carbon coated C@Cu-Fe MPs and and ann-Cu-Fe MPs (right).

Graph 4.9a shows that all three catalysts have similar recyclability, except the ann-Cu-Fe MPs that have a steeper decrease after the fourth run. It should be noted that the pristine Cu-Fe MPs required five hours to achieve the product **Bn-*triazole*-Ph**, whereas the carbon coated C@Cu-Fe MPs required 18 hours and the ann-Cu-Fe MPs need 10 hours. However, this lengthened reaction time did not correlate to an increase in copper content. Graph 4.9b shows that the amount of Cu in **Bn-*triazole*-Ph** for the carbon coated particles was on average 4-6 times less than the uncoated particles. This was an interesting point because longer reaction times generally correlate to higher Cu content in **Bn-*triazole*-Ph** (as was seen in Graph 4.5), because of prolonged exposure to the copper on the catalyst. Characterization of these particles, which will be discussed in

section 4.5, gave insight into how the structures and morphologies for pristine, carbon coated, and annealed-only particles translated into differences in catalytic activity and Cu loss. Overall, the carbon coated particles showed a significant decrease in Cu content in **Bn-*triazole*-Ph** and were the best performing, if Cu loss into the product of reaction is of concern.

4.5 Characterization of carbon coated Cu-Fe MPs and annealed-only Cu-Fe MPs

To better understand how these catalysts worked to catalyze the click reaction between benzyl azide and phenyl acetylene, a complete characterization of the particles was needed to understand their shape, size, morphology and chemical composition. As with the previous chapter, we employed several techniques such as transmission and scanning electron microscopy (TEM and SEM), coupled with Energy-dispersive X-ray spectroscopy (EDX), electron energy loss spectroscopy (EELS) spectroscopy and X-ray Photoelectron Spectroscopy (XPS). A full analysis of the Cu-Fe MPs was recently published in our group[36] which outlines mechanisms of growth of Cu onto the Fe MPs with detailed characterization similar to what was undertaken for these coated particles. Each set of particles was thus characterized to give an idea of what they looked like and how they may work.

4.5.1 Introduction to characterization of annealed particles

Annealing or thermal treatments of a material, has commonly been used in metallurgy to refine grain structure and relieve internal stress. In the case of Fe NPs, it has been shown that annealing can refine the crystalline structure and give physiochemical changes such as the recrystallization of the bulk metallic cores and changes to the surface oxides, such as thinning, dehydration, and migration of impurities toward surfaces[46]. Crane et al[46] vacuum annealed Fe NPs and Fe_3O_4 NPs and found both types of particles were arranged in chains and rings, due to their magnetic abilities. After annealing at 500^{o}C for 24h, they still observed the same arrangement except with some diffusion bonding between the otherwise discrete particles (Figure

4.1a, 4.1b). They found this occurred more in the Fe NPs, not only visually but also through a decrease in surface area determined by BET analysis.

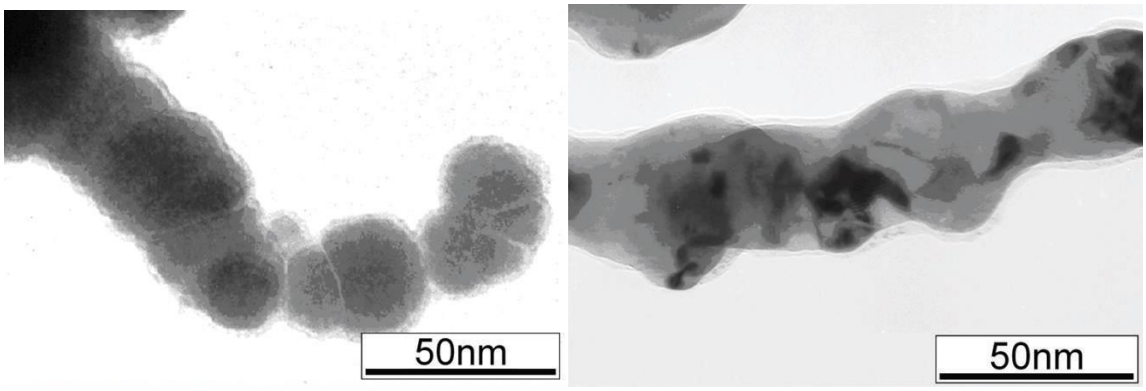

Figure 4.1a, 4.1b. a) Fe NPs before annealing (left) and **b)** after annealing at 500°C for 24h (right) under vacuum. Images taken from Crane et al.[46]

Vargas et al[47] prepared Fe_3O_4 NPs stabilized with oleic acid and oleylamine, to determine if there were size and morphology changes at different annealing temperatures. They found that, annealing at 300°C only resulted in slightly larger particles (from 5nm to 6nm) and was not a high enough temperature for decomposition of organics from the surface. Furthermore, there were insignificant changes in the morphology and crystallinity of the particles. This suggests low temperature annealing only induces a reduction in the number of defect centers and no real growth effects. High temperature annealing, however, showed decomposition of organics at 550°C. Moreover, there was a bimodal size distribution of the magnetite nanoparticles with 6 nm and 17 nm mean sizes, respectively.

In this section, characterization was done to determine the changes in size and morphology when the particles were carbon coated and/or annealed at two different temperatures. Techniques including SEM, TEM and XPS were used. We propose herein hypothesis to rationalize catalytic activity and Cu loss into **Bn-*triazole*-Ph** using the structural information gained.

4.5.2 Carbon Coated C@Cu-Fe MPs

To understand how the morphology of the Cu-Fe MPs changed when introducing glucose and annealing, SEM was done to visualize the surface of the carbon coated C@Cu-Fe MPs. Figure 4.2a shows what these particles look like and Figure 4.2b are the pristine Cu-Fe MPs as a comparison.

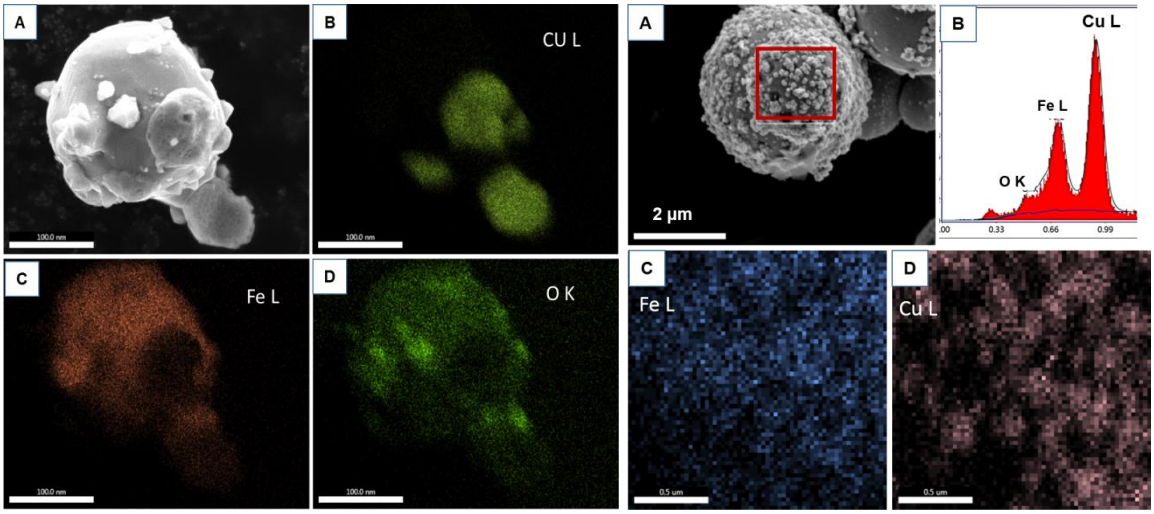

Figure 4.2a, 4.2b. a) SEM of C@Cu-Fe MPs with EDX maps of Cu, Fe and O (left). **b)** SEM of pristine Cu-Fe MPs with EDX maps of Cu and Fe (right).

The carbon coated C@Cu-Fe MPs looked very different from the pristine Cu-Fe MPs. The biggest difference was the distribution of Cu particles on the surface. In the carbon coated particles, there were large crystallites of copper concentrated together as opposed to the pristine Cu-Fe MPs which were small crystallites dispersed throughout the surface of the Fe. Furthermore, not all the crystallites on the coated particles were Cu. From the EDX mapping, there were also iron oxide crystallites on the surface. This suggests the iron oxide shell could have been disrupted and recrystallized into smaller crystallites.

XPS and Auger spectra for the C@Cu-Fe MPs were collected and presented in Figure 4.3a (top) and compared to the pristine Cu-Fe MPs in Figure 4.3b (bottom). Table 4.2 also outlines the percentages of each oxidation state present.

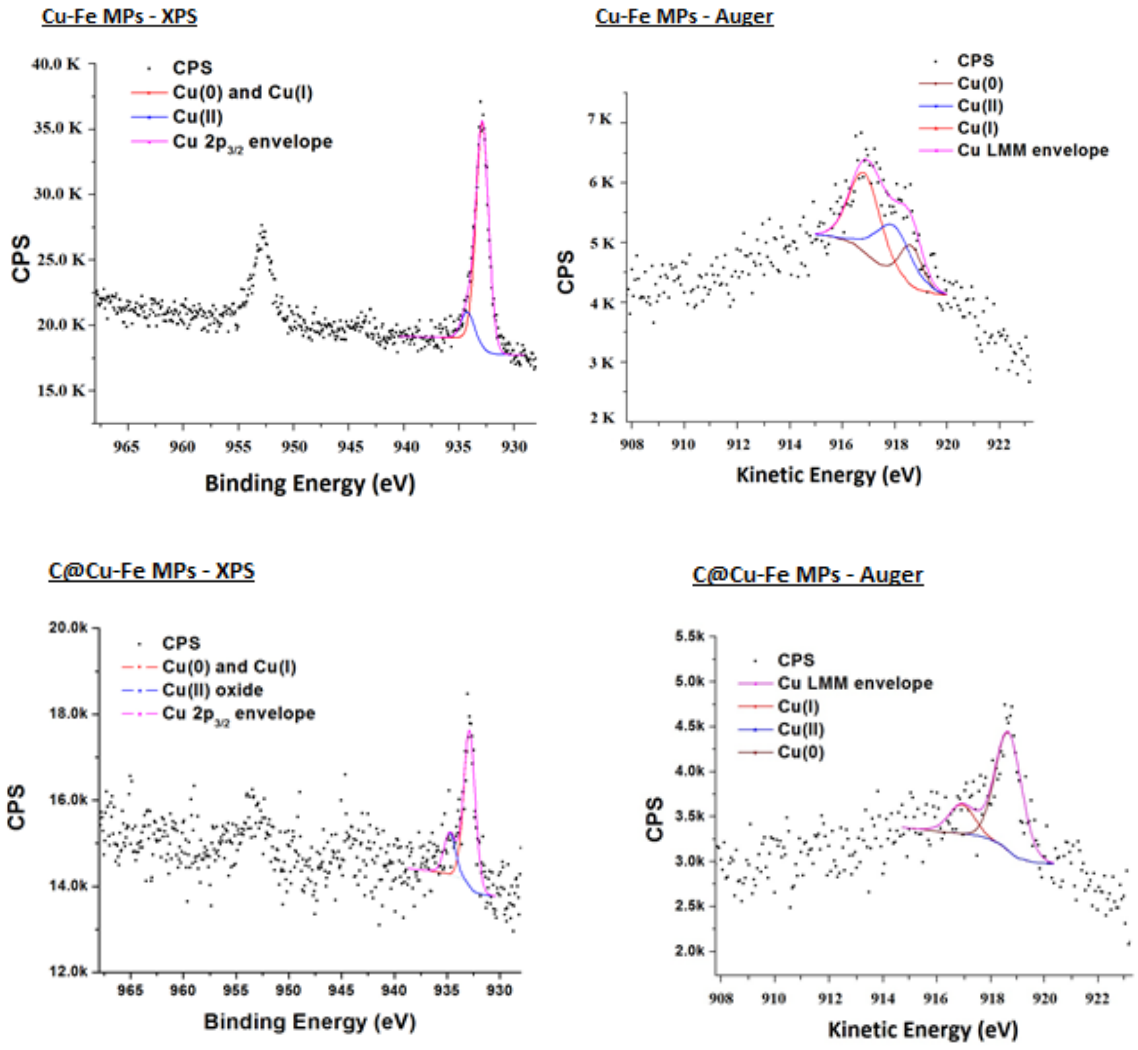

Figure 4.3a, 4.3b. XPS (left) and Auger (right) spectra of **a)** pristine Cu-Fe MPs (top) **b)** C@Cu-Fe MPs annealed at 800°C (bottom).

Oxidation state of Cu	% contained in Pristine Cu-Fe MPs	% contained in C@Cu-Fe MPs
Cu(0) – Cu Metal	23%	30%
Cu(I) – Cu_2O	63%	49%
Cu(II) - CuO	14%	20%

Table 4.2. Percentages of each oxidation state contained in pristine Cu-Fe MPs and C@Cu-Fe MPs.

4.5.2.1 Morphology and catalytic activity

Carbon coated particles were found to have a lower level of leaching during catalysis; an average of 2-3 times less over the course of four recycling runs, however,

the reaction took almost 4 times longer than with the uncoated Cu-Fe MPs (18h vs 5h). We rationalized this based on the Cu crystallites on the surface being much more concentrated in certain sections, (Figure 4.2a) compared to the pristine Cu-Fe MPs (Figure 4.2b). This meant less surface area and lower probability of interaction of the reagents with the Cu. Also, Table 4.2 shows that the amount of Cu(I) has decreased and the amount of Cu(II) has increased. This may have also played a role in the decrease in activity.

4.5.3. Annealed Cu-Fe MPs (ann-Cu-Fe MPs)

To determine the structure and morphology of the annealed Cu-Fe MPs, SEM was done to visualize the surface. Figure 4.4a, 4.4b are SEM images of the annealed at 800^{o}C Cu-Fe MPs. Figure 4.4c shows the EDAX of the surface.

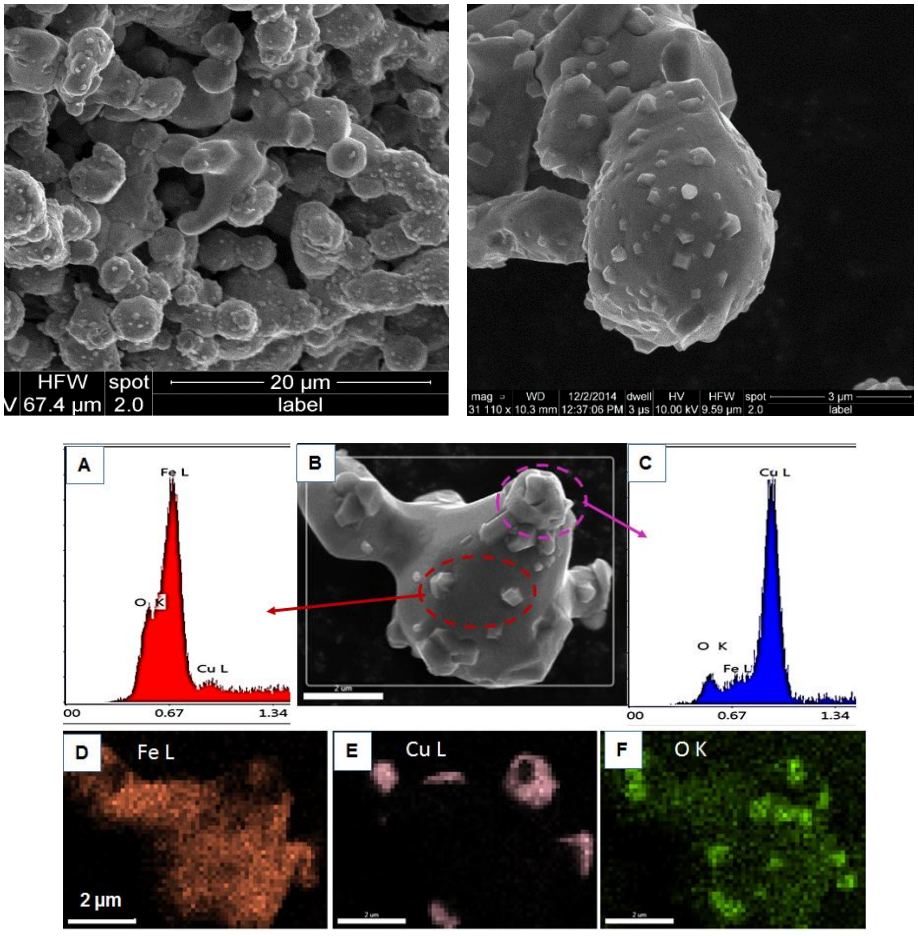

Figure 4.4a, 4.4b, 4.4c. a) SEM of the overall sample of ann-Cu-Fe MPs (top, left) **b)** Zoomed-in of one particle (top, right) **c)** EDX mapping of the crystallites found on the Fe MPs (bottom).

The ann-Cu-Fe MPs changed their shape and morphology quite drastically upon heating to 800°C, as was seen with the carbon coated. It appeared there were three major changes between these particles and the pristine Cu-Fe MPs. First, the Fe MPs fused together and formed interconnected networks. Figure 4.4a shows the formation of this Fe framework by diffusion bonding, which was also seen by Crane et al in Figure 4.1. Second, the EDX spectra showed that the smaller crystallites were actually iron oxides, and not Cu. This suggested the thin crystalline iron oxide shell broke apart and agglomerated into larger crystallites. Finally, the small Cu crystallites found in the pristine Cu-Fe MPs agglomerated into larger crystallites, which could have been caused by the iron oxide shell experiencing the same phenomenon.

It proved difficult to specifically select individual Cu crystallites to analyze by XPS to determine oxidation state. However, for the overall sample, we could determine the Cu oxidation as an average. Figure 4.5a and 4.5b show the XPS and Auger spectra of pristine Cu-Fe MPs (top) and the ann-Cu-Fe MPs (bottom).

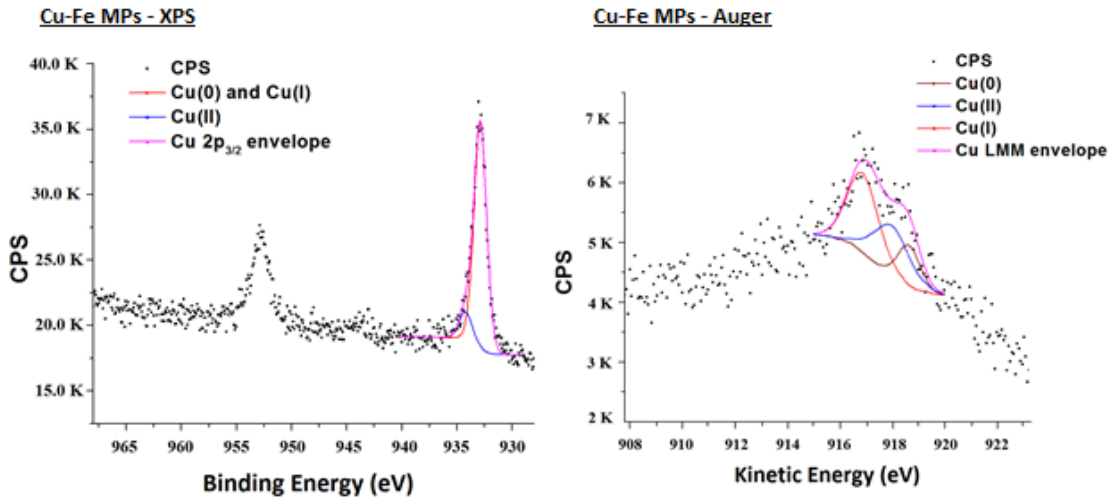

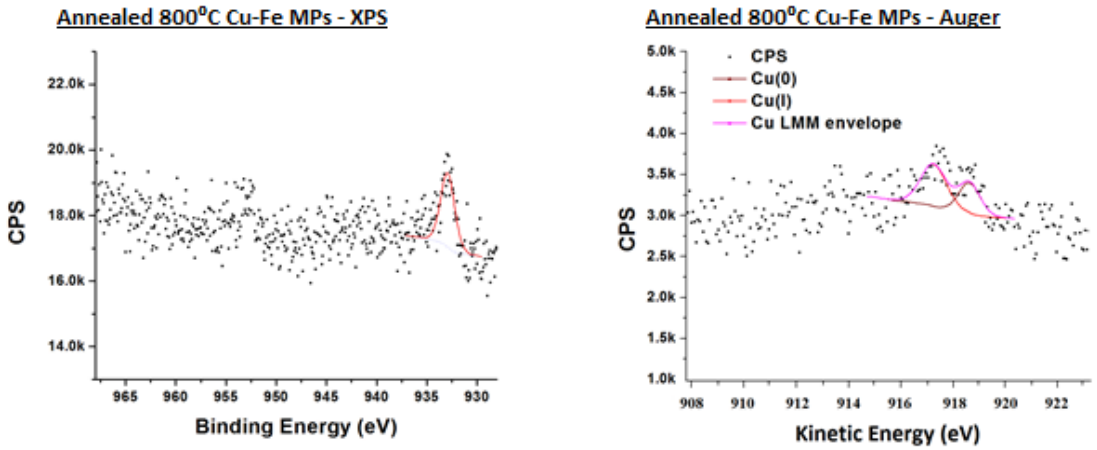

Figure 4.5a, 4.5b. XPS (left; top, bottom) and Auger (right; top, bottom) spectra of **a)** pristine Cu-Fe MPs (top; left, right) **b)** Cu-Fe MPs annealed at 800°C (bottom; left, right).

Oxidation state of Cu	% contained in Pristine Cu-Fe MPs	% contained in annealed 800°C Cu-Fe MPs
Cu(0) – Cu Metal	23%	38%
Cu(I) – Cu_2O	63%	62%
Cu(II) - CuO	14%	0%

Table 4.3. Percentages of each oxidation state contained in pristine Cu-Fe MPs and annealed 800°C Cu-Fe MPs.

It can be seen based on the XPS spectrum, the pristine Cu-Fe MPs, Figure 4.5a, contained mostly Cu(0) and Cu(I) with some Cu(II). Interestingly, the annealed sample had no Cu(II) and the same amount of Cu(I), as seen in Table 4.3.

4.5.3.1 Morphology and catalytic activity – annealed Cu-Fe MPs

The annealed Cu-Fe MPs had less leaching but required longer reaction time than the pristine Cu-Fe MPs. This could be explained by the fact the annealed particles had a smaller distribution of large Cu crystallites meaning smaller surface area. This implied slower reaction, but also slower leaching. Interestingly, the amount of Cu(I) was the same in the pristine Cu-Fe MPs as in the annealed counterparts (Table 4.2), this explaining that the reaction time difference was not so large, with 5h for pristine particles vs 10h for annealed one.

4.6 Conclusions

Our goal of attempting to decrease the amount of Cu loss through Cu leaching and catalyst detachment was successful. We found that pristine Cu-Fe MPs used without modification could catalyze the click reaction between benzyl azide and phenyl acetylene in 5 hours with about 260µg/g of Cu in **Bn-*triazole*-Ph** after the first run. When we coated these same particles with carbon at 800^{o}C, the amount of Cu in **Bn-*triazole*-Ph** dropped to about 60µg/g of Cu after the first run. The annealing of the Cu-Fe MPs at 800^{o}C was helpful for decreasing Cu loss but the presence of the carbon layer in conjunction with the annealing at 800^{o}C was vital to decrease leaching an average of 4-6 times compared to the pristine Cu-Fe MPs. With this decrease in leaching, reaction times were extended almost four times when the carbon coated particles were used and two times with just annealing. We hypothesized that perhaps the carbon coating inhibited direct Cu contact with the azide and alkyne which slowed the reaction in addition to the larger Cu crystallites present after exposure to 800^{o}C annealing temperature. However, we believe to have created a more heterogeneous catalyst with the carbon coating because despite the longer reaction times, this did not correspond to greater leaching as it did with the pristine Cu-Fe MPs. During characterization, we were unable to visualize the carbon layer and could not comment on its size and morphology. Our carbon coated Cu-Fe MPs at 800^{o}C are a good option for use in CuAAC when a low-leaching catalyst is required which does not need further purification after magnet removal.

4.7 References

1. Meldal, M.; Tornøe, C. W., Cu-Catalyzed Azide−Alkyne Cycloaddition. *Chem. Rev. (Washington, DC, U. S.)* **2008,** *108* (8), 2952-3015.
2. Struthers, H.; Mindt, T. L.; Schibli, R., Metal chelating systems synthesized using the copper(i) catalyzed azide-alkyne cycloaddition. *Dalton Trans.* **2010,** *39* (3), 675-696.
3. Hein, J. E., Fokin, V. V., Copper-catalyzed azide-alkyne cycloaddition (CuAAC) and beyond: new reactivity of copper(i) acetylides. *Chem. Soc. Rev.* **2010,** *39* (4), 1302-1315.
4. Rostovtsev, V. V.; Green, L. G.; Fokin, V. V.; Sharpless, K. B., A Stepwise Huisgen Cycloaddition Process: Copper(I)-Catalyzed Regioselective "Ligation" of Azides and Terminal Alkynes. *Angewandte Chemie International Edition* **2002,** *41* (14), 2596-2599.

5. Chan, T. R.; Hilgraf, R.; Sharpless, K. B.; Fokin, V. V., Polytriazoles as Copper(I)-Stabilizing Ligands in Catalysis. *Org. Lett.* **2004,** *6* (17), 2853-2855.
6. Worrell, B. T.; Malik, J. A.; Fokin, V. V., Direct Evidence of a Dinuclear Copper Intermediate in Cu(I)-Catalyzed Azide-Alkyne Cycloadditions. *Science* **2013,** *340* (6131), 457-460.
7. Decan, M. R.; Impellizzeri, S.; Marin, M. L.; Scaiano, J. C., Copper nanoparticle heterogeneous catalytic 'click' cycloaddition confirmed by single-molecule spectroscopy. *Nat Commun* **2014,** *5*.
8. Ahmad Fuaad, A.; Azmi, F.; Skwarczynski, M.; Toth, I., Peptide Conjugation via CuAAC 'Click' Chemistry. *Molecules* **2013,** *18* (11), 13148-13174.
9. Letelier, M. E.; Lepe, A. M.; Faúndez, M.; Salazar, J.; Marín, R.; Aracena, P.; Speisky, H., Possible mechanisms underlying copper-induced damage in biological membranes leading to cellular toxicity. *Chem.-Biol. Interact.* **2005,** *151* (2), 71-82.
10. Gaetke, L. M.; Chow, C. K., Copper toxicity, oxidative stress, and antioxidant nutrients. *Toxicology* **2003,** *189* (1–2), 147-163.
11. Song, L.; Connolly, M.; Fernández-Cruz, M. L.; Vijver, M. G.; Fernández, M.; Conde, E.; de Snoo, G. R.; Peijnenburg, W. J. G. M.; Navas, J. M., Species-specific toxicity of copper nanoparticles among mammalian and piscine cell lines. *Nanotoxicology* **2014,** *8* (4), 383-393.
12. Agard, N. J.; Prescher, J. A.; Bertozzi, C. R., A Strain-Promoted [3 + 2] Azide−Alkyne Cycloaddition for Covalent Modification of Biomolecules in Living Systems. *J. Am. Chem. Soc.* **2004,** *126* (46), 15046-15047.
13. Jewett, J. C.; Bertozzi, C. R., Cu-free click cycloaddition reactions in chemical biology. *Chem. Soc. Rev.* **2010,** *39* (4), 1272-1279.
14. Sletten, E. M.; Bertozzi, C. R., A Hydrophilic Azacyclooctyne for Cu-Free Click Chemistry. *Org. Lett.* **2008,** *10* (14), 3097-3099.
15. Agard, N. J.; Baskin, J. M.; Prescher, J. A.; Lo, A.; Bertozzi, C. R., A Comparative Study of Bioorthogonal Reactions with Azides. *ACS Chem. Biol.* **2006,** *1* (10), 644-648.
16. Yan, W.; Lien, H.-L.; Koel, B. E.; Zhang, W.-x., Iron nanoparticles for environmental clean-up: recent developments and future outlook. *Environmental Science: Processes & Impacts* **2013,** *15* (1), 63-77.
17. Macdonald, J. E.; Kelly, J. A.; Veinot, J. G. C., Iron/Iron Oxide Nanoparticle Sequestration of Catalytic Metal Impurities from Aqueous Media and Organic Reaction Products. *Langmuir* **2007,** *23* (19), 9543-9545.
18. Liendo, M.; Navarro, G.; Sampaio, C., Nano and Micro ZVI in Aqueous Media: Copper Uptake and Solution Behavior. *Water, Air, Soil Pollut.* **2013,** *224* (5), 1-8.
19. Li, X.-q.; Zhang, W.-x., Iron Nanoparticles: the Core−Shell Structure and Unique Properties for Ni(II) Sequestration. *Langmuir* **2006,** *22* (10), 4638-4642.
20. Hudson, R.; Li, C.-J.; Moores, A., Magnetic copper-iron nanoparticles as simple heterogeneous catalysts for the azide-alkyne click reaction in water. *Green Chem.* **2012,** *14* (3), 622-624.
21. Ishikawa, S.; Hudson, R.; Moores, A.; Li, C. J., LIGAND MODIFIED CuFe2O4 NANOPARTICLES AS MAGNETICALLY RECOVERABLE AND REUSABLE CATALYST FOR AZIDE-ALKYNE CLICK CONDENSATION. *Heterocycles* **2012,** *86* (2), 1023-1030.
22. Simpson, E. R.; Clyne, C.; Rubin, G.; Boon, W. C.; Robertson, K.; Britt, K.; Speed, C.; Jones, M., AROMATASE—A BRIEF OVERVIEW. *Annu. Rev. Physiol.* **2002,** *64* (1), 93-127.
23. Simpson, E. R., Sources of estrogen and their importance. *The Journal of Steroid Biochemistry and Molecular Biology* **2003,** *86* (3–5), 225-230.
24. (a) Njar, V. C. O.; Grun, G.; Hartmann, R. W., Evaluation of 6,7-Aziridinyl Steroids and Related Compounds as Inhibitors of Aromatase (P-450arom). *J. Enzyme Inhib. Med. Chem.* **1995,**

9 (3), 195-202; (b) Vinggaard, A. M.; Hnida, C.; Breinholt, V.; Larsen, J. C., Screening of selected pesticides for inhibition of CYP19 aromatase activity in vitro. *Toxicol. in Vitro* **2000,** *14* (3), 227-234.
25. Ohno, K.; Araki, N.; Yanase, T.; Nawata, H.; Iida, M., A Novel Nonradioactive Method for Measuring Aromatase Activity Using a Human Ovarian Granulosa-Like Tumor Cell Line and an Estrone ELISA. *Toxicol. Sci.* **2004,** *82* (2), 443-450.
26. Zheng, D.; Seferos, D. S.; Giljohann, D. A.; Patel, P. C.; Mirkin, C. A., Aptamer Nano-flares for Molecular Detection in Living Cells. *Nano Lett.* **2009,** *9* (9), 3258-3261.
27. Nutiu, R.; Li, Y., Structure-Switching Signaling Aptamers. *J. Am. Chem. Soc.* **2003,** *125* (16), 4771-4778.
28. Yildirim, N.; Long, F.; Gao, C.; He, M.; Shi, H.-C.; Gu, A. Z., Aptamer-Based Optical Biosensor For Rapid and Sensitive Detection of 17β-Estradiol In Water Samples. *Environ. Sci. Technol.* **2012,** *46* (6), 3288-3294.
29. Kolb, H. C.; Finn, M. G.; Sharpless, K. B., Click Chemistry: Diverse Chemical Function from a Few Good Reactions. *Angewandte Chemie International Edition* **2001,** *40* (11), 2004-2021.
30. King, T. L.; Brucker, M. C., *Pharmacology for women's health*. Jones and Bartlett Publishers: Sudbury, Mass., 2011.
31. Dervaux, B.; Du Prez, F. E., Heterogeneous azide-alkyne click chemistry: towards metal-free end products. *Chemical Science* **2012,** *3* (4), 959-966.
32. Masnadi, M.; Yao, N.; Braidy, N.; Moores, A., Cu(II) Galvanic Reduction and Deposition onto Iron Nano- and Microparticles: Resulting Morphologies and Growth Mechanisms. *Langmuir* **2014**.
33. (a) Cintas, P.; Barge, A.; Tagliapietra, S.; Boffa, L.; Cravotto, G., Alkyne-azide click reaction catalyzed by metallic copper under ultrasound. *Nat. Protoc.* **2010,** *5* (3), 607-616; (b) Carboni, B.; Benalil, A.; Vaultier, M., Aliphatic amino azides as key building blocks for efficient polyamine syntheses. *The Journal of Organic Chemistry* **1993,** *58* (14), 3736-3741.
34. Castonguay, A. B., M.; Masnadi, M.; Feng, Y.; Bao, H.; Li, C.J.; Maysinger, D.; Moores, A., Magnetic Cu@Fe Catalysts for the Synthesis of Biologically Relevant Molecules via Click Chemistry. *submitted* **2015**.
35. Kovacs, S.; Zih-Perenyi, K.; Revesz, A.; Novak, Z., Copper on Iron: Catalyst and Scavenger for Azide-Alkyne Cycloaddition. *Synthesis-Stuttgart* **2012,** *44* (24), 3722-3730.
36. Masnadi, M.; Yao, N.; Braidy, N.; Moores, A., Cu(II) Galvanic Reduction and Deposition onto Iron Nano- and Micro-Particles: Resulting Morphologies and growth Mechanisms. *Langmuir* **2014**.
37. Poulston, S.; Parlett, P. M.; Stone, P.; Bowker, M., Surface Oxidation and Reduction of CuO and Cu2O Studied Using XPS and XAES. *Surf. Interface Anal.* **1996,** *24* (12), 811-820.
38. (a) Rodionov, V. O.; Presolski, S. I.; Diaz, D. D.; Fokin, V. V.; Finn, M. G., Ligand-Accelerated Cu-Catalyzed Azide-Alkyne Cycloaddition: A Mechanistic Report. *J. Am. Chem. Soc.* **2007,** *129* (42), 12705-12712; (b) Aromí, G.; Barrios, L. A.; Roubeau, O.; Gamez, P., Triazoles and tetrazoles: Prime ligands to generate remarkable coordination materials. *Coord. Chem. Rev.* **2011,** *255* (5–6), 485-546.
39. Rodionov, V. O.; Fokin, V. V.; Finn, M. G., Mechanism of the Ligand-Free CuI-Catalyzed Azide–Alkyne Cycloaddition Reaction. *Angew. Chem.* **2005,** *117* (15), 2250-2255.
40. Barbaro, P.; Liguori, F. Heterogenized Homogeneous Catalysts for Fine Chemicals Production Materials and Processes.
41. (a) Li, H.; Zhou, H., Enhancing the performances of Li-ion batteries by carbon-coating: present and future. *Chem. Commun. (Cambridge, U. K.)* **2012,** *48* (9), 1201-1217; (b) Wang, Z.; Tian, W.; Liu, X.; Yang, R.; Li, X., Synthesis and electrochemical performances of amorphous

carbon-coated Sn–Sb particles as anode material for lithium-ion batteries. *J. Solid State Chem.* **2007,** *180* (12), 3360-3365; (c) Ponrouch, A.; Goni, A. R.; Sougrati, M. T.; Ati, M.; Tarascon, J.-M.; Nava-Avendano, J.; Palacin, M. R., A new room temperature and solvent free carbon coating procedure for battery electrode materials. *Energy & Environmental Science* **2013,** *6* (11), 3363-3371; (d) Wang, C.; Guo, Z.; Shen, W.; Xu, Q.; Liu, H.; Wang, Y., B-doped Carbon Coating Improves the Electrochemical Performance of Electrode Materials for Li-ion Batteries. *Adv. Funct. Mater.* **2014,** *24* (35), 5511-5521.
42. Zhang, D.; Wei, S.; Kaila, C.; Su, X.; Wu, J.; Karki, A. B.; Young, D. P.; Guo, Z., Carbon-stabilized iron nanoparticles for environmental remediation. *Nanoscale* **2010,** *2* (6), 917-919.
43. Lu, A. H.; Salabas, E. L.; Schuth, F., Magnetic nanoparticles: Synthesis, protection, functionalization, and application. *Angewandte Chemie-International Edition* **2007,** *46* (8), 1222-1244.
44. Grass, R. N.; Athanassiou, E. K.; Stark, W. J., Covalently Functionalized Cobalt Nanoparticles as a Platform for Magnetic Separations in Organic Synthesis. *Angewandte Chemie International Edition* **2007,** *46* (26), 4909-4912.
45. Huang, C.-H.; Wang, H. P.; Chang, J.-E.; Eyring, E. M., Synthesis of nanosize-controllable copper and its alloys in carbon shells. *Chem. Commun. (Cambridge, U. K.)* **2009,** (31), 4663-4665.
46. Crane, R. A.; Scott, T. B., The Effect of Vacuum Annealing of Magnetite and Zero-Valent Iron Nanoparticles on the Removal of Aqueous Uranium. *Journal of Nanotechnology* **2013,** *2013*, 11.
47. Vargas, J. M.; Lima, E.; Socolovsky, L. M.; Knobel, M.; Zanchet, D.; Zysler, R. D., Annealing Effects on 5 nm Iron Oxide Nanoparticles. *J. Nanosci. Nanotechnol.* **2007,** *7* (9), 3313-3317.
48. Bergmeier, S. C., Benzyl Azide. In *Encyclopedia of Reagents for Organic Synthesis*, John Wiley & Sons, Ltd: 2001.

4.8 Appendix

4.8.1 Materials and Reagents

All reactants were purchased from Sigma Aldrich and used as received unless otherwise noted. Organic azides (benzyl azide) was synthesized from the corresponding bromides via previously reported procedures[33a]. All reactions were carried out in an oxygen-free glovebox, except where noted, and all solvents were de-gassed for 20 minutes prior to use.

4.8.2 Synthesis of carbon coated Cu-Fe particles (C@Cu-Fe MPs)

The following procedure was used to prepare C@Cu-Fe particles. The particles were prepared and characterized by Mitra Masnadi, with the exception of the Cu content measured by ICP-OES, which was done by me.

To prepare the C@Cu-Fe particles, a 1:10 batch of Cu-Fe MPs was prepared as usual. First, 250mg of the 1:10 Cu-Fe MPs were weighed in a 250mL round bottom flask and vacuum and purged with argon. In another round bottom flask, 500mg of glucose was dissolved in 20mL milliQ water and degassed under argon for 20 minutes. This solution was then syringed into the flask containing the Cu-Fe MPs and sonicated for 30 minutes. In an air-free glovebox, this solution was transferred to a Parr chamber containing a glass sleeve. The system was closed off with an adapted swagglelock and vacuum and purged with argon. The system was kept closed and attached to the Parr system and heated to 160^{o}C while stirring at 500rpm for 4 hours, then allowed to cool to room temperature on its own, which took about 1-2 hours. On the bench top, oven the Parr chamber, the catalyst washed with degassed water three times, and with degassed acetone three times, in a 250mL beaker. The sample was dried in the vacuum oven overnight at 120^{o}C. The next day, the sample was loaded into the tube furnace, purged with argon and heated to 800^{o}C for two hours to burn off the glucose and leave an amorphous coating of carbon on the Cu-Fe MPs. Once the annealing was complete, the tube furnace was allowed to cool to room temperature while under a constant flow of argon. The sample was removed, and placed in a vial and kept in a desiccator until use.

4.8.3 Synthesis of annealed Cu-Fe particles (ann-Cu-Fe MPs)

The annealed at 800^{o}C Cu-Fe MPs were simply 250mg of 1:10 Cu-Fe MPs loaded into the tube furnace and purged with argon while heated to 800^{o}C for two hours. Once the annealing was complete, the tube furnace was allowed to cool to room temperature while under a constant flow of argon. The sample was removed, and placed in a vial and kept in a desiccator until use. Table 4.4 summarized the amount of copper (%Cu) contained in each type of particle used.

Type of Cu-Fe MP	%Cu (by ICP-OES)
Pristine Cu-Fe MPs	5.4%
Carbon coated C@Cu-Fe MPs	1.9%
Annealed 800^{O}C ann-Cu-Fe MPs	5.5%

Table 4.4. Percentage of Cu found in each type of particle studied in this chapter.

4.8.4 Synthesis of benzyl azide

Benzyl azide was prepared from benzyl bromide and sodium azide. All reagents were used without further purification. To begin, 8.254g of benzyl bromide was weighed into a 100mL Schlenk round bottom flask with 25mL DMF. The solution was stirred under argon for 10 minutes. To this solution, 3.9g of sodium azide was added slowly scoop-wise. This mixture was stirred under argon for another 10 minutes then the temperature was increased to 50^{O}C under reflux and heated overnight. The solution should turn a light brown-orange colour. Once the reaction is over, remove the flask from the heat and cool to room temperature. Add 50mL of water to the flask and stir for 15 minutes, then extract with ether and saturated NaCl solution (3 x 100mL) each, and collect the ether layer. Rotovap the ether and collect a yellow liquid. ^{1}H NMR was done to confirm purity (^{1}H NMR (400 MHz, $CDCl_3$) 7.45-7.31 (5H, m, Ph), 4.36 (2H, s, CH_2)) and matched with the literature.[48] Total yield is 81.1%.

4.8.5 Storing particles for 5h reactions – Cu-Fe MPs

Since the Cu-Fe MPs were recycled four times, only two reactions could be set up per day (5 hours each). To store the particles overnight to continue recycling run 3 and 4, we tested three different storage methods: 1) drying; 2) freezing in solvent in the freezer; 3) freezing in solvent in liquid nitrogen. All tests were done in duplicate and the product of reaction was analyzed for Cu content and %yield. Our tests of drying the particles showed more inconsistent leaching in the run 3 and 4 products. We also tried keeping the particles frozen in liquid nitrogen while also having them under vacuum, which we thought would be safer as to not form any liquid O_2 in a sealed vessel. However, since there was not a constant source of liquid nitrogen, it evaporated and

eventually one of the vials shattered. The data obtained from the freezer method gave the most consistent results and was overall the safest so we kept with this method.

Chapter 5 - Conclusions and Future Work

5.1 Summary and Conclusions

In this thesis, the use of magnetically retrievable particles to catalyze CuAAC reactions for biological molecules was investigated. These Fe core-Cu shell particles were ideal due to their heterogeneous nature, where the catalyst could be removed magnetically without the need for lengthy purification processes. Their abilities in the CuAAC of rhod-N_3 and ethisterone and/or benzyl azide and phenyl acetylene were probed along with determination of Cu loss from the catalyst. Four types of particles were prepared and tested in reaction: Cu@Fe NPs, Cu-Fe MPs, C@Cu-Fe MPs and annealed-Cu-Fe MPs. Each type of particle was characterized to determine potential reasons for their catalytic activity and Cu leaching tendencies.

In chapter 2, Cu@Fe NPs were prepared and attempted in catalysis. However, due in the inhomogeneity within catalyst sample and from batch to batch, there were problems with reproducibility despite several attempts to modify reaction parameters. It was thought that, the 100-150nm Fe particles were too small and underwent drastic Fe depletion during galvanic reduction, and thus magnetic loss. This led to portions of the catalyst being very copper-rich and some very copper-poor and thus having inconsistencies in catalytic ability. To potentially reduce this impact, in chapter 3 a larger Fe core was used, namely Fe MPs, which were in the range of 0.5-5µm in size. This proved to be helpful, because the reaction showed much more consistency and several reaction parameters and Cu leaching profiles could be assessed. It was found that, a 5mol% reaction, using 0.25M concentration of reactants in $CHCl_3$ were the best conditions for catalysis. This reaction took 16h to achieve 93% ± 5% conversion. Moreover, this reaction showed the least amount of Cu loss, where simply magnetically retrieving the catalyst left behind 961.2µg/g of Cu. These conditions were also better than the homogenous version using CuI/DIPEA, which took 24h to achieve 84% ± 5% with 1985.0µg/g of Cu in the product after filtration through Celite. The Cu-Fe MPs and the rhod-testo product from a 5mol% Cu-Fe MP reaction were both tested in MCF-7

breast cells for toxicity. An MTT assay was done and found the Cu-Fe MPs were not toxic to the breast cells in the pM, nM and µM range and the Cu-containing **rhod-*triazole*-testo** product was not toxic to the breast cells in the pM, and nM range. This was a very promising find which will allow for further development of an aromatase sensor.

In chapter 4, there was investigation of modifying the Cu-Fe MPs to attempt to further decrease the Cu loss from the catalyst. Coating the particles with carbon (C@Cu-Fe MPs) by annealing the Cu-Fe MPs in a solution of glucose at 800^{o}C was able to decrease Cu loss by an average of 4-6 times. These Cu-Fe MPs were also annealed only at 800^{o}C and they also decreased the Cu loss but only after the first run about two-fold. Therefore, the carbon coating played a key role in decreasing the Cu loss, not just the annealing. This decrease in Cu loss came at the expense of longer reaction time, however, applications requiring low levels of Cu contamination without need for purification could benefit from these modified particles.

5.2 Future Work

While there were reproducibility issues with the Cu@Fe NPs, there has been some preliminary work to anneal these particles and visualize the resulting structures. The structures showed a thin layer of Cu at the surface with less Cu-rich particles present, and more Cu distribution at the surface than the MPs. Based on these present structures, we believe these annealed Cu@Fe NPs could exhibit less Cu loss due to less dangling Cu species that were susceptible to being detached. Catalytic tests and ICP-OES measurements of the product of a click reaction would need to be done along with further characterization, specifically XPS, to determine the surface Cu content as well as the proportion of Cu(0), Cu(I) and Cu(II).

The Cu-Fe MPs used for the CuAAC of rhod-N_3 and ethisterone to produce rhod-testo were successful and thus the second part of this project to develop the AuNP nanosensor in collaboration with Dr. Dusica Maysinger in Pharmacology and McGill is possible and will hopefully be performed.

As for the carbon coating decreasing the Cu loss from the catalyst, visualizing this

coating has proven to be difficult. XPS showed an increase in %C at the surface versus the pristine Cu-Fe MPs; however, determining the exact nature of this carbon coating was elusive. Learning more about this coating would allow for more thoughtful analyses of the mechanism for decrease in Cu loss and longer reaction time. One suggestion would be to use silica coated TEM grids and do an EDX mapping to visualize the regions of the particles that contain the amorphous carbon. Furthermore, early tests indicated perhaps the proportions of Cu(0), Cu(I) and Cu(II) could play a role in catalyst activity. Learning better particle synthesis techniques to control these proportions could also play a role in finding the optimal catalyst composition for increasing catalytic activity while decreasing Cu loss.